University of Alberta

Development of the Voltage-Gated Sodium and Potassium Currents Underlying Excitability in Zebrafish Skeletal Muscle

by

Christopher Alexander Coutts

A thesis submitted to the Faculty of Graduate Studies and Research
in partial fulfillment of the requirements for the degree of

Doctor of Philosophy
in
Physiology, Cell & Developmental Biology

Department of Biological Sciences

Fall 2009
Edmonton, Alberta

Examining Committee

Declan Ali, Biological Sciences

John Chang, Biological Sciences

Warren Gallin, Biological Sciences

Peter Nguyen, Physiology

Greg Goss, Biological Sciences

Mel Robertson, Biology, Queen's University

ABSTRACT

Excitable cells display dynamically regulated changes in the properties of ion currents during development. These changes are crucial for the proper maturation of cellular excitability, and therefore have the potential to affect more sophisticated functions, including neural circuits, movements, and behaviors. Zebrafish skeletal muscle is an excellent model for studying the development of ion channels and their contributions to excitability. They possess distinguishable populations of red and white muscle fibers, whose biological functions are well understood. The main objectives of this thesis were:

(1) To characterize the development of muscle excitability by examining properties of voltage-gated sodium and potassium currents expressed in embryonic and larval zebrafish during the first week of development.

(2) To elucidate some of the mechanisms by which ion current development might be controlled, beginning with activity-dependent and phosphorylation-dependent mechanisms.

These objectives were approached using whole-cell electrophysiological techniques to examine the voltage-dependent and kinetic properties of voltage-gated sodium and potassium currents in intact zebrafish skeletal muscle preparations. Mutant *sofa potato* zebrafish, which lack functional nicotinic acetylcholine receptors, were then utilized

to determine whether synaptic activity at the neuromuscular junction is required for proper ion current development. Finally, protein kinases were activated pharmacologically in order to determine whether they were able to modulate ion currents during development.

The results revealed that properties of ion currents undergo a developmental progression, including increased current density, accelerated kinetics, and shifts in voltage-dependence; these developments correlated well with the maturation of muscle action potentials and the movements and behaviors they mediate. *Sofa potato* mutants were found to be deficient in certain aspects of ion current development, but other aspects appeared to be unaffected by a lack of synaptic activity. Protein kinase A demonstrated the ability to drastically reduce potassium current density; however the effects of PKA were similar at all developmental stages.

Overall, these findings provide novel insight into the roles played by voltage-gated currents during the development of excitability in zebrafish skeletal muscle, and expand the rapidly growing body of knowledge about ion channel function in general.

ACKNOWLEDGEMENTS

I'm not one to drag these sorts of things out, so I will keep this short and sweet; however I should note that I could easily fill many pages with the gratitude I have for the following people.

First and foremost, I'd like to acknowledge the tremendous support and guidance I've received from my supervisor, Declan Ali. Always there when I need him, and yet somehow never overbearing, Declan embodies all of the best qualities of supervisors I have known, and none of the faults. He has truly been a source of inspiration.

Next, I would like to thank the members of my supervisory committee, John Chang, Warren Gallin, and Peter Nguyen, for the knowledgeable and thoughtful insights you have contributed over the years. Thanks are also due to the members of my candidacy and defense examining committees, including Greg Goss, Klaus Ballanyi, and Mel Robertson, for their thought-provoking questions, and also to the committee chairs, Mike Belosevic and Reuben Kaufman, for keeping us all in line.

I'd also like to acknowledge the contributions, scientific and otherwise, of my lab-mates over the years, particularly those of Kessen Patten and Leslie Balt, for whom I have a tremendous amount of respect and admiration.

Credit is due to the Natural Sciences and Engineering Research Council of Canada, the Department of Biological Sciences, and the Province of Alberta for their generous financial support.

I must also thank the friends I've made along the way, for ensuring that I balanced my studies with generous helpings of drunken debauchery. I won't attempt to name you all, for fear of missing someone, however

there are a few people that stand out in this regard: Kessen Patten, Scott Parks, Martin Tresguerres, James Stafford, Ben Montgomery, and Dave Graham.

Finally, I thank Janelle Pakan and my parents, Robert and Gisela Coutts, for the support and encouragement they've provided me in all my endeavors.

TABLE OF CONTENTS

LIST OF TABLES

LIST OF FIGURES

LIST OF ABBREVIATIONS

4-AP	4-amino pyridine
AKAP	A-kinase anchoring protein
ANOVA	analysis of variance
BAPTA	1,2-bis(o-aminophenoxy)ethane-N,N,N',N'-tetraacetic acid
C_m	membrane capacitance
CA1	*Cornu Ammonis* area 1
CaP	caudal primary motoneuron
cAMP	3'-5'-cyclic adenosine monophosphate
CaMK	Calcium/calmodulin-dependent protein kinase
ChoCl	choline chloride
DHPR	dihydropyridine receptor
DMSO	dimethyl sulfoxide
dpf	days post fertilization
EGTA	ethylene glycol tetraacetic acid
ERK	extracellular signal-related kinases; see also ‘MAPK’
Fsk	forskolin
hpf	hours post fertilization
HSP	heat-shock protein
IBMX	isobutylmethylxanthine
K_{Ca}	calcium- and voltage-gated potassium channel
K_V	voltage-gated potassium channel
KChAP	potassium channel associated protein
KChIP	potassium channel interacting protein

KCNE	potassium channel, group E; see also ‘MiRP’
MAPK	mitogen-activated protein kinase
MEK	mitogen-activated protein kinase; see also ‘MAPK/ERK’
mEPC	miniature endplate current
mEPP	miniature endplate potential
minK	mitogen associated protein kinase kinase kinase kinase; see also ‘MiRP’
MiP	middle primary motoneuron
MiRP	mink-related peptides; see also ‘minK’
mRNA	messenger ribonucleic acid
Na_V	voltage-gated sodium channel
nAChR	nicotinic acetylcholine receptor
PKA	protein kinase A
PKC	protein kinase C
R_m	membrane resistance
R_S	series resistance
RoP	rostral primary motoneuron
RT-PCR	reverse transcription-polymerase chain reaction
RyR	ryanodine receptor
SEM	standard error of mean
Shh	Sonic hedgehog
SR	sarcoplasmic reticulum
sop	*sofa potato* mutant
TTX	tetrodotoxin
V_{50}	voltage of half-activation

1. INTRODUCTION

1.1 Role of voltage-gated ion channels in cellular excitability

Electrical activity in nerve and muscle is responsible for many vital processes, including movement, sensation, and cognition. This electrical excitability is mediated in large part by the permeability of cellular membranes to various inorganic ions through transmembrane glycoproteins called ion channels. There is an incredible diversity of ion channels not only between species, but even within an individual organism; a typical mammalian genome can contain as many as several hundred genes for ion channel subunits (Hille, 2001). One method of classifying ion channels is according to the various stimuli that serve to activate and open them, including changes in membrane potential, mechanical deformations, light, chemical stimuli such as neurotransmitters, second messengers, and even changes in intracellular ion concentrations.

The family of ion channels that will be the focus of this thesis is activated by changes in membrane potential. Once activated, these voltage-gated channels act as aqueous pores in the membrane, allowing ions to passively flow down their electrochemical gradients at a rate ($>10^6$ ions/second) approaching that of free diffusion (Hille, 2001). The ability of these channels to be selectively permeable only to a restricted class of small, inorganic ions at such a high rate truly makes them “superb chemists” (Miller, 2000). The classical examples of these channels are the

voltage-gated sodium-, potassium-, and calcium-selective channels of nerve and muscle membranes. The direction of ion flow is determined by electrochemical gradients across the membrane, which are actively maintained by various membrane transport mechanisms, most notably the sodium-potassium pump. In general, the extracellular concentration of sodium, calcium, and chloride ions is greater than intracellular, while the opposite is true for potassium (K^+) ions. Ion flow through channels is manifested as electrical current across the membrane, which has a direct effect on membrane potential, as dictated by Ohm's Law:

$$\boldsymbol{V = I\,R}$$

Where ***V*** is membrane potential, ***I*** is current, the direction of which is defined as the movement of positive charge, and ***R*** is transmembrane resistance. Neighboring voltage-gated channels detect local changes in membrane potential and are activated in turn, ultimately resulting in a regenerative and self-propagating electrical phenomenon known as the action potential.

The action potential is biphasic, and can be described as a wave of membrane depolarization followed by a repolarization to near resting membrane potential within 1-2 ms. As Hodgkin and Huxley so elegantly described in their four seminal papers (Hodgkin & Huxley, 1952a, b, c; Hodgkin *et al.*, 1952), the depolarizing phase of the action potential is typically due to an increased membrane sodium (Na^+) conductance, later

discovered to be due to the influx of Na^+ ions through voltage-gated channels, which is followed by an efflux of K^+ ions due to an increase in K^+ conductance, which serves to repolarize the membrane.

The biphasic nature of the action potential is due to the ability of voltage-gated ion channels to exist in one of three distinct conformational states: resting (or deactivated), activated, and inactivated (Hille, 2001). From the non-conducting resting state, which typically occurs at a membrane potential at or near the resting membrane potential of the cell, voltage-gated channels are activated by sufficient depolarization to undergo a conformational change which will allow the channel to form an aqueous pore that is permeable to ion flow. Voltage-sensing regions of the channel, which are highly positively charged, are repelled by the intracellular depolarization, causing them to move extracellularly within the membrane. This, in turn, induces a conformational change which allows the channel's activation gate(s) to open and ions to permeate. Once activated, the channels can then either revert to the resting state following a repolarization of the membrane potential (deactivation), or undergo further conformational change to become inactivated. The inactivated state is an additional non-conducting state that is distinct from the resting or deactivated state. The process of inactivation is mechanistically different from that of deactivation; typically, after the activation gate opens, a cytoplasmically located portion of the channel diffuses into the mouth of the pore and blocks conduction (Hille, 2001). The initiation of inactivation

is not directly dependent upon membrane potential, which allows it to occur despite prolonged and continuous depolarization; however repolarization is required for a channel to revert from the inactivated to the resting state, such that it is once again ready to be activated.

The movement of ions across the cell membrane during the concerted opening and closing of multiple ion channels can be recorded in the form of ionic current using electrophysiological techniques. The properties of these currents have implications not only for the underlying activity of individual channels, but also for the excitability of the cell as a whole; voltage-gated currents affect the generation, propagation, shape, speed, and refractoriness of action potentials. In this way, voltage-gated channels are able to detect, amplify, and reshape electrical activity in excitable cells (Armstrong & Hille, 1998).

1.1.1 Voltage-gated Na^+ channels and currents

The genes encoding voltage-gated Na^+ channels (Na_V) have been highly conserved throughout evolution, which is likely due to the critical role they play in cellular excitability (Hille, 2001; Goldin, 2002). The first voltage-gated channel to be cloned was a Na_V channel of the electric eel (Noda *et al.*, 1984), from which a primary structure was deduced (Catterall, 1988); however the best-characterized Na_V channels to date are those from mammalian species (Goldin, 2002). There are 9

functionally confirmed isoforms of Na_V channel (Na_V 1.1-1.9) encoded by the mammalian genome, whose amino acid sequences are more than 75 percent identical (Wood & Baker, 2001; Goldin, 2002; Catterall *et al.*, 2005). Na_V channels are composed of one α subunit (~260 kD), which contains the voltage-sensing and pore-forming regions, and is associated with one or two of several β subunits in mammals (Catterall, 1988; Hille, 2001). The α subunit has four homologous domains (I-IV), each containing six hydrophobic α helix transmembrane segments (S1-S6) (Figure 1.1). The fourth transmembrane segment (S4) of each domain acts as the voltage-sensor with a positively charged amino acid at every third position (Catterall, 1988). The S5-S6 linker forms part of the pore by dipping into and out of the lipid bilayer and it also contains the sequence of amino acids necessary to confer Na^+ ion selectivity (Hille, 2001). The intracellular loop between domains III and IV serves as the inactivation gate, acting as a blocking particle by binding to a site at the intracellular mouth of the pore (Stuhmer *et al.*, 1989; Vassilev *et al.*, 1989; West *et al.*, 1992).

For the most part, Na_V channels are expressed in a tissue-specific manner. For example, some channels are expressed primarily in the central and peripheral nervous systems (Na_V1.1, 1.2, 1.3, 1.6, 1.7), and others are found in dorsal root ganglia (Na_V1.8, 1.9), skeletal muscle (Na_V1.4), and cardiac muscle (Na_V1.5) (Catterall *et al.*, 2005). This distribution suggests that the Na_V channel isoforms may have diverse functions to perform; however, the currents carried by these channels are

remarkably similar in appearance, characteristics, and perhaps most importantly, in their primary purpose – to generate action potentials. In general, Na_V currents have the following characteristics: they activate rapidly, within fractions of a millisecond from the onset of a stimulus, and they inactivate rapidly and often completely, usually within a few milliseconds. The high rate at which Na_V currents are activated is responsible for the rapid membrane depolarization of the action potential, and Na_V current inactivation allows the membrane to repolarize, albeit with the help of a voltage-gated K^+ (K_V) current.

1.1.2 K_V channels and currents

Of all voltage-gated ion channels, the K_V channels are the most diverse, both structurally and functionally. To date, there are 12 subfamilies (K_V 1-12), grouped according to their phylogenetic relatedness (Gutman *et al.*, 2003; Gutman *et al.*, 2005). The first of these to be cloned were the *Shaker*, *Shab*, *Shaw* and *Shal* channels in *Drosophila*, making up what are now known as the K_V 1-4 subfamilies (Kamb *et al.*, 1987; Papazian *et al.*, 1987; Tempel *et al.*, 1987; Pongs *et al.*, 1988; Butler *et al.*, 1989), and the rest were identified, for the most part, in mammalian studies performed since then. Each subfamily has several members with distinct functional properties, and some of these have splice variants.

Functional K_V channels are composed of a tetramer of α subunits, each subunit being structurally and functionally similar to a single domain of a Na_v channel (Figure 1.1). Together, the four α subunits assemble to form a structure similar to a single Na_V channel α subunit. Each of the four K_V channel α subunits possesses an S4 voltage-sensor and an S5-S6 pore-forming and selectivity filter region. Contrary to Na_V channels, many K_V channels do not possess the ability to inactivate. Those that do use either α subunit N-terminal sequences acting as inactivation balls (α-balls) or similar inactivation balls can be provided by certain subtypes of auxiliary β subunits (β-balls) (Hille, 2001; Li *et al.*, 2006). There are several types of auxiliary subunits that can co-assemble with K_V α subunits to modify their surface expression and functional properties (see INTRODUCTION 2.1.3) (Rettig *et al.*, 1994; Chouinard *et al.*, 1995; Li *et al.*, 2006).

K_V channels are expressed by virtually all excitable cells, including those that don't support action potentials, but the tissue distribution is not as consistent or straight-forward as that of Na_V channels. There does appear to be some localization on a subcellular level in mammalian neurons, however; K_V 1 subunits are found primarily in axons and terminals, K_V 2 and K_V 4 subunits are found on soma and dendrites, and K_V 3 subunits can be located in any of these areas depending on the type of cell and isoform in question (Trimmer & Rhodes, 2004). K_V channels need not be homomeric; closely related subunits or splice variants can

assemble into fully functional channels. The large number of possible structural combinations, together with the often mosaic pattern of subcellular localization, results in an enormous diversity of K_V channels with complex biological functions. This complexity does not arise by chance; it is tightly regulated and often follows a distinct progression from an immature to a mature state during development.

1.2 Development of Na_V and K_V channels

The vast majority of early work on voltage-gated ion channels was performed on mature nerve and muscle cells. Mature cells are readily available and possess a sophisticated suite of voltage-gated ion channels that are optimized for specific cellular functions. Gaining knowledge of the developmental processes and timetable by which this maturation is achieved has since become the focus of much interest. Excitable cells have been found to display dynamically regulated changes in the density, kinetics, and voltage-dependence of ion channels during development, often with demonstrable effects on cell excitability and even behaviour. For example, studies in several different species have shown that action potential shortening during postnatal ventricular myocyte maturation is due to an increase in a transient outward K_V current density (Kilborn & Fedida, 1990; Jeck & Boyden, 1992; Nuss & Marban, 1994; Sanchez-Chapula *et al.*, 1994; Wahler *et al.*, 1994). In spinal neurons of *Xenopus*, developmental increases in Na_V and K_V current density and K_V activation

rate underlie a decrease in the duration of action potentials (Barish, 1986; O'Dowd *et al.*, 1988; Lockery & Spitzer, 1992; Vincent *et al.*, 2000). Similarly, in developing rat spinal neurons, Na_V current density and kinetics are increased, along with an increase in K_V current density, resulting in concurrent developmental increases in action potential rate and firing frequency (Gao & Ziskind-Conhaim, 1998). Examples of shifting voltage-dependence take place in developing hippocampal astrocytes and chick cardiac ventricular muscle. In these animals, fewer Na_V channels are in an inactivated state at resting membrane potentials in immature cells, making them more excitable, and sometimes even generating spontaneous activity (Sontheimer *et al.*, 1992; Sada *et al.*, 1995). Thus, it has become clear that many properties of voltage-gated ion channels are different in immature cells than in their mature counterparts, and these changes alter cellular excitability. Somewhat less well understood, however, are the mechanisms underlying such developmental changes.

1.2.1 Mechanisms underlying Na_V and K_V channel development

With the abundance of data illustrating the effects of Na_V and K_V current development on cellular excitability, the need arises to understand the mechanisms responsible for bringing these changes about. Recent studies have demonstrated a variety of possible mechanisms for cells to utilize in the maturation of excitability, including

regulation of gene expression, modulation of channel activity by protein kinases, and the influence of various auxiliary subunits.

1.2.1.1 Regulation of voltage-gated channel gene expression

There is evidence to suggest that the diversity of Na_V and K_V current properties observed in developing nerve and muscle cells can be achieved via differential expression of α subunits. These approaches use molecular genetics and/or protein biochemistry to identify the molecular identities of functionally identified currents present in cells at different developmental stages. In some cases, mRNA analyses were performed at the single-cell level (RT-PCR), allowing correlation between expression of specific transcripts with the functional currents present in a given cell; for example, there is an up-regulation of K_V 1.1 and K_V 2.2 in *Xenopus* spinal neurons during the period in which delayed-rectifier K_V current density increases (Gurantz *et al.*, 1996). The transient outward K_V current present in early neonatal (postnatal days 1-2) rat ventricular myocytes appears to be mediated by K_V 1.4 channels, whereas by postnatal day 5 there is a switch to K_V 4.2/4.3 channel along with a change in the current kinetics (Guo *et al.*, 1996; Xu *et al.*, 1996; Guo *et al.*, 1997; Wickenden *et al.*, 1997). $Na_V1.1$ and $Na_V1.6$ are both expressed in zebrafish Rohon-Beard mechanosensory neurons, whose Na_V current density increases during development; antisense morpholinos for $Na_V1.1$ were only effective in reducing Na_V currents at younger ages, whereas $Na_V1.6$ morpholinos

increased in effectiveness as development proceeded (Pineda *et al.*, 2005). These results appear to indicate that developmental upregulation of Na_V currents were the result of an increased expression of Na_V 1.6 channels. Increased expression of Na_V 1.6 channels also appears to underlie the developmental increase in Na_V current density observed in murine spinal motoneurons; in the absence of the gene encoding Na_V 1.6, this developmental increase failed to occur (Carlin *et al.*, 2008).

1.2.1.2 Modulation of Na_V and K_V channels via phosphorylation or dephosphorylation

Many aspects of cellular function are regulated by the phosphorylation of proteins. It has been estimated that a third of cellular proteins can be reversibly phosphorylated; a protein's state of phosphorylation is determined by the relative activities of various kinases and phosphatases within the cell (Depaoli-Roach *et al.*, 1994). Modulation of the phosphorylation-state of ion channels is another mechanism by which ionic currents may be altered during development.

Na_V and K_V channels have consensus sequences for various protein kinases. For example, Na_V channels possess multiple potential phosphorylation targets for both protein kinase A (PKA) and protein kinase C (PKC), which are located on the intracellular loops linking α subunit domains I-II and III-IV (Sigel & Baur, 1988; Dascal & Lotan, 1991; Chen *et*

al., 1995). There is evidence to suggest that Na_V channel isoforms are modulated in a differential manner by PKA and PKC. In neurons, both kinases have been shown to decrease current amplitude (Sigel & Baur, 1988; Dascal & Lotan, 1991; Gershon *et al.*, 1992; Li *et al.*, 1993; Smith & Goldin, 1996), but in heart muscle they have opposite effects (Schreibmayer *et al.*, 1994). Activation of PKC in cultured embryonic rat brain neurons resulted in reduced Na_V current amplitude and slowing of the inactivation kinetics, and had similar effects when rat brain Na_V channels were expressed in Chinese hamster ovary cells, but the mutation of a single serine residue on the intracellular loop linking domains III and IV abolished the effects of PKC (Numann *et al.*, 1991; West *et al.*, 1991). The effects of PKA in these same preparations was slightly different; it also reduced Na_V current amplitude, however current kinetics were unaffected (Li *et al.*, 1992). Interestingly, PKA appears to have no effect on Na_V currents in skeletal muscle (Frohnwieser *et al.*, 1997).

The majority of research on phosphatase actions on Na_V channels has been performed in the rat brain, where protein phosphatases (PP) 2A and 2B were shown to have different specificities for several serine residues phosphorylated by PKA (Murphy *et al.*, 1993). The convergence of PKC- and PKA-mediated phosphorylation of Na_V channels noted above (Li *et al.*, 1993) could be due to an inhibition of dephosphorylation of PKA sites by PP2A or PP2B in the presence of PKC (Kondratyuk & Rossie, 1997). Although PP2A- and PP2B-like are the only protein phosphatases

that have been pharmacologically and immunologically identified in rat brain to date (Chen *et al.*, 1995), PP1 activity has been implicated by the ability of phosphorylated DARPP-32 (a PP1-specific inhibitor) to reduce Na_V current amplitudes in striatal neurons (Schiffmann *et al.*, 1998).

K_V channels possess consensus sequences for phosphorylation by multiple kinases, including PKA, PKC, mitogen-activated protein kinase/extracellular signal-related kinase (MAPK/ERK), and calcium/calmodulin-dependent protein kinase II (CaMKII) on the intracellular C-terminal portions of each α subunit. Also identified is a potential site for PKA modulation on the N-terminal (Adams *et al.*, 2000; Anderson *et al.*, 2000). Activation of PKC attenuates K_V 1.4 and K_V 4.2/4.3 currents, and removes the inactivation of K_V 3.4 (Covarrubias *et al.*, 1994; Murray *et al.*, 1994; Nakamura *et al.*, 1997). Activation of PKC in *Aplysia* bag cell neurons had no effect on any of several types of K_V currents present (DeRiemer *et al.*, 1985), whereas activation of PKA caused a reduction in current amplitude (Kaczmarek & Strumwasser, 1984; Strong, 1984; Shuster *et al.*, 1985). In certain preparations, PKA and PKC have similar effects; K_V currents in cultured astrocytes (MacVicar *et al.*, 1987; Akerman *et al.*, 1988) and oligodendrocytes (Soliven *et al.*, 1988), as well as those in murine dorsal root ganglion cells (Grega *et al.*, 1987), are reduced by both PKC and PKA activation. These results suggest that certain K_V channels, or perhaps a closely-associated regulatory protein, can be common substrates for several types of kinases, and that

phosphorylation at the various consensus sites can have diverse effects on channel function.

Protein phosphatases have also been implicated in the modulation of K_V channels. An investigation into the mechanism of angiotensin II-induced increase in delayed rectifier K_V current of rat hypothalamic neurons found that this effect was inhibited by nanomolar okadaic acid, a potent phosphatase inhibitor (Kang *et al.*, 1994). It was later discovered that anti-PP2A antibodies blocked this angiotensin II effect (Huang *et al.*, 1996). A reduction in transient outward currents from recombinant mouse brain K_V channels was found to be due to dephosphorylation by PP2B (Hoger *et al.*, 1991), and a later study found that PP2B also accelerated the inactivation kinetics, whereas CaMKII resulted in deceleration (Roeper *et al.*, 1997).

1.2.1.3 Auxiliary subunits

It is important to consider the fact that voltage-gated channels are not sitting isolated in cell membranes; they are surrounded by large complexes of auxiliary and scaffolding proteins. Some of these proteins are very tightly associated with channels for their entire functional existence, while other interactions may be only transient in nature. These interactions can have various functional consequences, including altered surface expression, trafficking, stabilization, and voltage-dependence and

kinetics of gating (Hille, 2001). It therefore stands to reason that some of these auxiliary subunits may regulate the changes in ion channel activity observed during development.

Both Na_V and K_V channels are associated with their own β subunits, and there are several isoforms for both. Na_V channels are associated with β1 and β2 subunits in neurons, but only with β1 subunit in muscle (Roberts & Barchi, 1987). Even in neurons, however, the β2 subunit appears to have no effect on channel activity, whereas without the β1 subunit, Na_V channels are no longer functional (Messner *et al.*, 1986). β1 subunits have been shown to alter Na_V current amplitude, kinetics of activation and inactivation, and the voltage-dependence of inactivation (Denac *et al.*, 2000).

K_V channel β subunits consist of 3 subfamilies (K_V β 1-3), each containing several splice variants (Rettig *et al.*, 1994; Scott *et al.*, 1994; Majumder *et al.*, 1995; McCormack *et al.*, 1995). K_V β subunits are ~400 residues in length, and form tetramers in K_V channel complexes to complement the α subunit tetramer; the four α subunits of each K_V channel combine with four β subunits in a 1:1 ratio (Parcej *et al.*, 1992). K_V β 1 and 3 have been shown to confer the ability to inactivate in K_V channels that would otherwise do so only very slowly or not at all (Rettig *et al.*, 1994; Heinemann *et al.*, 1996). While not involved in inactivation, K_V β 2 has been shown to act as a chaperone protein, increasing surface

expression, glycosylation, and proper folding of K_V 1.2 α subunits (Shi *et al.*, 1996). K_V β subunits can accelerate both activation and inactivation kinetics (Leicher *et al.*, 1998). K_V channels also associate with a number of other auxiliary proteins, including K_V channel interacting proteins (KChIPs), which generally slow the inactivation of K_V 4 channels (An *et al.*, 2000; Bahring *et al.*, 2001); K_V channel associated protein (KChAP), which increases the amplitudes of several K_V subfamilies (Wible *et al.*, 1998); group E potassium channel (KCNE)-encoded proteins (e.g. minK and minK-related peptides – MiRPs), which have many diverse effects on various K_V channel subfamilies (Li *et al.*, 2006); and even A-kinase anchoring proteins (AKAPs), which serve to localize PKA to sites of action, along with other kinases and phosphatases (Li *et al.*, 2006).

1.2.2 Controlling the development of cellular excitability: genetic programs versus synaptic activity

The developmental expression of ion channels can be governed by cell autonomous genetic programs, as established during cell differentiation, or external factors such as hormones, growth factors, and synaptic input, or a combination of these (Mennerick & Zorumski, 2000; Spitzer *et al.*, 2002; Moody & Bosma, 2005; Spitzer, 2006). The focus here will be on the role played by synaptic activity, as some of the possible roles played by gene transcription in ion current development have already been mentioned above. Electrical activity has been shown to regulate several

essential neuronal characteristics during neural development, including axonogenesis, synapse formation, neurotransmitter expression, and channel expression (Spitzer, 1991; Shatz, 1994; Katz & Shatz, 1996). This activity-dependence is often limited to critical windows during development, when excitability is initially established, which is consistent with the developmental progression of ion channel expression during embryonic development.

Over the course of development, murine hippocampal neurons express six members of the K_V 1 subfamily of channels (K_V 1-6) in a specific pattern, resulting in a 7- to 8-fold increase in K_V current (Grosse *et al.*, 2000). It was discovered that application of clostridial toxins (e.g., tetanus, botulinum) selectively blocked the developmental upregulation of some K_V channels (K_V 1.1, 1.2, and 1.4), but not others (K_V 1.3, 1.5, and 1.6). These toxins were potentially acting at the synaptic level, by inhibiting the release of neurotransmitters, and/or by interfering with the trafficking of K_V 1.1, 1.2, and 1.4 into the membrane. In order to distinguish between these two possibilities, a Na_V channel blocker (tetrodotoxin: TTX) was applied to abolish action potentials, thereby blocking synaptic activity without directly interfering with channel trafficking. Application of TTX mimicked the effects of the clostridial toxins, indicating that the proper development of K_V 1.1, 1.2, and 1.4 channels is dependent on synaptic activity. Interestingly, developmental regulation of

K_V 1.3, 1.5 and 1.6 in the same preparation appear to be independent of synaptic input (Grosse *et al.*, 2000).

It has been proposed that the effects of synaptic activity might be compensatory (Moody & Bosma, 2005), as indicated by the upregulation of K_V channels as seen above; therefore, one might expect activity to downregulate Na_V channel expression. Indeed, in developing hippocampal and cortical neurons, activity results in an internalization of Na_V channel proteins and downregulation of α subunit mRNAs (Dargent *et al.*, 1994; Lara *et al.*, 1996; Paillart *et al.*, 1996). In contrast, neurons in the central nervous system of *Drosophila* upregulate both Na_V and K_V currents in an activity-dependent manner, but calcium currents are unaffected by blockade of synaptic input (Baines *et al.*, 2001).

Thus, the complex patterns of ion channel development that occur in excitable cells appear to be under the influence of synaptic input from extrinsic sources in some instances, but in others there appears to be an intrinsic genetic program in place that is capable of controlling the development of excitability autonomously.

1.3 Zebrafish skeletal muscle as a model for the development of cellular excitability

Zebrafish (*Danio rerio*) are tropical, freshwater fish, and are one of over 2000 species of minnows (Family Cyprinidae), measuring

approximately four centimeters long as adults (Schilling & Webb, 2007). Their geographical range consists of the waterways around the Ganges river in Southern and Southeastern Asia. A recent field study has revealed that they occur primarily in still and slow-moving waters with silt-covered bottoms and submerged or overhanging vegetation, and ranging in temperature between roughly 25 and 40 °C, with a pH of approximately 6 to 8 (Engeszer *et al.*, 2007). Based on their field data, Engeszer and colleagues have hypothesized the following natural history for zebrafish: Adults reside in shallow, slow-moving streams or vegetated pools, feeding on insects, until the rainy season begins. Then they move out into flooded areas and rice paddies to spawn, where the offspring feed and grow until they return to the streams along with the receding flood waters at the end of the wet season.

The zebrafish is an important model for the study of vertebrate developmental biology, including nervous system and musculature development (Holley & Nusslein-Volhard, 2000; Bassett & Currie, 2003; Ingham & Kim, 2005; Ochi & Westerfield, 2007). Zebrafish embryos are fertilized and develop externally and are optically transparent (Figure 1.2). This facilitates experimental observation and manipulation with cellular, molecular, and genetic approaches *in vivo*, which gives them a major advantage over mammalian models of development. In particular, the developing zebrafish has proven to be especially valuable for studying aspects of neuromuscular electrophysiology in an intact preparation

(Westerfield *et al.*, 1986; Devoto *et al.*, 1996; Ali *et al.*, 2000a; Buss & Drapeau, 2000, 2002). Another advantage of the zebrafish neuromuscular preparation is its simplicity compared to mammalian and even amphibian preparations; there are relatively few types of neuronal and muscle cells in the developing embryo and larva, and they possess well-defined, distinct morphologies. It is therefore possible to obtain patch-clamp recordings from identifiable hindbrain, spinal cord, and muscle cells *in vivo*.

The majority of the zebrafish genome has been sequenced, and the zebrafish genomic toolbox now includes both forward and reverse genetics. One of the more recent and notable reverse genetic approaches used to elucidate gene function and pathways in zebrafish is the microinjection of morpholinos (Nasevicius & Ekker, 2000). Morpholinos are antisense oligonucleotide analogs with a morpholine group replacing the pentose ring; they are a genetic knockdown technology which blocks translation or prevents correct splicing into a mature mRNA (Summerton & Weller, 1997). Large-scale mutagenesis screens in zebrafish have led to the discovery of a large number of mutations in more than 400 genes that disrupt embryonic development and many of these transgenic mutants are readily available (Granato & Nusslein-Volhard, 1996). Several mutations have been found that affect ion currents, including those of voltage-gated calcium, Na_V, and K_V channels (Ribera & Nusslein-Volhard, 1998; Rottbauer *et al.*, 2001; Arnaout *et al.*, 2007; Nakamura & Coetzee, 2008).

Indeed, the zebrafish is increasingly utilized as an animal model for the study of voltage-gated ion channels and their currents (Novak *et al.*, 2006a; Novak *et al.*, 2006b; Nakamura & Coetzee, 2008), particularly those found in the heart (Langheinrich *et al.*, 2003; Arnaout *et al.*, 2007; Hassel *et al.*, 2008; Mittelstadt *et al.*, 2008; Scholz *et al.*, 2009), retina (Connaughton & Maguire, 1998; Vessey *et al.*, 2005; Yu & Li, 2005), and central nervous system (Ribera & Nusslein-Volhard, 1998; Nakayama & Oda, 2004; Pineda *et al.*, 2006; Fein *et al.*, 2008; Yonkers & Ribera, 2008). However, only a few of these studies examined the development of channels, or its effect on the physiology or behavior of the animal. One such study found that the ability of zebrafish embryos to respond to a touch stimulus at 27 hours post fertilization (hpf) was dependent on a developmental increase in Na_V current amplitude in Rohon-Beard mechanosensory neurons, which in turn is responsible for producing action potentials with larger overshoots and shorter durations; several touch-insensitive zebrafish mutants were shown to lack a developmental increase in Na_V current amplitude (Ribera & Nusslein-Volhard, 1998). Nonetheless, very little is known about the development of voltage-gated channels found in zebrafish skeletal muscle.

1.3.1 Development of zebrafish skeletal muscle

Vertebrate skeletal muscles perform many different tasks; thus there is a diversity of muscle characteristics in order to match muscle

performance to its biological function. Some muscle fibers are specialized for slow, steady contraction, while others are specialized for rapid movements. These fibers can be distinguished by their biochemical, metabolic, and histochemical properties, including contraction rate, fatigue resistance, and electrical properties of their membranes (Randall *et al.*, 2002). Based on criteria such as these, two major groups of vertebrate skeletal muscle are recognized – tonic fibers and twitch fibers. Tonic fibers contract very slowly, due to the types of myosin they express, but they are also very fatigue-resistant. Tonic fibers do not produce action potentials, because they aren't required to spread excitation; motoneurons that innervate them make multiple synapses along their entire length, thus spreading the depolarization throughout the muscle. Due to this type of excitation, tonic fibers are able to respond to motoneuronal input with graded contractions, rather than the all-or-none contractions observed in twitch fibers. Twitch fibers (also known as phasic fibers) contract and fatigue relatively quickly. Their ability to respond to motoneuronal input with an all-or-none twitch contraction is facilitated by the production of action potentials (Randall *et al.*, 2002).

Zebrafish skeletal muscle fibers, as in most species of fish, can be broadly classified into two main groups based on their coloration – red and white. The red color is due to the relative amount of the oxygen-storing protein myoglobin present; red fibers contain relatively high concentrations compared to white fibers (Randall *et al.*, 2002). Red and white muscle

differs in additional ways, however, including fiber diameter, speed and force of contraction, enzyme composition, and metabolism. Red fibers are smaller, contract more slowly and with less force, have more mitochondria than white fibers, and express myosin isoforms that are specialized for slow, continuous contraction and oxidative metabolism. White fibers have distinct fast myosins and glycolytic metabolism, making them more suited for high-force, short-duration contractions (Randall *et al.*, 2002).

It has recently been discovered that white muscle fibers support action potentials, whereas red muscle fibers do not (Buckingham & Ali, 2004), indicating that zebrafish red fibers may actually be tonic muscles, while the white fibers are of the twitch variety (Randall *et al.*, 2002). Given these molecular and functional differences, it is not surprising that red and white muscle fibers play different roles in zebrafish motility; red fibers are primarily responsible for slow, rhythmic swimming, whereas white fibers generate the powerful 'C-bend' that initiates the escape response (Fetcho, 1987, 1992).

Differences between red and white muscle fibers become evident early on during development. Muscles are formed by the differentiation of mononucleate myoblasts into post-mitotic myocytes that then fuse to form multinucleate muscle fibers. In amniotes, the differentiation of muscle fibers is temporally separated; red fibers form first, followed by white fibers (Batty, 1984; Veggetti *et al.*, 1993; Stoiber & Sanger, 1996). The process of myogenesis in zebrafish begins during gastrulation (~70-75% epiboly),

when the subset of mesodermal cells that will ultimately give rise to somatic skeletal muscle begin the initial transcription of myogenic genes for transcription factors such as *myoD* and *mef2A,C,D* (Ticho *et al.*, 1996; Weinberg *et al.*, 1996). By the end of gastrulation (~10 hpf), muscle precursor cells (myoblasts) have positioned themselves at the midline and adjacent to the notochord (Figure 1.3A). The notochord secretes signaling glycoproteins such as Sonic hedgehog (Shh) that induce the most medial of the myoblasts to become so-called 'adaxial' cells, which will later transform into red muscle fibers after somite formation is completed. Somite formation is an important characteristic of vertebrate mesoderm development. They begin as balls of mesoderm that form in a rostro-caudal order. In lower vertebrates, such as fish, the somite mainly gives rise to muscle (Morin-Kensicki & Eisen, 1997). Zebrafish somites form at a rate of one every 20-30 minutes beginning at ~10 hpf and continuing on to about 24 hpf to create a total of 30-34 somites (Devoto *et al.*, 1996).

Following somite formation, adaxial cells elongate and migrate out to the lateral surface of the somite and differentiate into red muscle fibers. The remaining precursor cells, so-called 'lateral pre-somitic' cells, differentiate into white muscle fibers (Devoto *et al.*, 1996; Blagden *et al.*, 1997; Ochi & Westerfield, 2007). By 36 hpf, red fibers have formed a layer one cell thick just beneath the skin, and the bulk of the remaining axial musculature is comprised of white fibers (Figure 1.3B) (van Raamsdonk *et al.*, 1987). The situation in the adult zebrafish is much the same, although

red fibers have migrated toward and converged at the midline, such that they form a band running the length of the body axis, just dorsal and ventral to the midline (Figure 1.3C).

1.3.2 Innervation of zebrafish skeletal muscle during development

Red and white muscle fibers also differ in terms of innervation; both red and white fibers receive input from multiple motoneurons, however red fibers receive synaptic input only from secondary motoneurons, whereas white fibers are innervated by both primary and secondary motoneurons (van Asselt *et al.*, 1993). Zebrafish motoneurons are classified into groups, primary and secondary, based on several key anatomical and morphological differences between them (Westerfield *et al.*, 1986). There are three primary motoneurons per hemi-segment, as compared to 20-25 secondaries. Primary motoneurons are born before secondaries (~10 hpf versus ~16 hpf) and they are the first to begin extending axons into the periphery (~17 hpf versus ~26 hpf). Primary motoneurons are located more dorsal and medial in the spinal cord than secondary motoneurons, and they have larger cell bodies, axons, and fields of muscle fiber innervations. The three primary motoneurons in each myotomal hemi-segment innervate muscle only within their home segment, and can be distinguished by their relative positions in the spinal cord and their fields of innvervation. The most rostral primary motoneuron (RoP) innervates fibers in the dorsal-most region of the ventral hemi-segment; the middle primary

(MiP) innervates dorsal muscle; the caudal primary (CaP) innervates the ventral-most muscle (Eisen *et al.*, 1986; Myers *et al.*, 1986; Westerfield *et al.*, 1986).

1.3.3 Excitation and contraction of zebrafish skeletal muscle

In order to understand muscle function, it is necessary to examine its cellular and molecular properties. Like other vertebrates, red and white muscle fibers in zebrafish receive excitatory cholingergic input from primary and secondary motoneurons via activation of nicotinic acetylcholine receptors (nAChRs) (Liu & Westerfield, 1988; Nguyen *et al.*, 1999). The synaptic activity resulting from nAChR activation has been characterized during development. Compared to those recorded at ~1 day post fertilization (dpf), miniature endplate currents (mEPCs) recorded at 6 dpf had larger amplitudes (~10-fold), higher frequency (~3.5-fold), and faster kinetics (up to 5-fold) (Nguyen *et al.*, 1999). Similarly, miniature endplate potentials (mEPPs) recorded between 1 and 5 dpf in both red and white muscle fibers exhibited increased frequency and amplitude, and the kinetic properties of mEPPs in red fibers also increased (Buss & Drapeau, 2000). These synaptic events are responsible for generating the depolarization that initiates excitation of the muscle membrane via activation of Na_V channels.

In mammalian skeletal muscle, there is a developmental switch from TTX-insensitive Na_V 1.5 α subunits expressed in neonates to relatively TTX-sensitive Na_V 1.4 channels that predominate in the adult (Trimmer *et al.*, 1989; Kallen *et al.*, 1990). In adults, Na_V 1.4 channels are expressed and distributed in the membrane in an activity-dependent manner; they are concentrated at the neuromuscular junction, where synaptic activity is high, and lower elsewhere in the membrane. Interestingly, Na_V 1.5 channels are expressed once again following denervation or paralysis, indicating that their expression is actually suppressed by synaptic activity (Awad *et al.*, 2001). A recent study reported the embryonic and larval gene expression patterns for all eight isoforms of Na_V 1.x channels in zebrafish (Novak *et al.*, 2006b). In zebrafish, Novak and colleagues (2006b) found that genes encoding both Na_V 1.4 and 1.5 are expressed in developing somites, which differentiate primarily into skeletal muscle, as described above. Interestingly, they are expressed in a similar manner to that seen in mammals; Na_V1.5 is expressed only transiently (19-30 hpf), whereas Na_V 1.4 is expressed from 24 hpf onwards. This would seem to indicate that the expression of Na_V channels in zebrafish muscle follows a similar, and perhaps an activity-dependent, progression as it does in mammals.

Only one other study has examined voltage-gated ion channels in zebrafish skeletal muscle (Buckingham & Ali, 2004), where the voltage-gated ion currents and action potentials of 4-6 dpf larvae are described.

Not surprisingly, red and white fibers were found to have distinct electrical phenotypes. White fibers were found to exhibit Na_V currents and fast-inactivating A-type K_V currents. They also support action potentials, whereas the outer red fibers appear to be devoid of Na_V currents, and therefore don't support action potentials. The only current observed in red fibers is a low amplitude delayed rectifier K_V current. Buckingham and Ali described ion currents at only one developmental period, thereby setting the stage for a thorough investigation of ion current maturation.

Once a sufficient number of voltage-gated channels have been activated, and excitation of the cell membrane has been achieved, it spreads to the T-tubule system, where voltage-dependent dihydropyridine receptors (DHPRs) are activated. DHPRs are physically linked to calcium-permeant ryanodine receptors (RyRs) in the sarcoplasmic reticulum (SR). DHPR activation, and subsequent physical deformation, induces RyRs to open and release the calcium sequestered in the SR into the cytoplasm. Intracellular free calcium ions then bind to and allow activation of the contractile machinery of the cell, and muscle contraction is initiated (Randall *et al.*, 2002).

As previously mentioned, membrane excitation in white (twitch) muscle is spread by action potentials, whereas red (tonic) fibers rely on the summation of synaptic activity from sites all along their length to generate sufficient membrane depolarization for contraction to occur. In addition, red muscle fibers are extensively electrically coupled via gap

junctions, allowing them to share synaptic input among neighboring cells (Buss & Drapeau, 2000; Luna *et al.*, 2004; Luna & Brehm, 2006). In fact, both red and white muscle fibers are coupled, but not to equal functional extents; the synaptic and membrane properties of red fibers allow them to share electrical signals much more effectively than white fibers. Coupling in red fibers can be detected across as many as 5 somites. In both muscle types, there is a trend towards fiber uncoupling during development; the average number of coupled fibers decreases by ~70% between 1 and 3 dpf, and then remains constant as late as 5 dpf. Coupling was never observed between red and white fibers (Buss & Drapeau, 2000). Thus, synaptic input initializes a sequence of events, which relies heavily upon the activity of voltage-gated ion channels, in order to cause muscle contraction.

1.3.4 Development of zebrafish locomotive behaviours

Motor activities and behaviours begin early and mature rapidly in developing zebrafish embryos and larvae (Saint-Amant & Drapeau, 1998), beginning with spontaneous alternating contractions of the trunk as they are initially contacted by primary motoneurons (~17 hpf) (Melancon *et al.*, 1997). These spontaneous contractions quickly peak in frequency (~1 Hz) at ~19 hpf and then continue, declining in frequency, over the following 6 hours. Interestingly, the spontaneous contractions are not eliminated by lesions at the level of the hindbrain, and have been shown to be controlled

by primitive spinal circuits (Saint-Amant & Drapeau, 2000). At ~21 hpf, embryos begin to exhibit vigorous alternating contractions in response to touch that are similar to the spontaneous contractions, but approximately twice as fast (~30 ms contraction time versus ~60 ms for spontaneous contractions). At ~26 hpf, secondary motoneurons begin innervating muscle, and dechorionated embryos develop the ability to briefly and slowly swim away from touch stimuli. The frequency of induced swimming contraction cycles increases during development to a rate of ~30 Hz at 36 hpf, a rate that is comparable to that in adult fish (Liu & Westerfield, 1988). Over the next 48 hours, embryos hatch out of the chorion. Spontaneous beat and glide swimming isn't observed until just prior to the time larvae begin feeding at ~5-6 dpf. Thus, zebrafish progress from their first tentative movements at less than 1 dpf to fully mature swimming behavior within the first week of development. Importantly, this developmental progression of zebrafish behaviors correlates well with the concurrent maturation of synaptic activity that is occurring, as described above.

1.4 Rationale and objectives

Excitable cells display dynamically regulated changes in the properties of ion channels and their currents during development. These changes are frequently crucial for the proper maturation of cellular excitability, and therefore have the potential to affect more sophisticated functions, including neural circuits, movement, behavior, and disease

states. Channel development often occurs in complex patterns; it cannot always be understood as a simple continuum of events that leads to a mature set of properties; there can be several distinct phases of electrical activity, each with its own role to play in cellular development. Moreover, these developmental progressions toward excitability are often quite different between species, cells, and even the types of channels found within individual cells. Nonetheless, much can be gained in the form of general knowledge by integrating the results achieved from a multitude of seemingly unique systems, including zebrafish skeletal muscle.

Zebrafish skeletal muscle is an excellent model for studying the development of ion channels and their contributions to excitability. They possess distinguishable populations of red, tonic and white, twitch muscle fibers, whose biological functions are well understood. Furthermore, properties governing the excitability of these fibers can be correlated with the simple, well-characterized muscle-driven behavior of the organism as a whole. While studying the maturation of ion currents in an animal model as widely used as zebrafish is useful in and of itself, it will also expand knowledge of the development of cellular excitability in general.

Thus, en route to the broader goal of understanding the process by which cells become excitable during development, the specific goals of this thesis were threefold:

1.4.1 To characterize the development of Na_V and K_V currents in zebrafish skeletal muscle

Considering the important role that Na_V and K_V channels play in the excitability of fish skeletal muscle fibers, surprisingly little is known about their development. Most previous studies on developing muscle have been performed on dissociated fibers or cultured myocytes, whereas the zebrafish preparation offers the possibility of investigating the developmental profiles of these currents in muscle fibers *in vivo*. In addition, the specific differences between red and white fibers have not been investigated in developing preparations. In order to explore ion current development in zebrafish skeletal muscle more thoroughly, the properties of Na_V and K_V currents of red and white skeletal muscle fibers were investigated in developing zebrafish. In addition, action potentials generated at different ages were studied in order to gain insight into how current development affects muscle excitation.

1.4.2 To determine whether synaptic activity plays a role in the development of Na_V and K_V currents

Having established that ionic currents undergo several developmental changes, the next step was to investigate some of the possible mechanisms underlying such phenomena. In some types of excitable cells the development of voltage-gated currents is controlled by synaptic input, while in others it is not. In order to determine the effect that

an absence of synaptic input might have on Na_V and K_V current development, zebrafish *sofa potato* (*sop*$^{-/-}$) mutants were studied, which lack nAChRs in the membranes of skeletal muscle fibers due to a point mutation in the δ subunit (Ono *et al.*, 2004). These mutant muscle fibers are therefore completely devoid of synaptic input, and will lack any of the developmental cues they might normally receive from such synaptic activation.

1.4.3 To determine whether kinases modulate voltage-gated ion channels during development

Ion channels are important phosphorylation targets of protein kinases such as PKA (Hell *et al.*, 1995; Jonas & Kaczmarek, 1996; Johnson *et al.*, 1997; Anderson *et al.*, 2000; Vargas & Lucero, 2002; Hoshi *et al.*, 2003; Vogalis *et al.*, 2003; Vijayaragavan *et al.*, 2004). Channel phosphorylation can lead to many changes in current characteristics, including altered current density and voltage-dependence, similar to those observed in developing muscle fibers. Numerous studies have shown that kinases like PKA and PKC modulate K_V currents, and A-type currents in particular, but never in muscle (Hoffman & Johnston, 1998; Yao & Wu, 2001; Yuan *et al.*, 2002; Hu & Gereau, 2003; Kim *et al.*, 2005; Liao *et al.*, 2005; Hu *et al.*, 2008; Liu *et al.*, 2008). Skeletal muscle fibers are known to express PKA and PKC (Chahine *et al.*, 1993; Xu & Salpeter, 1995; Hoover *et al.*, 2001; Patten *et al.*, 2007), and it is likely that they modulate

muscle ion channels, but little is known about the functional consequences of this modulation in muscle. In this study, the ability of PKA to modulate A-type K_V currents in white muscle was investigated at several developmentally relevant ages. These experiments focused on the A-type currents in white muscle, rather than the non-inactivating K_V currents in red muscle, due to their robustness, well-characterized properties, and the opportunity to better evaluate the physiological outcome of any modulation in the form of action potentials. The effect of PKC activation on A-type currents was also investigated, however the results were somewhat inconsistent; future work will aim to resolve these issues (APPENDIX 1). In addition, a study of modulation of Na_V currents by kinases was aborted early on due to large and inconsistent fluctuations in current amplitude over time under control conditions (APPENDIX 1).

Thus, with regard to PKA modulation of A-type K_V currents in white skeletal muscle, the following hypotheses were tested: 1) skeletal A-type K_V channels are regulated by PKA; 2) this regulation affects the ability of white muscle fibers to fire action potentials; and 3) PKA modulates A-type currents differentially during development.

Figure 1.1 Simplified diagrams of Na_V and K_V channel α subunit topologies. The Na_V α subunit has four homologous domains, each containing six hydrophobic α-helix transmembrane segments (S1 – S6). The fourth transmembrane segment (+++) of each domain acts as the voltage-sensor with a positively charged amino acid at every third position. The S5 – S6 linker forms part of the pore and it also contains the sequence of amino acids necessary to confer Na^+ ion selectivity. The intracellular loop between domains III and IV serves as the inactivation gate (black circle), acting as a blocking particle by binding to a site at the intracellular mouth of the pore. Functional K_V channels are composed of a tetramer of α subunits, each subunit being structurally and functionally similar to a single domain of a Na_v channel. Together, the four α subunits assemble to form a structure similar to a single Na_V channel α subunit. Each of the four K_V channel α subunits possesses an S4 voltage-sensor and an S5-S6 pore-forming and selectivity filter region, similar to the four domains of the Na_V α subunit. Some of the K_V channels that are able to inactivate use their α subunit N-termini as inactivation particles.

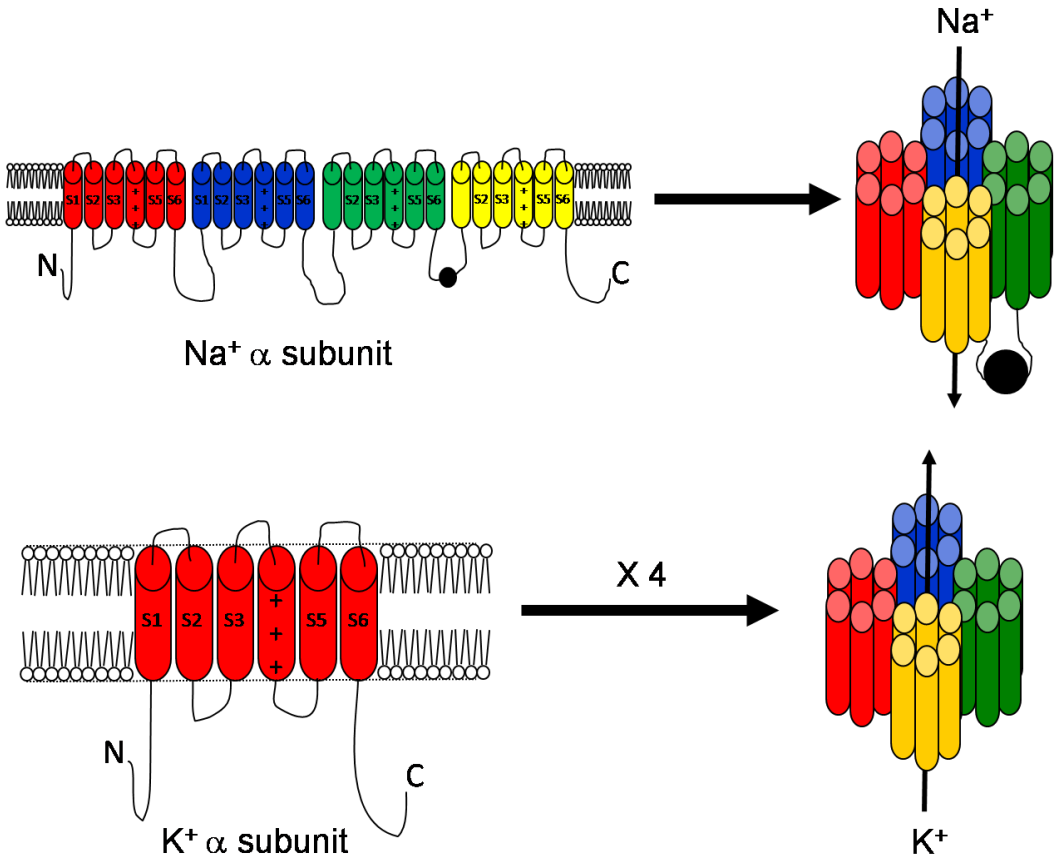
Na+
S1
S2
S3
S5
S6
S7
N
C
Na+ α subunit
X 4
K+
K+ α subunit

Figure 1.2 Pictures of zebrafish embryos and larva. At 1 dpf, embryos exhibit some residual coiling contractions, and begin to respond to touch stimuli. 2 dpf embryos no longer contract spontaneously, but respond vigorously to touch stimuli. Embryos begin hatching out of the chorion and becoming larvae at around 2 dpf, and are normally finished by 3 dpf. At 6 dpf, larvae exhibit robust escape responses and beat-and-glide swimming. Note: the 1 and 2 dpf embryos have been dechorionated for illustrative purposes. Scale bar = ~100 μm.

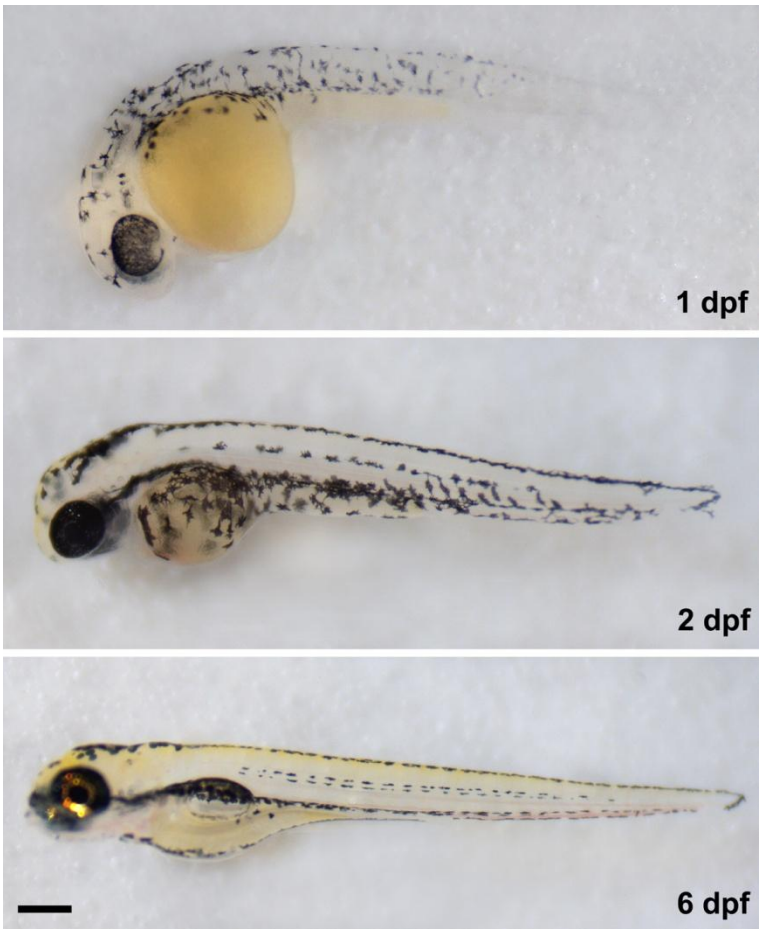
1 dpf
2 dpf
6 dpf

Figure 1.3 Muscle anatomy of the developing zebrafish. **(A)** Schematic transverse section of the caudal trunk is shown as it appears in the segmental plate prior to somite formation (15 hpf). Adaxial cells (red) in the segmental plate, elongate shortly after somite formation. The lateral presomitic cells, which will later differentiate into white fibers, are shown in white. **(B)** Adaxial cells have finished their radial migration away from the notochord to become a layer of superficial red muscle fibers (36 hpf). The lateral presomitic cells do not migrate, but differentiate into white muscle cells remaining deep in the myotome. **(C)** Schematic drawing of the same myotome in the adult zebrafish. Red muscle fibers migrate further toward the midline and form a band running the length of the body axis, just dorsal and ventral to the midline. In these schematic transverse sections, dorsal is up. ‘nc’ = notochord, ‘sc’ = spinal chord.

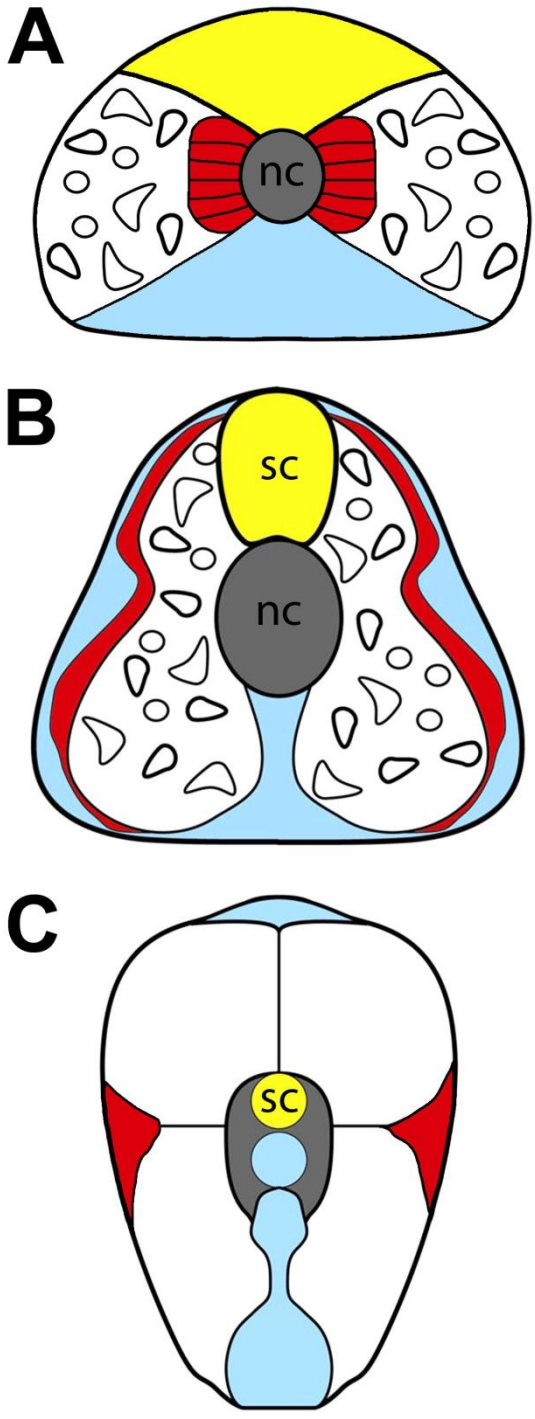
A
nc
B
sc
nc
C
sc

2. MATERIALS AND METHODS

2.1 Animals

Wild-type (WT) zebrafish were obtained from a breeding facility (Carolina Biological Supply Co., Burlington, NC) or were bred from the Oregon AB line. Embryos of the *sofa potato* (tj19d) strain were kindly provided by Dr. Hans Georg Frohnhofer from the Tubingen Zebrafish Stockcenter, at the Max-Planck Institute for Developmental Biology, Germany. The mutation was studied in homozygous offspring ($sop^{-/-}$) that were obtained by crossing heterozygous ($sop^{+/?}$) adults. Embryos and larvae were reared at 28.5 °C, and all experimental procedures were performed at room temperature (20-23 °C). All zebrafish were maintained according to established procedures (Westerfield, 1995) and all procedures were carried out in compliance with the guidelines stipulated by the Canadian Council for Animal Care and the University of Alberta.

2.2 Dissection

Zebrafish embryos and larvae of ages ranging from 1-6 dpf were anaesthetized in a solution of 0.02% tricaine (MS-222; Sigma Chemical, St. Louis, MO) dissolved in extracellular physiological saline (Table 2.1) before and during dissection. Larvae were pinned through the notochord, decapitated, and skin overlaying axial skeletal muscle was removed with a pair of fine forceps (Dumont #5). Red and white muscle fibers were identified and clearly distinguishable under Nomarski Differential

Interference Contrast (DIC) optics based on anatomical position and orientation (Buckingham & Ali, 2004). The outer layer of red muscle fibers are oriented parallel to the notochord, whereas the inner white muscle fibers are approximately 30-40° to the midline (Figure 2.1). Muscle fibers from musculature dorsal and ventral to the midline were similar and subsequently pooled.

2.3 Solutions and drugs

Electrophysiological solutions were prepared as in Tables 2.1 and 2.2. The pH of all extracellular solutions was adjusted to 7.8 with NaOH or KOH, while the pH of all intracellular solutions was adjusted to 7.4 with CsOH or KOH. The final osmolarity of all solutions was adjusted to 290±2 mOsm. D-tubocurarine (10-15 μM) was added to all extracellular solutions to block nAChR activity, except when recording mEPCs. All solutions and drugs were bath-applied via gravity flow at a rate of 1-2 mL/min. Chemicals and drugs were obtained from Sigma-Aldrich (St. Louis, MO, USA) unless otherwise indicated.

2.3.1 Voltage-clamp experiments

During all voltage-gated recordings, the gap-junction blocker carbenoxolone (100 μM) was added to the extracellular saline in order to reduce electrical coupling between cells. Carbenoxolone is a close

chemical derivative of 18 β-glycyrrhetinic acid, and both compounds have been used to block gap junctions (Personius *et al.*, 2001; Luna *et al.*, 2004). A period of 5 minutes was allowed for gap-junction blockers to take effect, and currents were recorded in the following 25 minutes, after which the preparations were discarded. This ensured that all preparations were incubated in the blockers for a maximum of 30 minutes. Over this short period of time, the gap-junction blockers had no detrimental effects on isolated currents; the data were compared with results obtained from a few recordings of electrically-isolated cells in older aged animals, in which electrical coupling was limited and no gap-junction blockers were needed (Buss & Drapeau, 2000; Luna *et al.*, 2004). There was no difference in the peak current density and steady state characteristics of uncoupled fibers of the same age, recorded in the presence or absence of carbenoxolone.

2.3.2 Recording miniature endplate currents

Tetrodotoxin (TTX; Tocris Bioscience, Bristol, UK) was added to the extracellular solution (1 μM) for mEPC recordings in order to prevent evoked synaptic events, but allow for the occurrence of spontaneous synaptic events.

2.3.3 Activation and inhibition of PKA

Forskolin (Fsk; *Coleus forskohlii*) and N-[2-[[3-(4-Bromophenyl)-2-propenyl]amino]ethyl]-5-isoqu inolinesulfonamide dihydrochloride (H-89) were purchased from Calbiochem (San Diego, CA). Forskolin (25 μM), H-89 (10 μM) and 3-Isobutyl-1-methylxanthine (IBMX; 500 μM) were prepared in dimethyl sulfoxide (DMSO), aliquoted, and stored at -20°C. The final concentration of DMSO in the bathing saline did not exceed 0.3%; thus all DMSO controls were performed using 0.3% DMSO in K^+-isolating saline. 4-Aminopyridine (4-AP; 5 mM) was applied to block A-type K_V currents completely.

2.4 Electrophysiological recordings

Patch-clamp electrodes were prepared from borosilicate glass and fire-polished to resistances of 1-2 MΩ. Signals were amplified using an Axopatch 200B amplifier (Axon Instruments) and displayed using pClamp 8.02 software (Axon Instruments). Series resistance (R_s) was compensated by at least 80-90% using the amplifier's compensation circuitry, and experiments were aborted if R_s changed by more than 15%. Cell capacitance was measured by the amplifier's circuitry. Capacitative and leak currents were subtracted online using a P/4 protocol provided with the pClamp software.

2.4.1 Voltage-clamp experiments

Na_V and K_V currents were sampled using a Digidata 1322A (Axon Instruments) at 400 and 100 kHz, respectively, and were low-pass filtered at 10 kHz. Adequate space-clamping was confirmed by ensuring that there were never any uncontrolled regenerative inward currents (Eliasof *et al.*, 1987), that the peak of the Na_V currents all occurred within 500 μs of the onset of depolarization (Sontheimer *et al.*, 1992), and that tail currents were superimposable when normalized. In addition, currents recorded from very small patches of membrane (in the cell-attached patch-clamp configuration) had virtually identical kinetic properties compared to whole-cell currents (APPENDIX 2).

2.4.2 Current-clamp experiments

For current clamp experiments, muscle fibers were held at -70 mV and positive current was injected (for 1 ms or 12 ms, depending on the experiment) to bring the cell to threshold. It was usually necessary to inject 0.6-2.0 nA of current to induce cells to fire action potentials. In paired pulse (action potential recovery) experiments, the initial stimulus was followed by a second stimulus of equal amplitude, at intervals beginning at 40 ms and decreasing to 8 ms, in 2 ms increments. For high frequency experiments, fibers were stimulated with 20 x 1 ms pulses over a 500 ms time period (40 Hz). This stimulation paradigm was chosen

because it approximated bouts of fictive swimming (Buss & Drapeau, 2002).

2.4.3 mEPCs

mEPCs were recorded from white skeletal muscle fibers in whole-cell patch-clamp mode with the membrane potential clamped at -60 mV. Recordings were performed with an Axopatch 200B and mEPCs were captured with pClamp 8.1 software. Data were sampled at 50 KHz and low-pass filtered at 10 kHz.

2.5 Electrophysiological analysis

Voltage- and current-clamp whole-cell recordings were analyzed using Clamp-fit (pClamp 8.02; Axon Instruments) and miniature endplate recordings were analyzed using Axograph X software (Axograph). All plots were created using SigmaPlot 10.0 (Systat). Liquid junction potentials of 4.3 and 6.7 mV were calculated for Na^+- and K^+-isolating solutions, respectively, and were corrected for in all plots.

2.5.1 Voltage-clamp protocols: K_V currents

Outward K_V currents were evoked using stepwise depolarizations from -60 mV to 30 mV in 10 mV increments from a holding potential of -90

mV. Division of peak current amplitude by cell capacitance gives an estimation of peak current density, thereby normalizing current amplitude to cell size. Current-voltage (IV) plots were generated by plotting the peak current density evoked by each voltage step.

The steady-state activation properties of A-type K_V currents were determined from isochronal, isopotential tail currents as described previously (Buckingham & Ali, 2004). K_V currents were evoked using a series of voltage steps from a holding potential of -90 mV to a range of potentials from -40 to 40 mV in 10 mV increments (Figure 2.2A). This pre-conditioning series of voltage steps served to activate channels long enough to reach peak current amplitude, and were then followed by an isopotential step to -30 mV to evoke tail currents (Figure 2.2A). The use of an isopotential step allows the influence of driving force (defined as the difference between membrane potential and the Nernst potential of the ion) on current amplitude to be removed, thereby allowing current amplitude to represent the relative conductance (G) of the membrane at a given potential. Thus, when the amplitudes of the tail currents were normalized (maximum = 1, minimum = 0) and plotted against the amplitude of the activating voltage step, they yielded a sigmoid curve. These curves were fitted with Boltzmann functions:

$$A = 1 / (1 + e^{[(V - V_{50}) / b]})$$

Where *A* is the activation variable, *V* is the potential of the depolarizing step, V_{50} is the potential of half activation and *b* is the Boltzmann slope factor.

A-type current steady-state inactivation properties were also determined from isochronal, isopotential tail currents. A series of pre-conditioning voltage steps from a holding potential of -90 mV to a range of potentials from -60 to 10 mV in 10 mV increments was followed by an isopotential step to 0 mV (Figure 2.2B). Here, the pre-conditioning series of voltage steps was of sufficient duration to both activate and then allow channels to inactivate. Tail currents were then evoked by the isopotential step, and represent relative conductance (Figure 2.2B). Sigmoid curves of normalized conductance were fitted with Boltzmann functions.

2.5.2 Voltage-clamp protocols: Na_V currents

Outward Na_V currents were evoked using stepwise depolarizations from -80 mV to 70 mV in 10 mV increments from a holding potential of -90 mV. Current-voltage (IV) plots for Na_V currents were generated, as described above for K_V currents, by plotting the peak current density evoked by each voltage step.

Na_V current steady-state activation properties were determined by calculating the driving force (V_m - E_{Na}) for Na_V currents evoked by the

voltage protocol described above. Membrane conductance (*G*) for Na^+ was then estimated by dividing the peak current (*I*) by the driving force:

$$G = I / (V_m - E_{Na})$$

Plotting normalized membrane conductance against the amplitude of the depolarizing pulse yielded a sigmoid curve that was normalized and fitted with a Boltzmann function.

Steady state inactivation properties of Na_V currents were determined in the same manner as for K_V currents.

2.6 α-Bungarotoxin labelling

Homozygous *sop*$^{-/-}$ mutants were identified prior to dissection by their immobility and lack of response to tactile stimulation. *Sop*$^{-/-}$ larvae were then dissected as described above and bathed for 30 minutes in 1 μM Alexa Fluor 488-conjugated α-bungarotoxin, a potent and irreversible nAChR antagonist. The preparation was continuously washed in extracellular recording solution at room temperature for 2-3 hrs to remove the unbound antagonist and to reduce non-specific binding. Preparations were imaged on a Leica DM LFSA upright microscope equipped with epi-fluorescence and controlled by OpenLab 8 software (Improvision).

2.7 Activation and inhibition of PKA

During experiments where drugs were bath-applied, the initial (control) recording was performed exactly two minutes after establishment of the whole-cell mode to allow for stabilization of the current. This initial recording is referred to as the t=0 minutes recording. Forskolin and IBMX were then bath applied to the preparation for 5 minutes, at which time a second recording was performed, which is referred to as the t=5 minutes recording. The PKA inhibitor H-89 was bath applied 5-7 minutes prior to the initial recording. Time controls and 0.3% DMSO controls were performed to determine if channel properties were changing either as a function of time or due to the presence of DMSO in the bathing solution.

During experiments where drugs were included in the pipette-filling (intracellular) solution, it was not possible to obtain an initial (control) recording in the absence of drug. Thus, only one recording was obtained, at 2 minutes following the establishment of the whole-cell mode.

2.8 Statistics

All data values are given as mean±SEM (standard error of mean). Statistical significance was assessed using the Student's paired and unpaired *t*-tests and one-way ANOVA followed by an all pairwise multiple comparison procedure (Fisher LSD method) on normally distributed, equal variance data sets. Systat software was used for all statistical analysis.

Significance was assigned when *P* values were <0.05. In chapter 3.1, ‘a’, ‘b’, and ‘c’ indicate that age groups differ significantly from 1, 2, and 3 dpf, respectively. Within chapter 3.2, ‘d’ indicates values that are significantly different between *sop*$^{-/-}$ mutants and corresponding ages in *sop*$^{+/?}$ siblings. Within *sop*$^{+/?}$ and *sop*$^{-/-}$ groups, ‘e’ indicates values that are significantly different from 1 dpf and ‘f’ indicates values that are significantly different from 3 dpf. In chapter 3.3, * denotes significance from the control group at $p<0.05$, ** denotes significance at $p<0.01$ and *** denotes significance at $p<0.001$.

Figure 2.1 Patch-clamping from identified red and white skeletal muscle fibers in zebrafish embryos and larvae. Immobilized and anesthetised fish had skin overlaying axial skeletal muscle removed with a pair of fine forceps. Red arrows indicate the edges of red fibers on either side of a space where several red fibers have been teased away with a spent recording electrode. White arrow heads indicate the edge of a white fiber in the cleared space. Fiber types can be identified based on anatomical position and orientation; the outer layer of red muscle fibers are oriented parallel to the midline, whereas the inner white muscle fibers are approximately 30-40° to the midline. Note the presence of the patch pipette positioned above a white fiber.

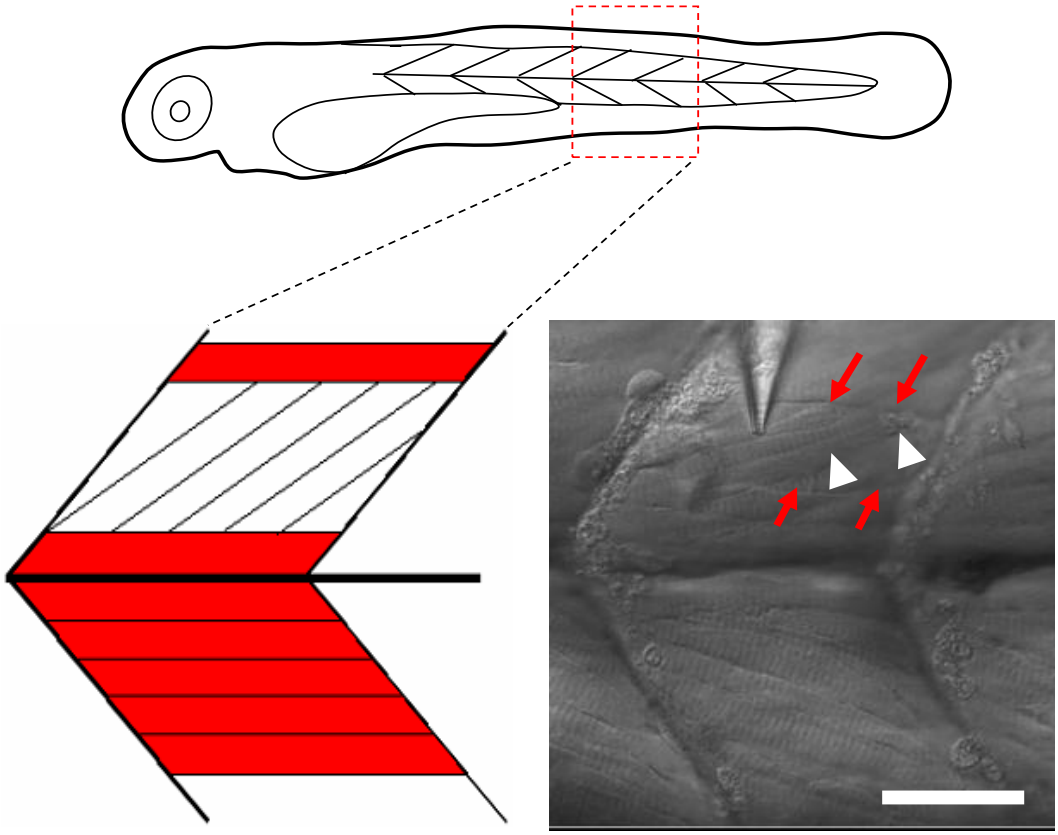

Figure 2.2 Voltage protocols used to examine the steady-state properties of activation and inactivation of A-type K_V currents. **(A)** Steady-state activation was determined from isochronal, isopotential tail currents. K_V currents were evoked using a series of voltage steps from a holding potential of -90 mV to a range of potentials from -40 to +40 mV in 10 mV increments. This pre-conditioning series of voltage steps served to activate channels long enough to reach peak current amplitude, and were then followed by an isopotential step to -30 mV to evoke tail currents. **(B)** A-type current steady-state inactivation properties were also determined from isochronal, isopotential tail currents. A series of pre-conditioning voltage steps from a holding potential of -90 mV to a range of potentials from -60 to 10 mV in 10 mV increments was followed by an isopotential step to 0 mV. Tail currents were measured approximately at the positions of the red lines. Scale bar = 25 μm.

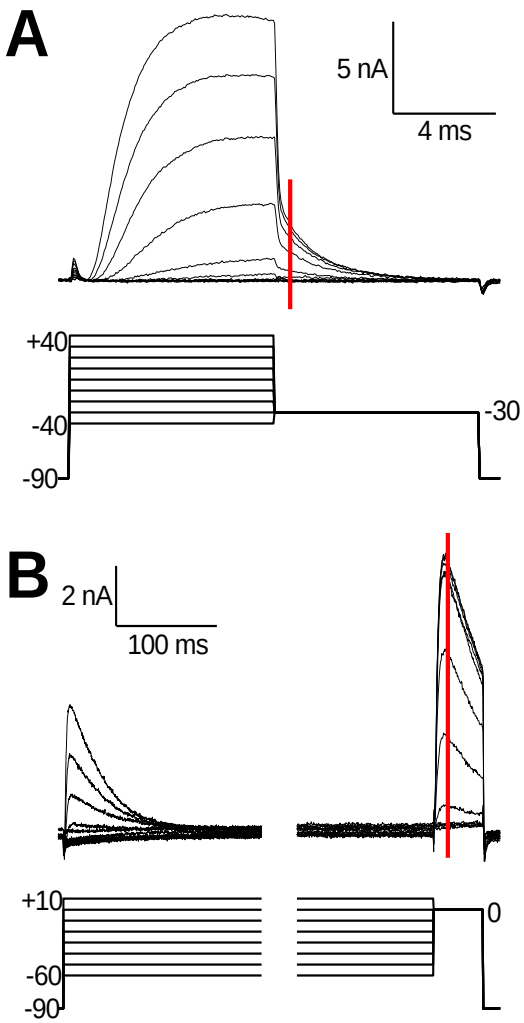
A
5 nA
4 ms
+40
-40
-90
-30
B
2 nA
100 ms
+10
-60
-90
0

Table 2.1 Extracellular solution composition

Solution	NaCl	KCl	ChoCl	CsCl	$CaCl_2$	$MgCl_2$	$CdCl_2$
Physiological	134	2.9	-	-	2.1	1.2	-
Na^+-isolating	130	-	-	2.9	-	10	0.7
K^+-isolating	-	2.9	130	-	-	10	0.7

All values are mM. All extracellular solutions contained 10 mM HEPES, 10 mM Glucose.

Table 2.2 Intracellular solution composition

Solution	NaCl	KCl	ChoCl	CsCl	$CaCl_2$	D-gluconic acid	EGTA	BAPTA
Physiological	8	6	-	-	-	140	10	-
Na^+-isolating	8	-	-	126	-	-	-	5
K^+-isolating	-	134	4	-	-	-	-	5
mEPCs	8	-	-	130	2	-	10	-

All values are mM. All intracellular solutions contained 10 mM HEPES, 4 mM MgATP, 0.4 mM LiGTP.

3. Development of Na_V and K_V currents in zebrafish red and white skeletal muscle fibers[1]

Na_V and K_V channels play key roles in the excitability of skeletal muscle fibers. The properties of skeletal muscle Na_V currents have been investigated in a number of organisms (Stanfield, 1972; Campbell & Hille, 1976; Adrian & Marshall, 1977; Duval & Leoty, 1978; Almers *et al.*, 1984; Lerche *et al.*, 1996; Ruff, 1996a, b; O'Leary, 1998). Skeletal muscle Na_V channels consist of an α subunit (260 kD or 285 kD for rat and rabbit respectively) and a β subunit (38 kD) (Casadei *et al.*, 1986; Roberts & Barchi, 1987), whereas neuronal Na_V channels consist of one α (260 kD) and two β subunits (β1, 36 kD and β2, 33 kD) (Catterall, 1992; Isom *et al.*, 1995; Goldin, 2001). Embryonic ($Na_V1.5$) and adult forms ($Na_V1.4$) of Na_V channels differ with respect to the extent of block by tetrodotoxin, and in their steady states of inactivation (Kallen *et al.*, 1990; Nuss *et al.*, 1995; Makielski, 1996). However, differences between the embryonic and adult Na_V currents may also arise from differences in the developmental expression of the β subunits (Sutkowski & Catterall, 1990; Wallner *et al.*, 1993; Patton *et al.*, 1994). To date there is very little information regarding the developmental properties of Na_V currents in fish. Moreover, the majority of previous studies on developing muscle, have been performed on dissociated fibers or cultured myocytes, whereas the zebrafish preparation offers the possibility of investigating the developmental

[1]A version of this chapter has been published. Coutts CA, Patten SA, Balt LN, Ali DW 2006. Journal of Neurobiology. 66(3):220-35.

profiles of these currents in muscle fibers *in situ*. Recently, an extensive study investigated the properties of Na_V currents in zebrafish spinal cord neurons (Pineda *et al.*, 2005), but there is virtually no information on the developing properties of Na_V currents in fish skeletal muscle. In addition, the specific differences between red and white fibers have not been investigated in developing preparations. Transcripts of Na_V channel cDNA have been isolated from the zebrafish central nervous system (Tsai *et al.*, 2001), but skeletal muscle transcripts remain elusive.

The major type of K_V channel associated with skeletal muscle fibers is an A-type inactivating outward current (Duval & Leoty, 1980a, b; Camacho *et al.*, 1996; Buckingham & Ali, 2004), while a delayed rectifier-like K_V current is associated with some slow-twitch muscle fibers (Duval & Leoty, 1980a, b; Buckingham & Ali, 2004). Because K_V channels are involved in setting the resting membrane potential and influencing the shape of the action potential, the timing of their appearance during development has been a focus of some investigations (Gurantz *et al.*, 1996; Meis & Deitmer, 1997; Bringmann *et al.*, 1999; Ribera, 1999; Bahrey & Moody, 2003; Falk *et al.*, 2003; Grande *et al.*, 2003; Hattori *et al.*, 2003), but virtually nothing is known about the changes that K_V currents might undergo in developing zebrafish. A number of studies have focused on the electrophysiological properties of developing K_V currents in neurons and muscle (Simoncini & Moody, 1991; Davis *et al.*, 1995; Gao & Ziskind-Conhaim, 1998; Currie & Moody, 1999; Gurantz *et al.*, 2000;

Spitzer *et al.*, 2000); however questions still remain regarding the developmental properties of the voltage-dependences of activation and inactivation.

In this study the steady-state and kinetic properties of voltage-gated Na_V and K_V currents of red and white skeletal muscle fibers in zebrafish ranging in age from 1-6 dpf were investigated. A number of characteristics of both Na_V and K_V currents were observed to change developmentally. Action potentials generated at the different ages reflected the changes in ionic current. These findings indicate that there are significant differences in the ionic current profiles between the red and white fibers and that a number of changes occur in the steady-state and kinetic properties of Na_V and K_V currents of developing zebrafish skeletal muscle fibers.

3.1 K_V current development

K_V currents were isolated by replacing all Na^+ ions with equimolar choline, calcium with cadmium, and including 5 mM BAPTA in the pipette to reduce muscle contractions. The identity of these currents was previously confirmed by pharmacological means (Buckingham & Ali, 2004). A series of depolarizing voltage steps from a holding potential of -90 mV to a range of potentials from -60 mV to 30 mV in 10 mV increments evoked outward currents that appeared at potentials more positive than approximately -10 mV in red fibers (Figures 3.1A and 3.2A) and that were

similar to delayed rectifier currents. There was an inactivating component of these outward currents that appeared at potentials more positive than approximately 10 mV. In white fibers, the outward currents appeared at approximately -20 mV (Figures 3.1B and 3.1C) and increased as the depolarizing potentials were made more positive. K_V current amplitudes for both red and white muscle fibers appeared to increase during development (Figure 3.1A&B). Current-voltage relationships of peak current density plotted against membrane potential revealed a sudden developmental increase in the peak current density in white but not red fibers between 1 and 2 dpf (Figure 3.2A&C). The difference between these two muscle fibers is striking; not only is the peak current density of the A-type current approximately 10-fold greater than the red, but there appears to be major developmental changes that occur between 1 and 2 dpf in the A-type current and not in the delayed rectifier.

In order to compare peak current densities between age groups, a membrane potential of 20 mV was chosen as one that would elicit well-defined, maximal currents regardless of the shift of voltage dependence of activation (see below). The peak current density of K_V currents in red fibers did not vary significantly in the first week of maturation (Figure 3.2B), although there was a trend towards larger values at 6 dpf. In contrast, the peak current density of white fibers increased nearly 4-fold between 1 dpf and 2 dpf animals, then remained relatively constant thereafter (Figure 3.2D).

The kinetics of K_V current activation and inactivation were then examined during development. The 10-90% rise time of red and white fibers decreased by 3- and 2-fold, respectively, after the first day of development (Figure 3.3A&B). When the A-type currents from white fibers were normalized for amplitude, it appeared that currents in 1 dpf embryos decayed at a slower rate than in older ages (Figure 3.1C). In order to determine the time constant of inactivation ($\tau_{inactivation}$), the decay phase of the current was fit with a single exponential function (Figure 3.3C). $\tau_{inactivation}$ was found to be 1.5 to 2 times longer at 1 dpf than at older ages (Figure 3.3D).

Having analyzed the current kinetics, the next step was to investigate steady-state activation and inactivation properties of the A-type K_V currents from white fibers (Figure 3.4A&B). There was a significant negative shift in the V_{50}s of both activation and inactivation between 3 dpf and 4-6 dpf age groups (Figure 3.4C&D, Table 3.3), indicating that the K_V currents in older animals are activated at less depolarized potentials. The slope factor did not appear to change during development (Figure 3.4E&F, Table 3.2).

3.2 Na_V current development

In order to isolate Na_V currents, extracellular potassium ions were replaced with cesium and calcium ions were replaced with cadmium. Na_V

currents were never evoked in red muscle fibers at any of the ages examined (Figure 3.5A). White muscle, in contrast, exhibited fast activating and inactivating inward currents that increased in amplitude during development (Figure 3.5B). These white muscle currents had previously been confirmed to be carried by Na^+ ions via TTX blockade (Buckingham and Ali, 2004). Currents were evoked by a series of depolarizing voltage steps from a holding potential of -90 mV to a range of potentials from -80 mV to 70 mV in 10 mV increments (Figure 3.5). When the peak current density was plotted against membrane potential, the inward Na_V currents of white fibers appeared at potentials more positive than -30 mV and reversed at approximately 50-60 mV (Figure 3.6A). The most obvious developmental change was a 2- to 3-fold increase in the peak current density of Na_V currents after 1 dpf, which was measured at the peak of the I-V relationship (0 mV; Figure 3.6B).

In terms of current kinetics, similarly to K_V currents, time constants of Na_V current inactivation were calculated by fitting the decay phase with single exponential functions (Figure 3.6C). $\tau_{inactivation}$ was significantly longer in 1 dpf animals, but only at more negative potentials (-30 mV; Figure 3.6D). Na_V current activation occurred so rapidly that signal interference from stimulus artifacts prevented accurate measurements of rise time.

Steady-state activation and inactivation properties were determined for Na_V currents at all ages (Figure 3.7A&B). There was significant

hyperpolarization in the V_{50}s of both activation and inactivation during development (Figure 3.7C&D, Table 3.3), but slope factors did not change (Figure 3.7E&F, Table 3.2).

The rate of recovery from inactivation was measured using a paired stimulus protocol (Figure 3.8A). A depolarization to -5 mV was applied for 4 ms to activate and then allow inactivation of the Na_V currents. The initial stimulus was followed by a recovery period (beginning at 9 ms, then decreasing to 0.5 ms) to allow partial recovery of the currents. A second stimulus of identical form to the first was then applied to determine the proportion of current recovery. A representative recording taken from a 3 dpf larvae is shown in Figure 3.8A. The potential of the interstimulus period was set at a value close to the resting membrane potential (-70 mV; Buss and Drapeau, 2000; Westerfield et al., 1986) in order to estimate the fractional recovery at or close to rest. The ratio of the amplitudes of currents evoked by the first and second test pulses was plotted against the duration of the recovery period (Figure 3.8B). The data were fit with single exponential functions (Figure 3.8B), from which half-times of recovery were calculated. The half-time of recovery from inactivation was not significantly different at any age, although the extent of recovery was greater in the 1 and 2 dpf ages compared with 3 and 4-6 dpf animals (Figure 3.8C).

3.3 Action potential development

Because several developmental changes were observed in the steady-state and kinetic properties of both Na_V and K_V currents, current-clamp recordings were obtained from muscle fibers at each age to determine whether the currents could affect properties of action potentials. Red fibers didn't exhibit evidence of action potentials at any age examined. Short (1 ms) and long (12 ms) depolarizing current steps were used to bring the fibers to threshold (Figure 3.9). The long (Figure 3.9A) stimuli were utilized in order to determine whether the cells were capable of firing multiple action potentials under conditions of prolonged depolarization; multiple action potentials were never evoked at any age (Figure 3.9A). The short stimulus served to excite the cells to threshold only, thereby allowing them to fire action potentials as physiologically as possible (Figure 3.9B). Measurements of action potential voltage threshold, amplitude and half-width were obtained from action potentials generated by the shorter, more physiological stimulus. Voltage threshold became more hyperpolarized in animals older than 1 dpf (Figure 3.10A). However, once an action potential occurred, its amplitude did not change significantly during development (Figure 3.10B). Lastly, the duration of the action potential, as indicated by measuring the half-width, decreased gradually and significantly as fibers matured (Figure 3.10C). Spontaneous action potentials were never observed during these experiments.

Figure 3.1 K_V currents recorded from red and white muscle fibers of developing zebrafish skeletal muscle. Stepwise depolarizations from a holding potential of -90 mV to a range of potentials from -60 to 30 mV in 10 mV increments give rise to outward currents when K^+-isolating solutions are used (see Table 2.1). **(A)** K_V currents in red muscle are largely non-inactivating throughout the duration of the stimulus, and increase markedly in amplitude between 1 dpf and 4-6 dpf. **(B)** White fibers exhibit A-type, fast-inactivating K_V currents that are greater in amplitude than red fiber currents. The A-type currents also increase in amplitude during development.

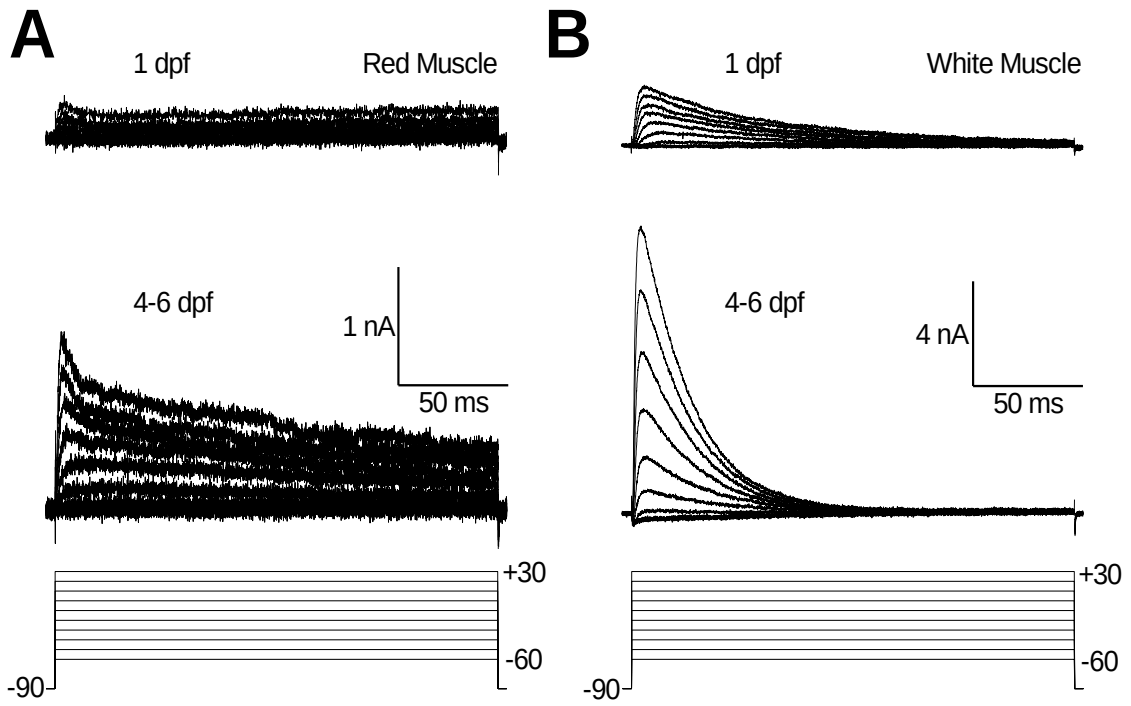
A
1 dpf
Red Muscle
4-6 dpf
1 nA
50 ms
+30
-60
-90
B
1 dpf
White Muscle
4-6 dpf
4 nA
50 ms
+30
-60
-90

Figure 3.2 Peak current density of K_V currents in red and white muscle fibers change during development. **(A)** Outward K_V currents in red muscle are evoked by voltages more positive than approximately -10 mV. **(B)** A comparison of peak current density between age groups at a potential of 20 mV revealed no significant developmental changes. **(C)** A-type currents in white muscle were evoked by voltages more positive than approximately -20 mV. **(D)** Quantification of peak current density at 20 mV indicates a significant increase in peak current density between 1 and 2 dpf. '**a**' **=** significantly different from 1 dpf. A liquid junction potential of 6.7 mV was accounted for in all plots.

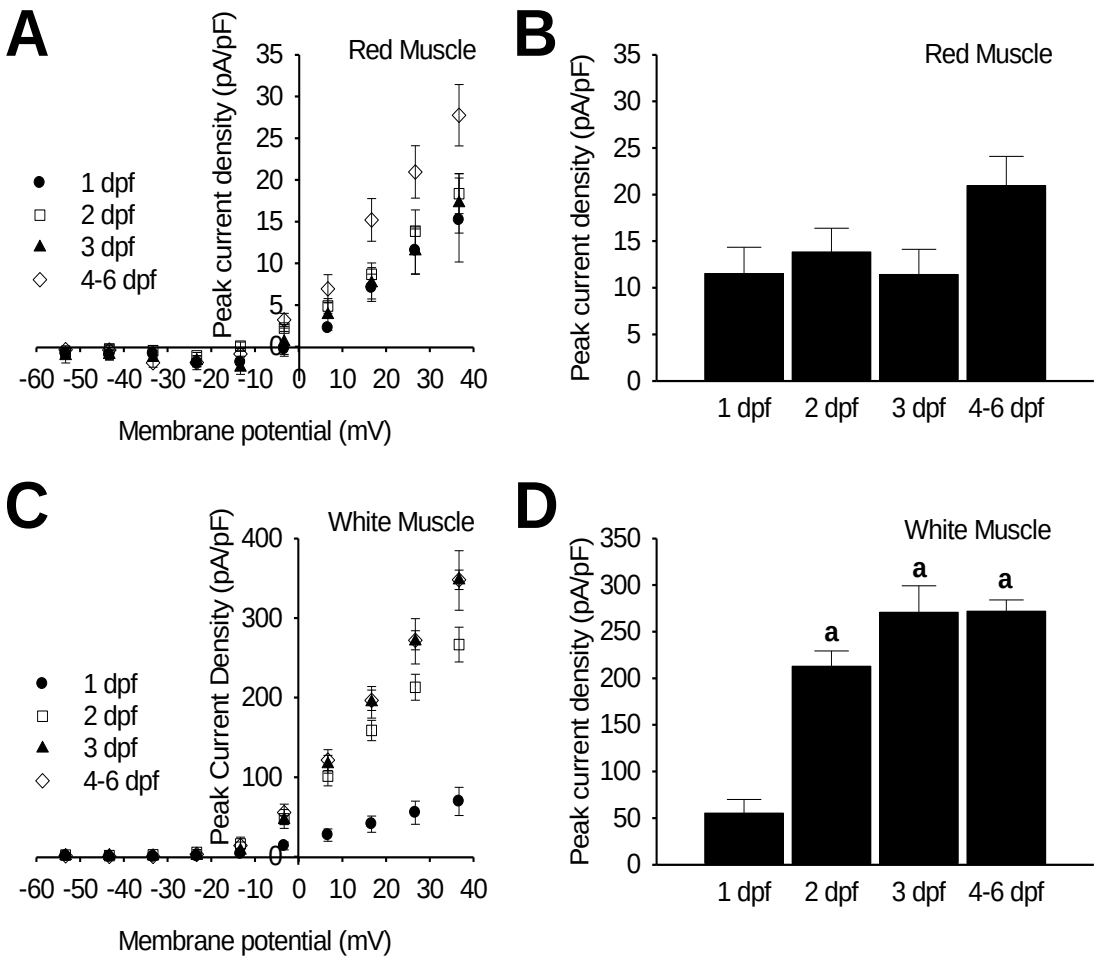
A
Red Muscle
Peak current density (pA/pF)
1 dpf
2 dpf
3 dpf
4-6 dpf
Membrane potential (mV)
B
Red Muscle
Peak current density (pA/pF)
1 dpf
2 dpf
3 dpf
4-6 dpf
C
White Muscle
Peak Current Density (pA/pF)
1 dpf
2 dpf
3 dpf
4-6 dpf
Membrane potential (mV)
D
White Muscle
Peak current density (pA/pF)
a
a
1 dpf
2 dpf
3 dpf
4-6 dpf

Figure 3.3 Kinetic properties of K_V currents in red and white skeletal muscle accelerate during development. **(A,B)** The duration of time taken for current to rise from 10-90% of its maximum amplitude decreased significantly after 1 dpf in both red and white muscle fibers. **(C)** A-type currents in white muscle evoked at 20 mV were normalized for amplitude and fit with single exponential functions, from which time constants of inactivation ($\tau_{inactivation}$) were calculated. **(D)** Currents from 1 dpf muscle fibers decayed significantly slower than those in older fibers. '**a**' = significantly different from 1 dpf, '**b**' = significantly different from 2 dpf.

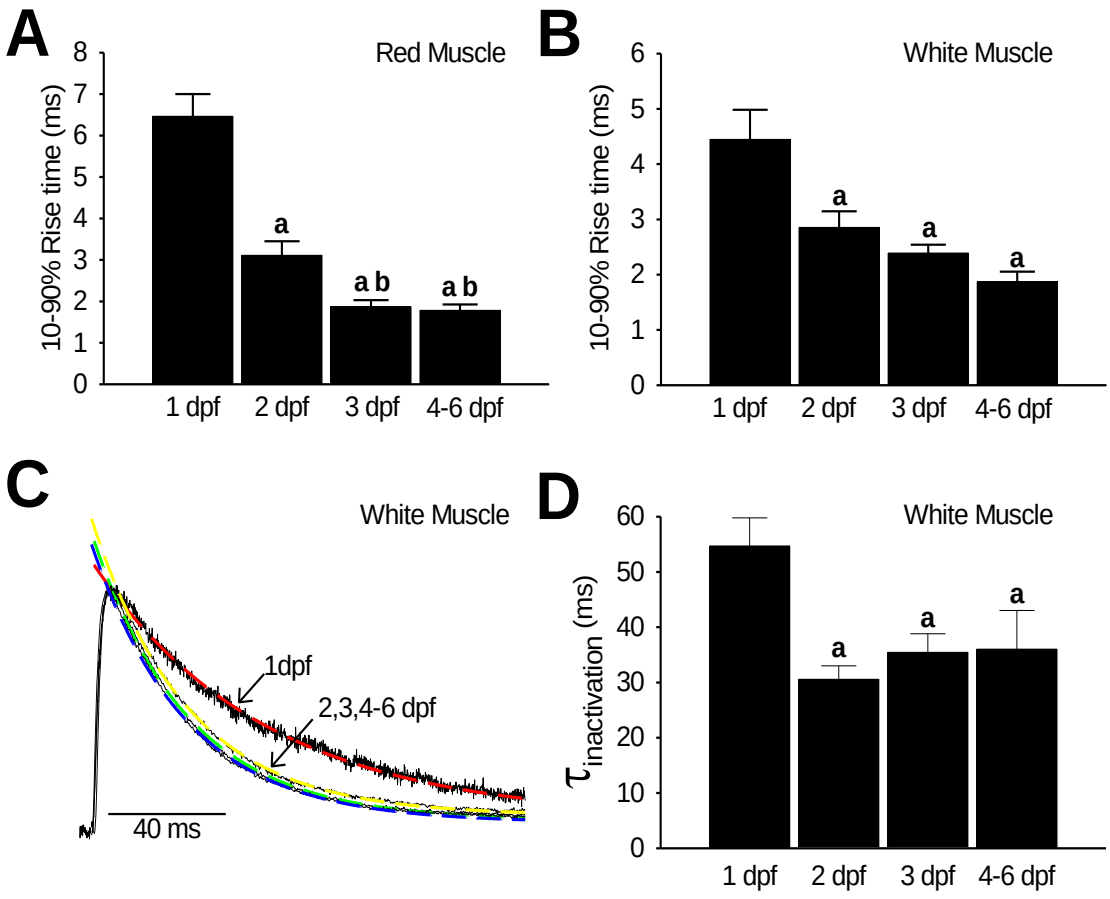
A
Red Muscle
10-90% Rise time (ms)
0
1
2
3
4
5
6
7
8
a
a b
a b
1 dpf
2 dpf
3 dpf
4-6 dpf
B
White Muscle
10-90% Rise time (ms)
0
1
2
3
4
5
6
a
a
a
1 dpf
2 dpf
3 dpf
4-6 dpf
C
White Muscle
1dpf
2,3,4-6 dpf
40 ms
D
White Muscle
τinactivation (ms)
0
10
20
30
40
50
60
a
a
a
1 dpf
2 dpf
3 dpf
4-6 dpf

Figure 3.4 Activation and inactivation V_{50}s and slope factors of A-type currents in white muscle become more hyperpolarized during development. **(A,B)** Steady-state activation and inactivation curves indicate that voltage-dependence undergoes a negative (hyperpolarizing) shift as animals increase in age. **(C,D)** Voltages of half-activation and inactivation obtained from the steady-state curves quantify the hyperpolarizing shifts in voltage-dependence. **(E,F)** Slope factors were similar at all ages. '**a**' = significantly different from 1 dpf, '**b**' = significantly different from 2 dpf, '**c**' = significantly different from 3 dpf. A liquid junction potential of 6.7 mV was accounted for in all plots.

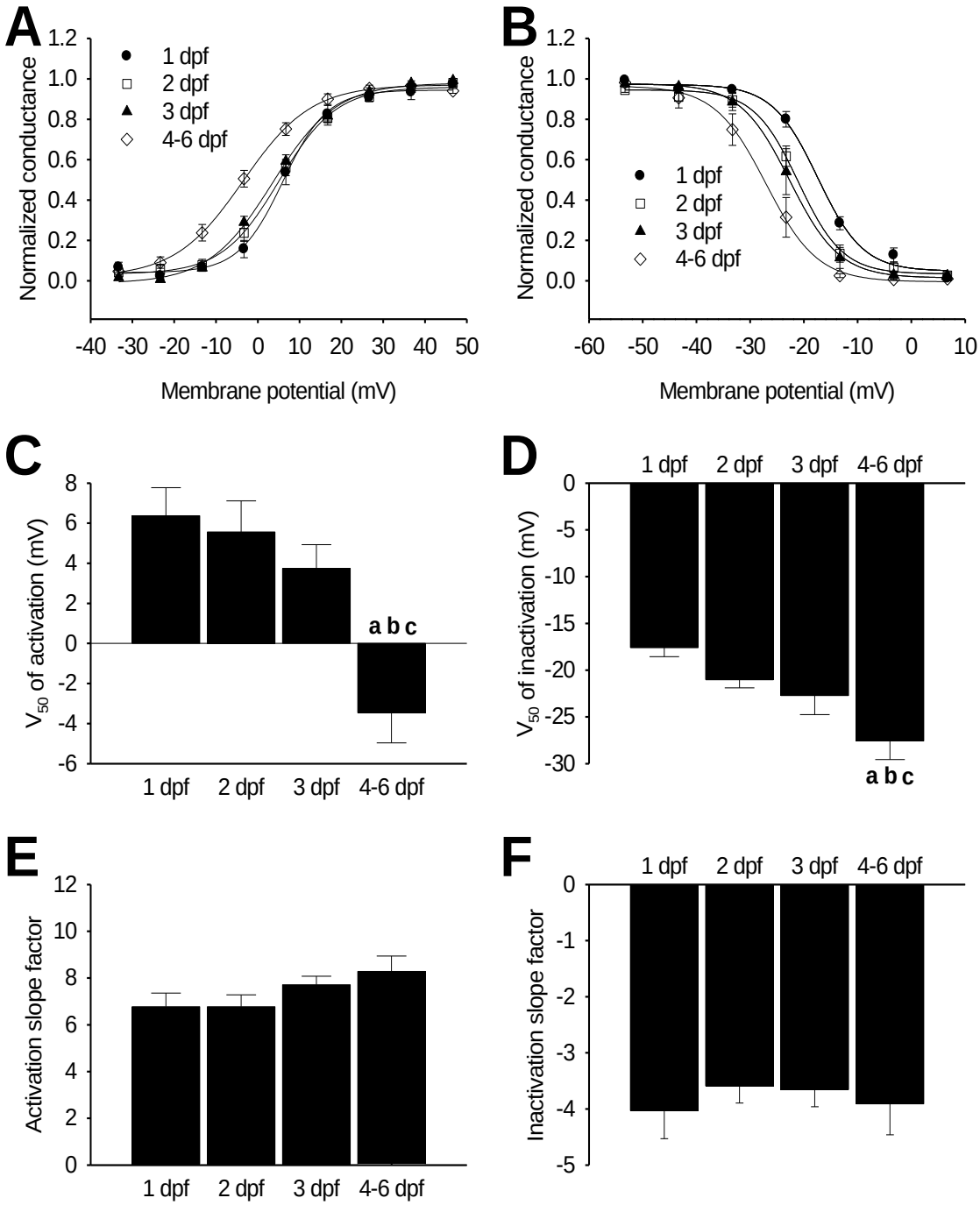
A
Normalized conductance
1.2
1.0
0.8
0.6
0.4
0.2
0.0
1 dpf
2 dpf
3 dpf
4-6 dpf
-40 -30 -20 -10 0 10 20 30 40 50
Membrane potential (mV)
B
Normalized conductance
1.2
1.0
0.8
0.6
0.4
0.2
0.0
1 dpf
2 dpf
3 dpf
4-6 dpf
-60 -50 -40 -30 -20 -10 0 10
Membrane potential (mV)
C
V50 of activation (mV)
8
6
4
2
0
-2
-4
-6
a b c
1 dpf 2 dpf 3 dpf 4-6 dpf
D
1 dpf 2 dpf 3 dpf 4-6 dpf
V50 of inactivation (mV)
0
-5
-10
-15
-20
-25
-30
a b c
E
Activation slope factor
12
10
8
6
4
2
0
1 dpf 2 dpf 3 dpf 4-6 dpf
F
1 dpf 2 dpf 3 dpf 4-6 dpf
Inactivation slope factor
0
-1
-2
-3
-4
-5

Figure 3.5 Na_V currents were exhibited by white muscle fibers, but not by red fibers, and increase in amplitude during development. **(A)** Stepwise, 5 ms depolarizations from a holding potential of -90mV to a range of potentials from -80 to 70 mV failed to evoke Na_V currents in red muscle at any age. **(B)** In contrast, white muscle exhibited rapidly activating and inactivating Na_V currents, which increased in amplitude during development.

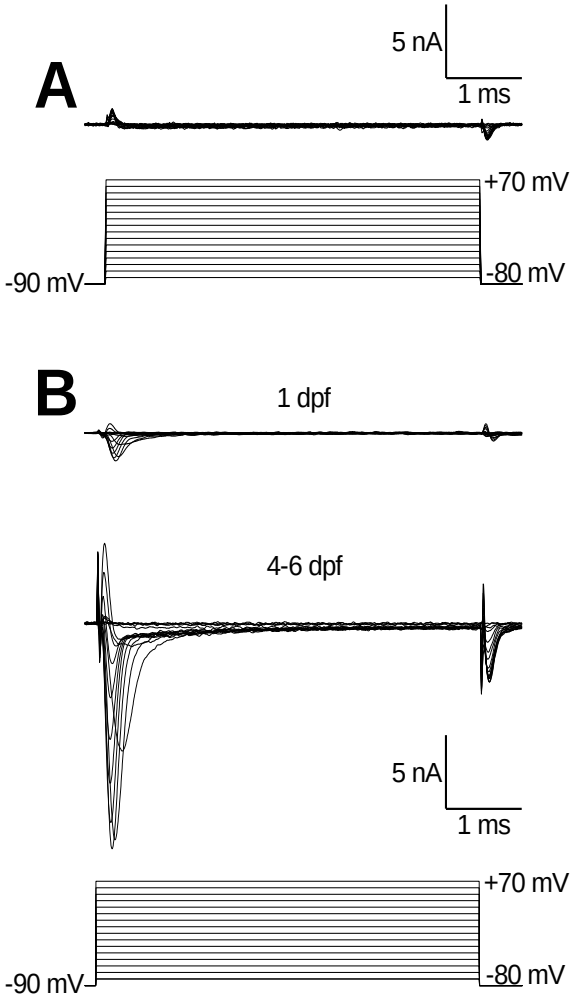
A
5 nA
1 ms
+70 mV
-90 mV
-80 mV
B
1 dpf
4-6 dpf
5 nA
1 ms
+70 mV
-90 mV
-80 mV

Figure 3.6 Peak current density and inactivation kinetics of Na_V currents change during development. **(A)** Current-voltage plots indicated that currents were evoked at potentials more positive than -40 mV, and reversed from inward to outward at approximately 50-60 mV. **(B)** Current density at the peak of the current-voltage relationship (~0 mV) was significantly smaller (less negative) at 1 dpf than in older animals. **(C)** The decay phases of Na_V currents from a variety of membrane potentials were fit with single exponential functions, from which time constants of inactivation ($\tau_{inactivation}$) were calculated. $\tau_{inactivation}$ appeared to be longer in younger animals at more negative potentials. **(D)** $\tau_{inactivation}$ at -30 mV was plotted for each age, showing that currents from 1 dpf muscle fibers decayed significantly slower than those in older fibers. '**a**' = significantly different from 1 dpf, '**b**' = significantly different from 2 dpf. A liquid junction potential of 4.3 mV was accounted for in all plots.

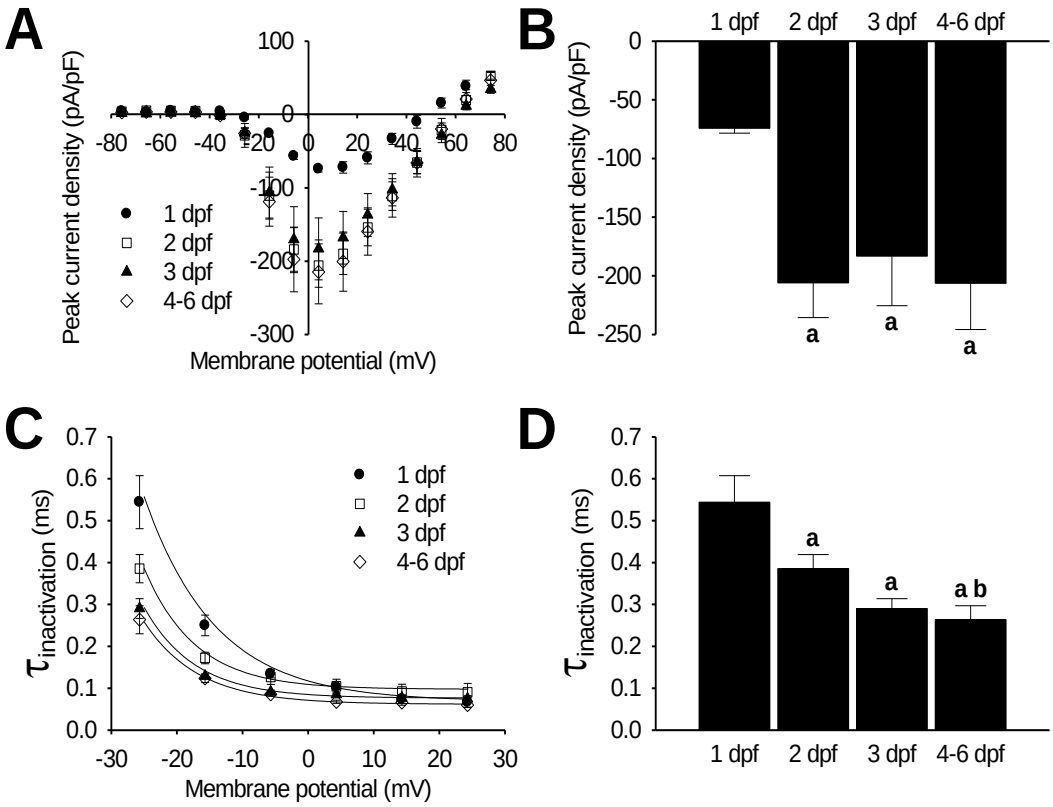
A
Peak current density (pA/pF)
Membrane potential (mV)
1 dpf
2 dpf
3 dpf
4-6 dpf
B
Peak current density (pA/pF)
1 dpf
2 dpf
3 dpf
4-6 dpf
a
a
a
C
τinactivation (ms)
Membrane potential (mV)
1 dpf
2 dpf
3 dpf
4-6 dpf
D
τinactivation (ms)
a
a
a b
1 dpf
2 dpf
3 dpf
4-6 dpf

Figure 3.7 Activation and inactivation V_{50}s and slope factors of Na_V currents become more hyperpolarized during development. **(A,B)** Steady-state activation and inactivation curves indicate that voltage-dependence undergoes a negative (hyperpolarizing) shift as animals increase in age. **(C,D)** V_{50}s of activation and inactivation obtained from the steady-state curves quantify the hyperpolarizing shifts in voltage-dependence. **(E,F)** Slope factors were similar at all ages. '**a**' = significantly different from 1 dpf, '**b**' = significantly different from 2 dpf. A liquid junction potential of 4.3 mV was accounted for in all plots.

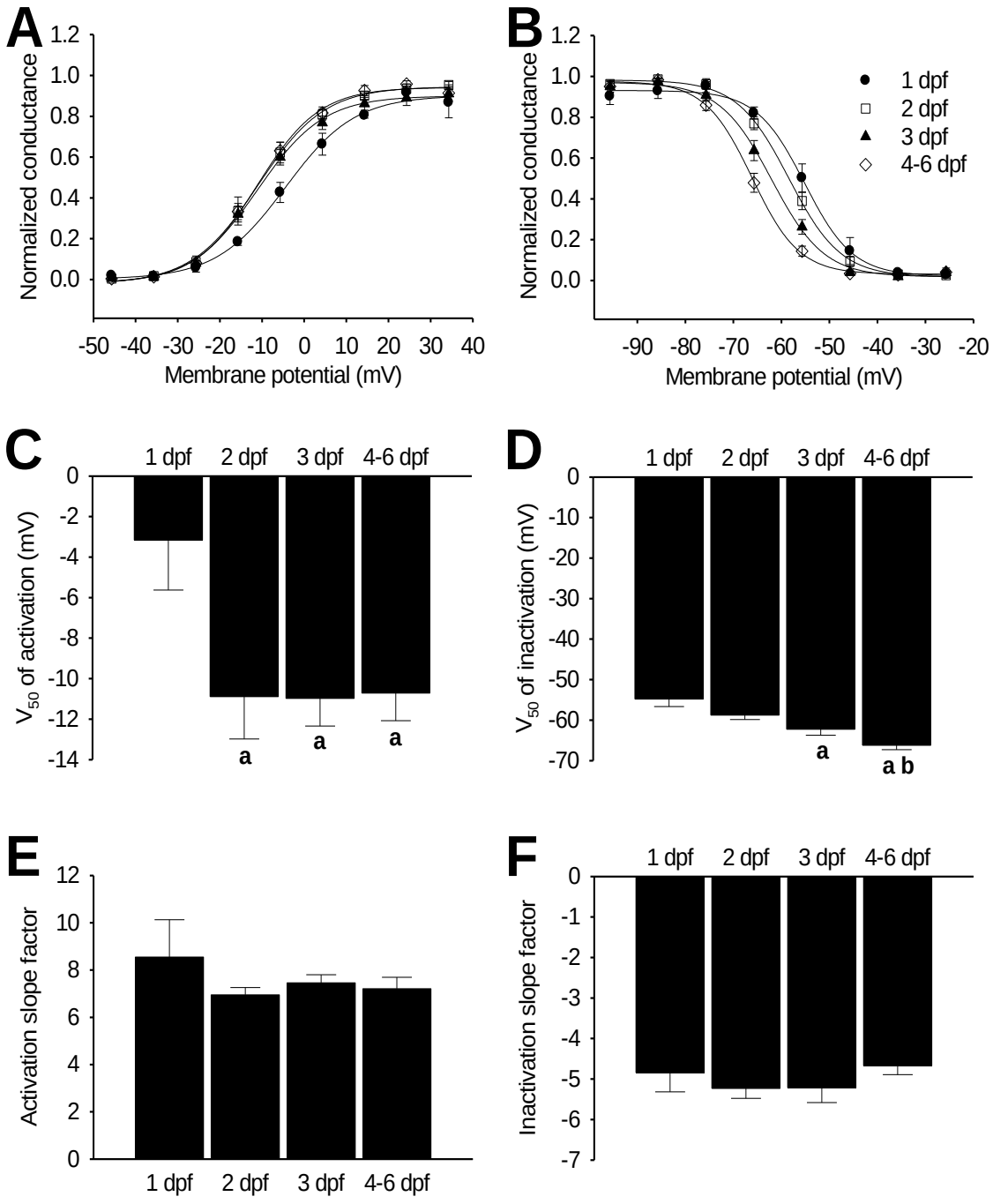
A
Normalized conductance
Membrane potential (mV)
B
1 dpf
2 dpf
3 dpf
4-6 dpf
C
V_{50} of activation (mV)
a
D
V_{50} of inactivation (mV)
a
a b
E
Activation slope factor
F
Inactivation slope factor

Figure 3.8 Na_V current inactivation recovery rate did not change during development. **(A)** Representative recording from a 3 dpf larva, illustrating that as the recovery period between stimuli was shortened, current amplitude evoked by the second stimulus decreased. **(B)** Fractional recovery was plotted against the duration of the recovery period. Na_V currents in 1 and 2 dpf fibers recovered to a greater extent than older fibers. **(C)** Half-times of recovery were calculated by fitting the fractional recovery over time (B) with single exponential functions. There were no developmental differences in half-times between age groups.

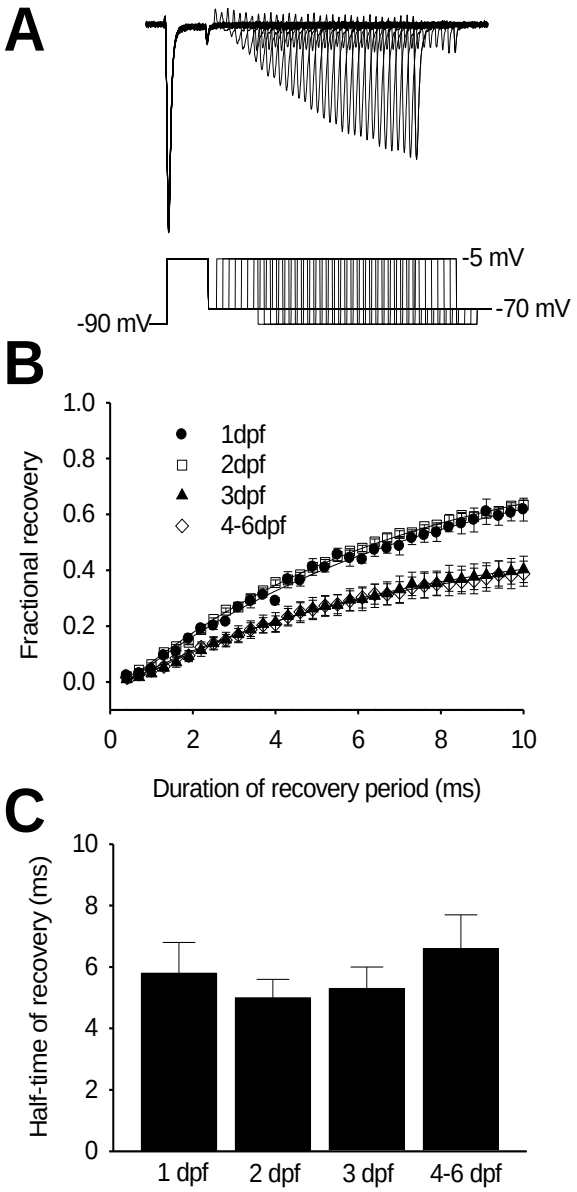
A
-5 mV
-70 mV
-90 mV
B
1dpf
2dpf
3dpf
4-6dpf
Fractional recovery
1.0
0.8
0.6
0.4
0.2
0.0
0
2
4
6
8
10
Duration of recovery period (ms)
C
Half-time of recovery (ms)
10
8
6
4
2
0
1 dpf
2 dpf
3 dpf
4-6 dpf

Figure 3.9 Development of action potentials recorded from white muscle fibers under current clamp conditions. Action potentials were evoked by depolarizing current stimuli of long (12 ms) and short (1 ms) durations from a holding potential of -70 mV. **(A)** Long stimuli evoked only single action potentials, regardless of stimulus amplitude. **(B)** Short stimuli are only sufficient in duration to bring cells to their threshold potential, allowing action potentials to progress without interference from injected current thereafter.

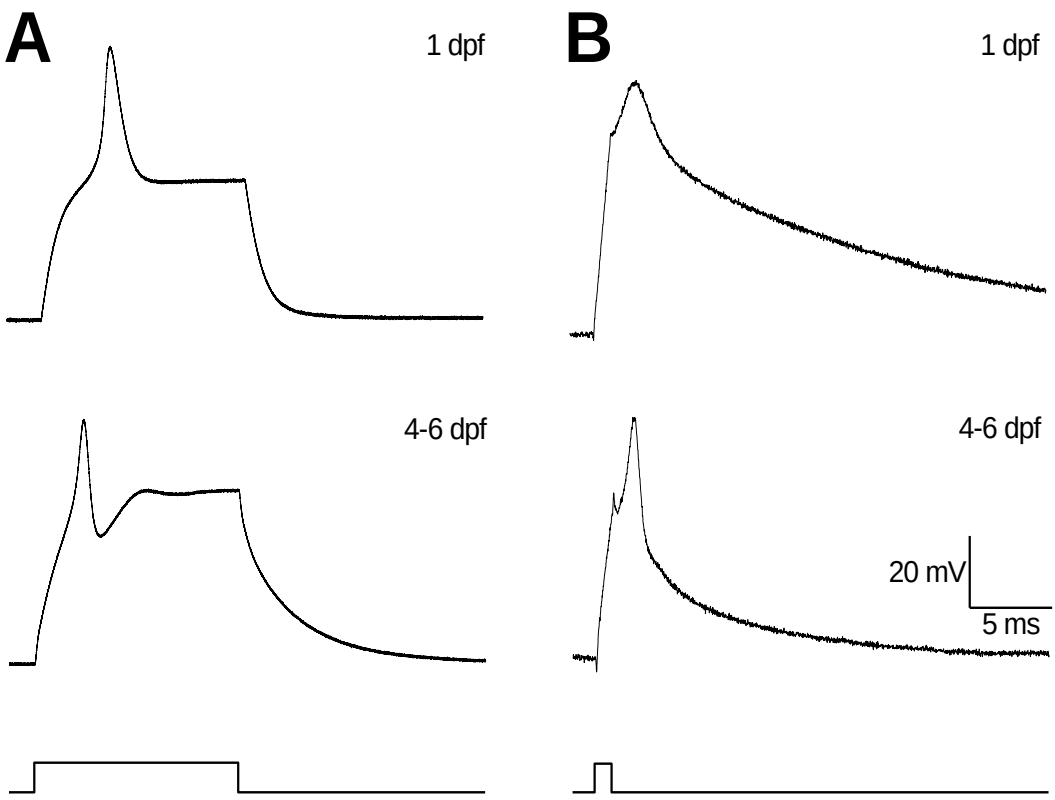
A
1 dpf
4-6 dpf
B
1 dpf
4-6 dpf
20 mV
5 ms

Figure 3.10 Action potentials evoked by short stimuli change during development. **(A)** The threshold potential required for action potential initiation became more hyperpolarized after 1 dpf. **(B)** Once evoked, action potential amplitudes were similar at all ages. **(C)** Action potential half-width, and therefore duration, was reduced significantly during development. ‘a’ = significantly different from 1 dpf.

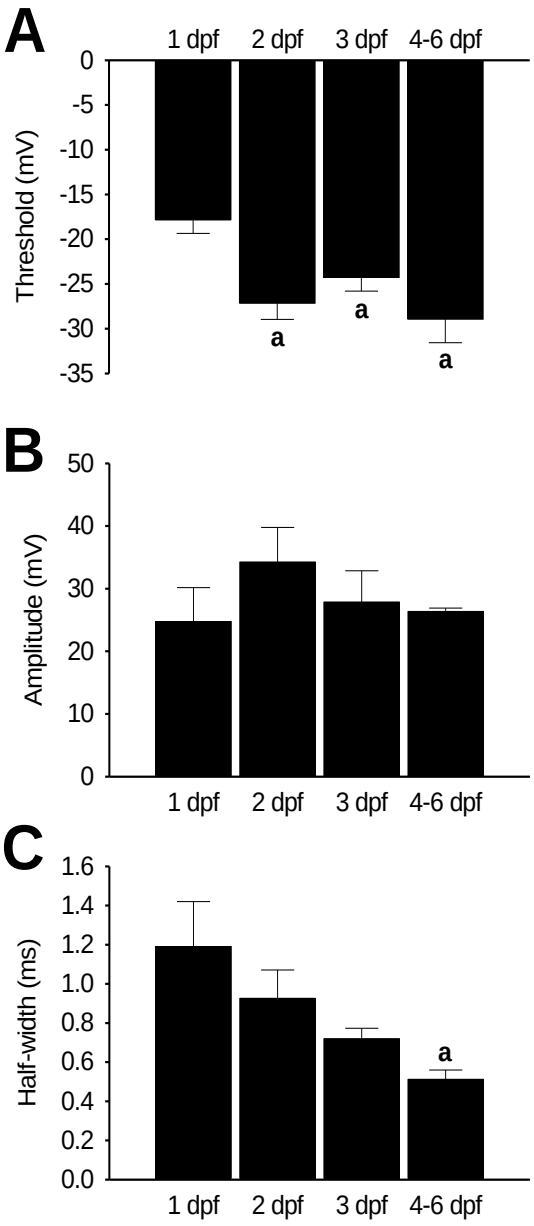
A
1 dpf
2 dpf
3 dpf
4-6 dpf
0
-5
-10
-15
-20
-25
-30
-35
Threshold (mV)
a
a
a
B
50
40
30
20
10
0
Amplitude (mV)
1 dpf
2 dpf
3 dpf
4-6 dpf
C
1.6
1.4
1.2
1.0
0.8
0.6
0.4
0.2
0.0
Half-width (ms)
a
1 dpf
2 dpf
3 dpf
4-6 dpf

Table 3.1 Values of red and white muscle fiber parameters during development

	Red Fibers			White Fibers		
	R_s (MΩ)	**R_m (MΩ)**	**C_m (pF)**	**R_s (MΩ)**	**R_m (MΩ)**	**C_m (pF)**
Na^+-isolating Saline						
1 dpf	-	-	-	3.8±0.7 (4)	292±103	18.8±1.8
2 dpf	-	-	-	3.2±0.3 (9)	225±76	40.9±5.0
3 dpf	-	-	-	3.4±0.2 (9)	303±28	38.8±4.8
4-6 dpf	-	-	-	3.6±0.7 (10)	248±36	44.8±5.3
K^+-isolating Saline						
1 dpf	5.4±0.9 (5)	660±201	12.8±0.8	5.2±0.6 (8)	249±84	18.2±1.8
2 dpf	4.4±0.7 (7)	350±134	24.1±0.7	4.1±0.5 (9)	396±130	30.7±3.6
3 dpf	3.9±0.7 (6)	345±101	28.3±1.2	3.3±0.3 (8)	149±107	65.6±7.3
4-6 dpf	3.2±0.2 (6)	324±75	33.2±1.1	2.5±0.2 (10)	117±15	77.1±3.0

R_s is series resistance, R_m is membrane resistance, C_m is membrane capacitance and dpf is days post fertilization. Values are means ± S.E.M. (n).

Table 3.2 Activation and inactivation slope factors of K_V and Na_V currents in developing white fibers

Age (dpf)	Activation Slope factor		Inactivation Slope factor	
	K_V	Na_V	K_V	Na_V
1	6.8±0.6 (5)	8.6±1.6 (4)	-4.0 ±0.5 (4)	-4.8±0.5 (4)
2	6.8±0.5 (7)	7.0±0.3 (7)	-3.6±0.3 (5)	-5.2±0.2 (9)
3	7.7±0.4 (7)	7.5±0.3 (7)	-3.7±0.3 (6)	-5.2±0.4 (7)
4-6	8.2±0.7 (9)	7.2±0.5(9)	-3.9±0.6 (6)	-4.7±0.2 (9)

Values are means ± S.E.M. (n).

Table 3.3 Activation and inactivation V_{50}s of K_V and Na_V currents in developing white fibers

Age (dpf)	Activation V_{50}		Inactivation V_{50}	
	K_V	Na_V	K_V	Na_V
1	6.4±1.4 (7)	-3.2±2.5 (4)	-17.6± 1.0(4)	-54.8±1.9 (4)
2	5.6±1.6 (7)	-10.9±2.1 [a] (7)	-21.0± 0.8 (5)	-58.8±1.1 (9)
3	3.7±1.2 (7)	-11.0±1.4 [a] (7)	-22.7±2.1 (6)	-62.2±1.5 [ab] (7)
4-6	-3.5±1.5 (9) [abc]	-10.7±1.4 [a] (9)	-27.6±2.0 (6)	-66.2±1.1 [abc] (9)

Values are means ± S.E.M. (n). [a]Significantly different from 1 dpf, [b]significantly different from 2 dpf, [c]significantly different from 3 dpf.

4. Development of Na_V and K_V currents in red and white skeletal muscle of zebrafish *sofa potato* mutants[2]

Having established that ionic currents undergo several developmental changes, the next step was to investigate some of the possible mechanisms underlying such phenomena. In some types of excitable cells the development of voltage-gated currents is controlled by synaptic input, while in others it is not. In order to determine the effect that an absence of synaptic input might have on Na_V and K_V current development, the zebrafish *sofa potato* (*sop*$^{-/-}$) mutation was studied.

The *sop* mutation was discovered in a screen targeting genes mediating locomotive behaviour of the zebrafish embryo and larva (Granato *et al.*, 1996). *Sop*$^{-/-}$ mutants lack nAChRs in the membranes of skeletal muscle fibers due to a leucine to proline point mutation at position 28 in the δ subunit (Ono *et al.*, 2004). Body musculature, motor neuron morphology and the release characteristics of acetylcholine at neuromuscular junctions are largely unaffected in these mutants (Li *et al.*, 2003; Panzer *et al.*, 2006). The absence of nAChRs means that *sop*$^{-/-}$ mutants are completely paralyzed, but their muscles are able to contract when depolarized by application of high K^+ solutions or electrical stimulation, indicating that the muscle fibers themselves are intact (Ono *et al.*, 2001). However, *sop*$^{-/-}$ mutants do have some deficiencies in muscle physiology. For example, the postsynaptic scaffolding protein rapsyn is not

[2] A version of this chapter has been accepted for publication. Coutts CA, Cunningham ME, Ali DW 2009. Developmental Neuroscience. In Press.

properly recruited to post-synaptic structures (Ono *et al.*, 2001) and there are minor ultra-structural defects in mutant muscle fibers, including narrower “wavy” myofibrils, decreased A-band width, shorter Z-lines and prominent M-lines (Etard *et al.*, 2005). It is not known whether the properties of voltage-gated currents that govern muscle excitability are affected in mutants that lack synaptic input.

Compared to their phenotypically wild-type siblings (*sop*$^{+/?}$), *sop*$^{-/-}$ mutants displayed altered development of K_V current density, but Na_V current density was similar. The steady-state properties of K_V currents were similar between *sop*$^{-/-}$ mutants and their normal siblings, but there was a significant difference in the voltage-dependence of Na_V current inactivation. These results indicate that some aspects of ion current development in skeletal muscle require synaptic activity, whereas others do not.

4.1 Sop$^{-/-}$ mutants lack nAChRs and synaptic activity in skeletal muscle

After successfully crossing zebrafish that were heterozygous (*sop*$^{+/-}$) for the *sofa potato* allele, *sop*$^{-/-}$ mutants were identified by their complete immobility, which was suggestive of a lack of muscle activation. Although the *sop* mutation has been studied by several groups (Ono *et al.*, 2001; Li *et al.*, 2003; Ono *et al.*, 2004; Panzer *et al.*, 2006), the phenotype

of the *sop*$^{-/-}$ mutants was confirmed again here in two ways. First, the labelling pattern of Alexa Fluor 488-tagged α-bungarotoxin, a potent nAChR antagonist, was examined in skeletal muscle (Figure 4.1A). At 6 dpf, *sop*$^{-/-}$ mutants exhibited a complete lack of staining (Figure 4.1A, right panel), whereas their phenotypically wild-type siblings (*sop*$^{+/?}$) show clusters of staining throughout the muscles (Figure 4.1A, left panel). Secondly, electrical activity in the form of miniature endplate currents (mEPCs) was recorded from red and white muscle fibers of 6 dpf larvae using patch-clamp electrophysiology (Figure 4.1B). Muscle fibers of *sop*$^{+/?}$ siblings exhibited mEPCs that were similar in frequency (0.1-1.7 Hz) and amplitude (200-700 pA) to those previously reported (Figure 4.1B, top) (Nguyen *et al.*, 1999; Todd *et al.*, 2004; Luna & Brehm, 2006), whereas mEPCs were completely absent in recordings from *sop*$^{-/-}$ mutants (Figure 4.1B, bottom). These observations confirm that *sop*$^{-/-}$ mutants lack nAChRs and therefore receive no cholinergic input from motorneurons.

4.2 K_V current development is deficient in *sofa potato* mutants

In order to determine whether a lack of cholinergic input would affect the development of K_V and Na_V currents in skeletal muscle, voltage clamp recordings from *sop*$^{-/-}$ mutants and their *sop*$^{+/?}$ siblings were compared. Recordings were obtained from red and white muscle fibers of zebrafish embryos and larvae at the ages of 1, 2, 3 and 6 dpf.

The K_V currents evoked from red muscle fibers are largely non-inactivating outward currents that exhibit a small inactivating component at voltages more positive than approximately 10 mV (Figure 4.2A). Current-voltage relationships, where peak current density was plotted against membrane potential, revealed that *sop*$^{-/-}$ mutants had normal current densities compared to their *sop*$^{+/?}$ siblings at 1, 2 and 3 dpf. However, at 6 dpf the current density of *sop*$^{-/-}$ mutants was significantly smaller than their 6 day old siblings (Figure 4.2B, Table 4.1). Between 3 and 6 dpf the peak current density at 30 mV increased in the *sop*$^{+/?}$ siblings, but not in the mutants (Figure 4.2A&B, Table 4.1).

White muscle fibers possess fast-inactivating A-type K_V currents (Buckingham & Ali, 2004) that appear at voltages more positive than -10 mV and are inactivated within 100 ms (Figure 4.3A). K_V currents of *sop*$^{+/?}$ siblings followed a developmental progression, increasing their current densities from 1 to 6 dpf, with significant increments occurring between 1 and 2 dpf, and again between 3 and 6 dpf (Figure 4.3B, Table 4.1). In *sop*$^{-/-}$ mutants, K_V currents exhibit the same developmental progression between the ages of 1 and 3 dpf, but they lack the developmental increase in current density between 3 and 6 dpf (Table 4.1). Because the current density accounts for the size of the cell relative to the peak current amplitude, a change in the current density suggests that there may be an effect on the K_V channel expression at the membrane.

Steady-state properties of A-type K_V currents in white muscle were then investigated (Figure 4.4). Conductance-voltage relationships for both activation and inactivation revealed no significant differences between the *sop*$^{-/-}$ mutants and their siblings with regard to the V_{50}s and slope factors (Figure 4.4, Tables 4.2&4.3).

4.3 Na_V current development in white muscle

White muscle fibers possess rapidly activating and inactivating inward Na_V currents (Buckingham & Ali, 2004) (Figure 4.5A). The current-voltage relationships for Na_V currents in *sop*$^{-/-}$ mutants were not found to be significantly different from their *sop*$^{+/?}$ siblings at any age (Figure 4.5B, Table 4.1). The developmental progression of the voltage-dependence of Na_V current activation and inactivation was also largely unaffected by the *sop*$^{-/-}$ mutation (Figure 4.6, Tables 4.2&4.3). However, there was a small but significant difference in the V_{50} of inactivation between the *sop*$^{-/-}$ mutants and their siblings at 6 dpf (Figure 4.6, Table 4.3).

Taken together, these results indicate that in both red and white muscle fibers, *sop*$^{-/-}$ mutants lacking synaptic activity at the neuromuscular junction exhibit normal K_V and Na_V currents during early stages of development (1-3 dpf). However, by 6 dpf K_V current density and the voltage-dependence of Na_V current inactivation in the *sop*$^{-/-}$ mutants are significantly different from their siblings.

Figure 4.1 *Sofa potato* mutants lack nicotinic acetylcholine receptors and cholinergic synaptic activity in skeletal muscle. **(A)** Alexa fluor 488-tagged α-bungarotoxin labels clusters of nAChRs throughout the axial muscle of phenotypically wild-type siblings (*sop*$^{+/?}$) at 6 dpf, but not in *sop*$^{-/-}$ mutants. **(B)** Whole-cell recordings from skeletal muscle of *sop*$^{+/?}$ zebrafish exhibit miniature end-plate currents (mEPCs), which are completely absent in *sop*$^{-/-}$ mutants. Scale bar: (A) = 50 μm.

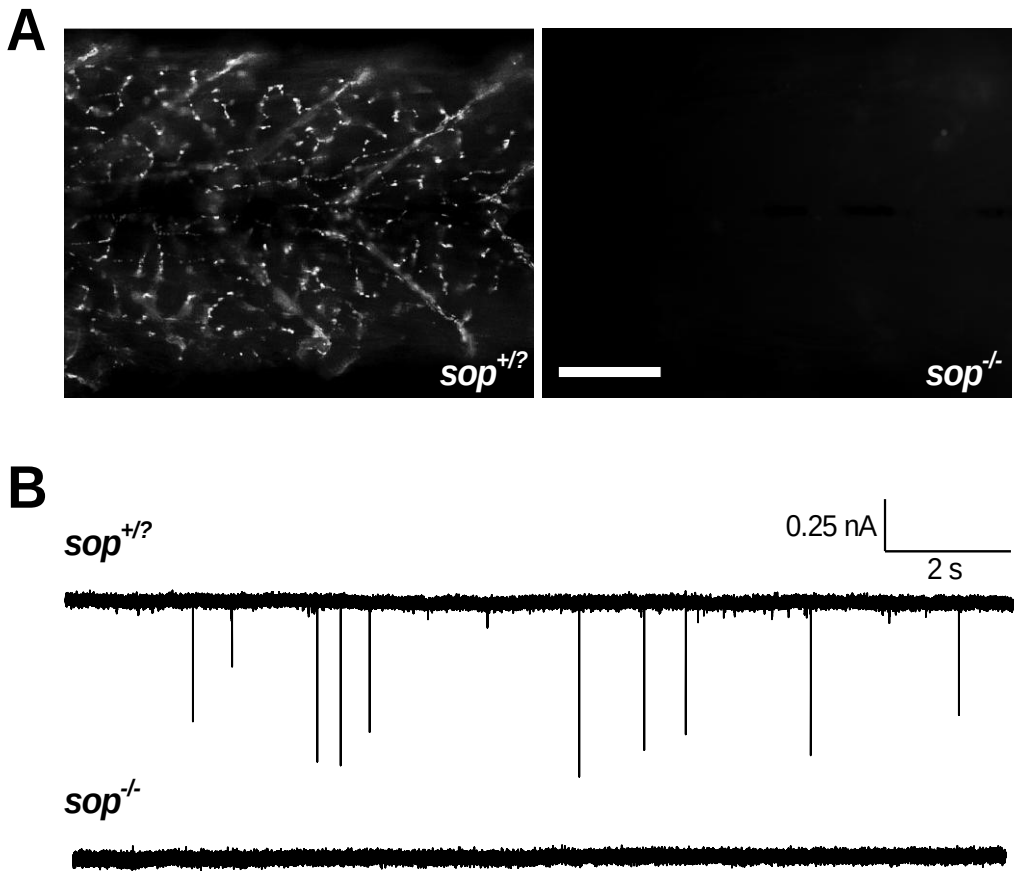
A
sop+/?
sop-/-
B
sop+/?
0.25 nA
2 s
sop-/-

Figure 4.2 Development of K_V currents in red muscle fibers of *sofa potato* mutants. **(A)** K_V currents evoked by a series of 200 ms voltage steps ranging from -60 to 30 mV in 10 mV increments at 6 dpf. The current amplitude in *sop*$^{-/-}$ mutants was markedly decreased compared with their phenotypically wild-type (*sop*$^{+/?}$) siblings. **(B)** Current-voltage relationships reveal that the peak current density of *sop*$^{-/-}$ mutants is similar to that of their *sop*$^{+/?}$ siblings from 1-3 dpf, but the *sop*$^{-/-}$ mutants lack a developmental increase in peak current density between 3 and 6 dpf. A liquid junction potential of 6.7 mV was accounted for in all plots.

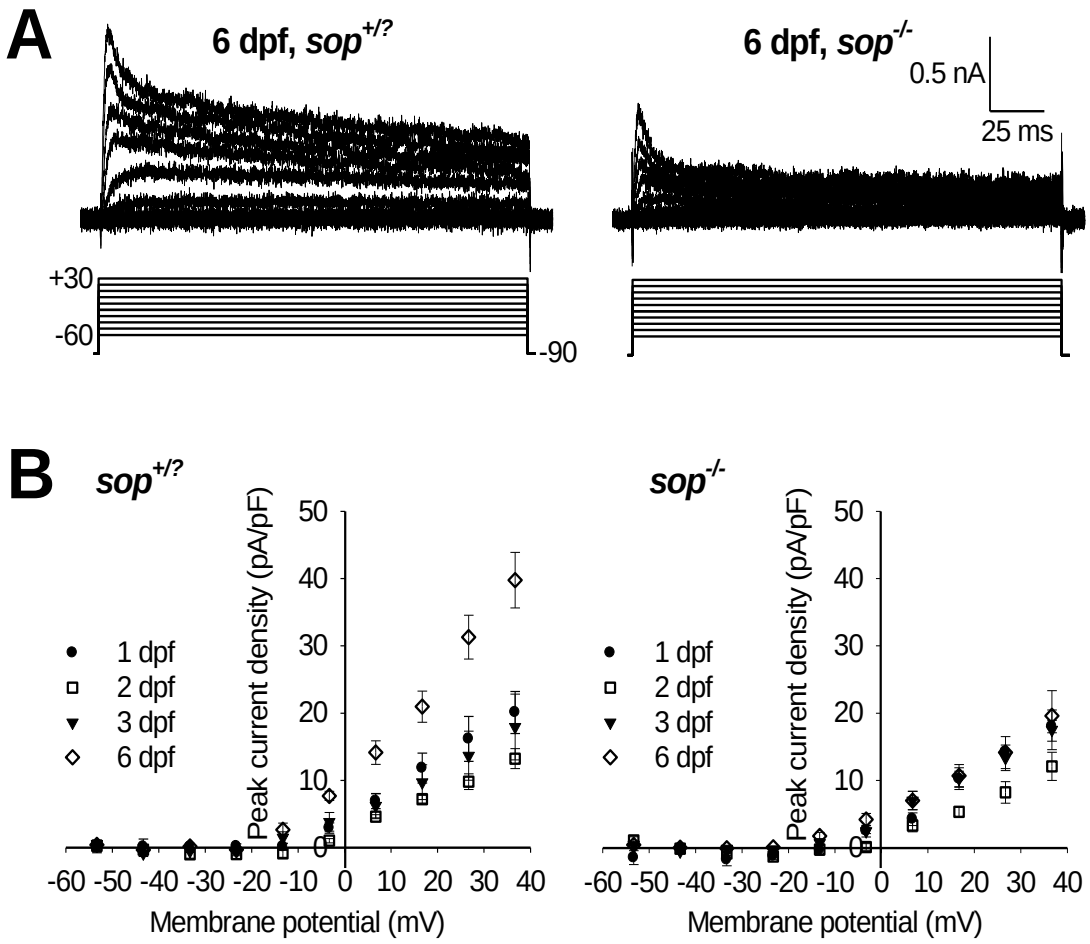
A
6 dpf, sop+/?
6 dpf, sop-/-
0.5 nA
25 ms
+30
-60
-90
B
sop+/?
sop-/-
Peak current density (pA/pF)
1 dpf
2 dpf
3 dpf
6 dpf
Membrane potential (mV)

Figure 4.3 Development of K_V currents in white muscle fibers of *sofa potato* mutants. **(A)** A-type K_V currents were evoked by a series of 200 ms voltage steps ranging from -60 to 30 mV in 10 mV increments at 6 dpf. The current amplitude in *sop*$^{-/-}$ mutants is markedly smaller than their *sop*$^{+/?}$ siblings. **(B)** Current-voltage relationships reveal that the peak current density of *sop*$^{-/-}$ mutants is similar to that of their *sop*$^{+/?}$ siblings from 1-3 dpf, but they lack the developmental increase in peak current density between 3 and 6 dpf. A liquid junction potential of 6.7 mV was accounted for in all plots.

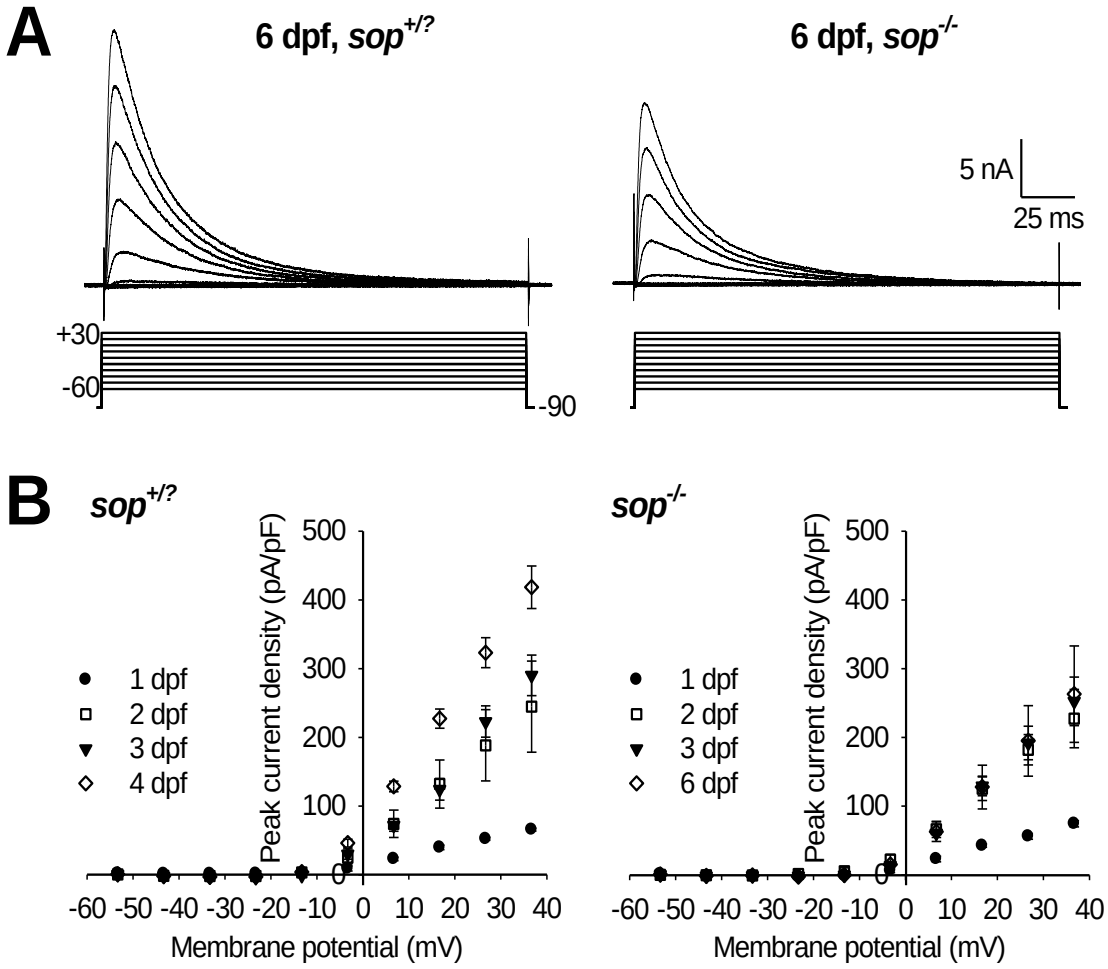
A
6 dpf, sop+/?
6 dpf, sop-/-
5 nA
25 ms
+30
-60
-90
B
sop+/?
sop-/-
1 dpf
2 dpf
3 dpf
4 dpf
6 dpf
Peak current density (pA/pF)
Membrane potential (mV)
500
400
300
200
100
0
-60 -50 -40 -30 -20 -10 0 10 20 30 40

Figure 4.4 Development of steady-state activation and inactivation properties of A-type K_V currents in white muscle of *sofa potato* mutants. Conductance-voltage plots were fit with Boltzmann functions to determine V_{50}s and slope factors of steady-state activation and inactivation. **(A)** Differences between V_{50}s of activation became significant only at 6 dpf, when *sop*$^{-/-}$ mutants display a negative shift from 3 to 6 dpf that isn't present in their *sop*$^{+/?}$ siblings. Slope factors were not significantly different at any age examined. **(B)** Neither the V_{50}s nor the slope factors of inactivation were different in *sop*$^{-/-}$ mutants compared to their *sop*$^{+/?}$ siblings. A liquid junction potential of 6.7 mV was accounted for in all plots.

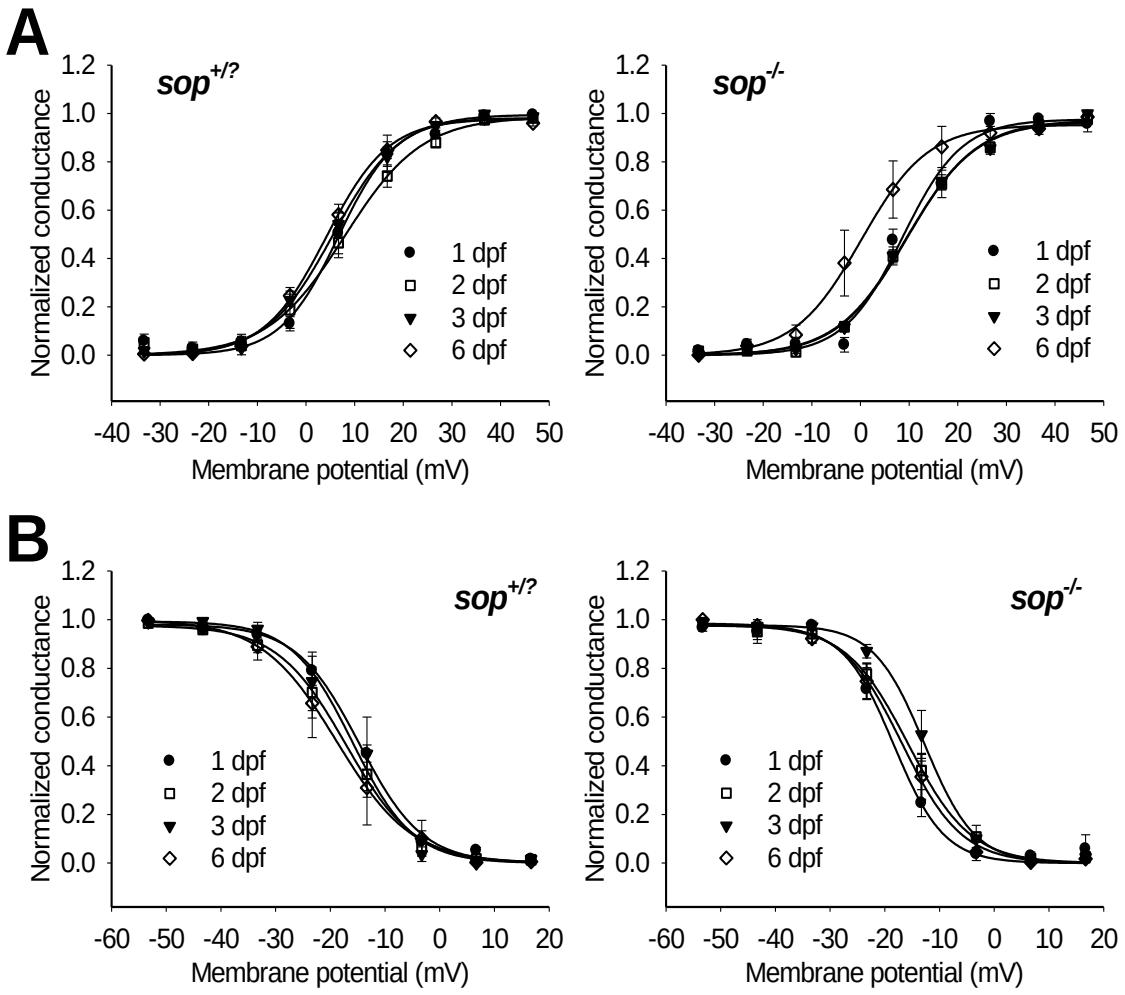
A
sop+/?
sop-/-
Normalized conductance
Membrane potential (mV)
1 dpf
2 dpf
3 dpf
6 dpf
B
sop+/?
sop-/-
Normalized conductance
Membrane potential (mV)
1 dpf
2 dpf
3 dpf
6 dpf

Figure 4.5 Development of Na_V currents in white muscle fibers of *sofa potato* mutants. **(A)** Na_V currents were evoked by a series of 5 ms steps ranging from -80 to 70 mV in 10 mV increments at 6 dpf. **(B)** Current-voltage relationships reveal that the peak current density of $sop^{-/-}$ mutants is similar to that of their $sop^{+/?}$ siblings at all ages examined. A liquid junction potential of 4.3 mV was accounted for in all plots.

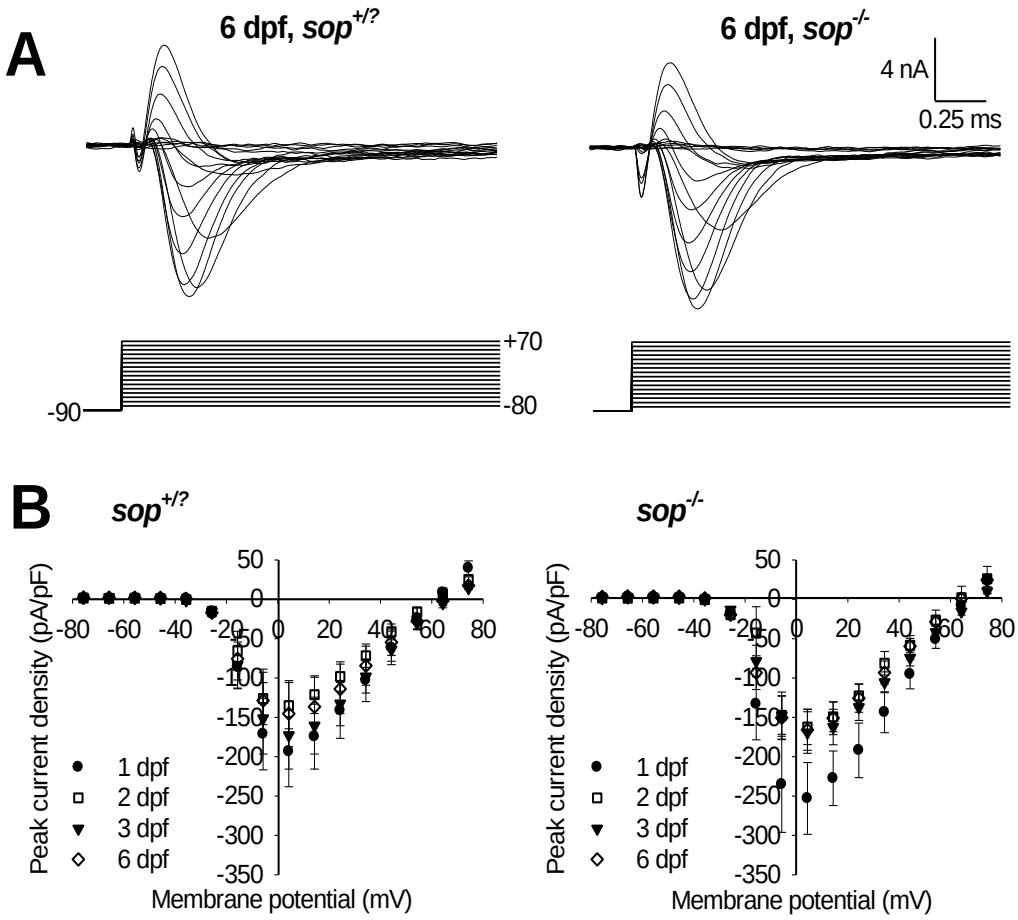
A
6 dpf, sop+/?
6 dpf, sop-/-
4 nA
0.25 ms
+70
-80
-90
B
sop+/?
sop-/-
Peak current density (pA/pF)
Membrane potential (mV)
1 dpf
2 dpf
3 dpf
6 dpf

Figure 4.6 Development of steady-state properties of Na_V currents in *sofa potato* white muscle. Conductance-voltage plots were fit with Boltzmann functions to determine V_{50}s and slope factors of steady-state activation and inactivation. **(A)** Neither the V_{50}s nor the slope factors of activation were different in *sop*$^{-/-}$ mutants compared to their *sop*$^{+/?}$ siblings. **(B)** Differences between V_{50}s of inactivation became significant only at 6 days post fertilization (dpf), when *sop*$^{-/-}$ mutants display a smaller negative shift from 3 to 6 dpf than their *sop*$^{+/?}$ siblings. Slope factors were not significantly different at any age studied. A liquid junction potential of 4.3 mV was accounted for in all plots.

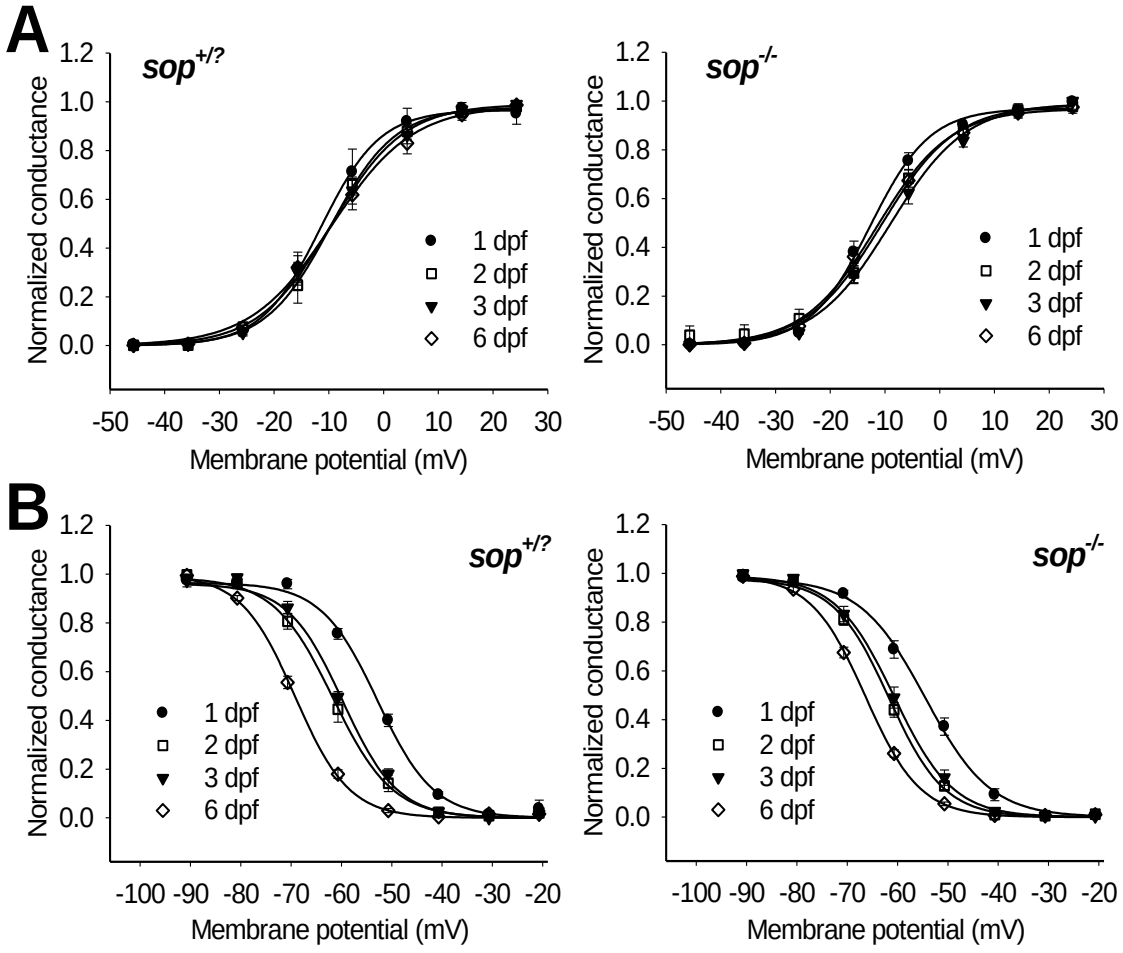
A
sop+/?
sop-/-
Normalized conductance
Membrane potential (mV)
1 dpf
2 dpf
3 dpf
6 dpf
B
sop+/?
sop-/-
Normalized conductance
Membrane potential (mV)
1 dpf
2 dpf
3 dpf
6 dpf

Table 4.1 Peak current density of K_V and Na_V currents in red white muscle fibers of developing *sofa potato* mutants

Current Type	Fiber Type	Age (dpf)	Peak Current Density (pA/pF)	
			***sop*$^{+/?}$**	***sop*$^{-/-}$**
K_V	**Red**	**1**	20.1±3.1 (*3*)	18.0±0.9 (*3*)
		2	13.2±1.5 (*4*)	12.1±2.1 (*5*)
		3	17.9±4.9 (*4*)	17.5±2.9 (*5*)
		6	39.7±4.1 (*5*)[f]	19.6±3.7 (*4*)[d]
	White	**1**	65.7±2.0 (*3*)	72.2±3.9 (*4*)
		2	244.6±66.2 (*7*)[e]	232.5±30.0 (*7*)[e]
		3	290.2±29.5 (*4*)	252.4±35.3 (*3*)
		6	441.4±26.8 (*5*)[f]	262.9±70.2 (*3*)[d]
Na_V	**White**	**1**	-193.5±44.6 (*4*)	-253.1±45.6 (*4*)
		2	-135.2±29.4 (*5*)	-162.2±22.4 (*9*)
		3	-172.6±43.2 (*4*)	-169.3±26.5 (*4*)
		6	-145.4±41.9 (*4*)	-165.8±26.1 (*6*)

Peak current density was calculated at a membrane potential of 30 mV for K_V currents and 0 mV for Na_V currents. 'dpf' is days post fertilization. [d] indicates values that are significantly different between *sop*$^{-/-}$ mutants and corresponding ages in *sop*$^{+/?}$ siblings. Within *sop*$^{+/?}$ and *sop*$^{-/-}$ groups, [e] indicates values that are significantly different from 1 dpf and [f] indicates values that are significantly different from 3 dpf. Values are means±SEM (*n*).

Table 4.2 Activation V_{50}s and slope factors of K_V and Na_V currents in white muscle fibers of developing *sofa potato* mutants

Current Type	Age (dpf)	Activation V_{50} (mV)		Activation Slope	
		***sop*$^{+/?}$**	***sop*$^{-/-}$**	***sop*$^{+/?}$**	***sop*$^{-/-}$**
K_V	**1**	7.6±1.9 (*3*)	9.6±1.7 (*3*)	5.2±0.8 (*3*)	6.1±0.6 (*3*)
	2	8.0±1.1 (*6*)	9.5±0.5 (*8*)	7.9±0.9 (*6*)	7.1±0.4 (8)
	3	5.6±0.6 (*5*)	9.5±0.6 (5)	6.8±0.5 (*5*)	9.5±0.6 (5)
	6	4.4±1.2 (*8*)	1.1±3.9 (*3*)	6.4±0.4 (*8*)	6.5±1.4 (*3*)
Na_V	**1**	-11.1±2.4 (*3*)	-12.9±1.3 (*3*)	5.4±0.7 (*3*)	5.5±0.5 (*3*)
	2	-9.7±0.7 (*4*)	-10.6±0.8 (*9*)	5.9±0.6 (*4*)	6.8±0.7 (*9*)
	3	-9.6±0.7 (*4*)	-9.0±0.6 (*4*)	6.7±0.6 (*4*)	6.9±0.5 (*4*)
	6	-9.2±2.0 (*5*)	-11.4±1.3 (*6*)	7.8±0.7 (*5*)	7.2±0.6 (*6*)

'dpf' is days post fertilization. Values are means±SEM (*n*).

Table 4.3 Inactivation V_{50}s and slope factors of K_V and Na_V currents in white muscle fibers of developing *sofa potato* mutants

Current Type	Age (dpf)	Inactivation V_{50} (mV)		Inactivation Slope	
		***sop*$^{+/?}$**	***sop*$^{-/-}$**	***sop*$^{+/?}$**	***sop*$^{-/-}$**
K_V	**1**	-14.9±1.0 (*3*)	-18.9±1.2 (*3*)	-5.9±1.3 (*3*)	-4.3±0.7 (*3*)
	2	-17.2±1.2 (*5*)	-15.7±0.5 (*4*)	-6.3±.0 (*5*)	-5.7±0.4 (*4*)
	3	-15.9±1.2 (*3*)	-12.7±0.7 (*4*)	-5.6±1.0 (*3*)	-4.6±0.7 (*4*)
	6	-18.0±4.3 (*4*)	-16.9±2.9 (*3*)	-5.4±0.6 (*4*)	-5.0±0.7 (*3*)
Na_V	**1**	-53.1±0.6 (*6*)	-54.1±1.2 (*6*)	-5.4±0.3 (*6*)	-6.5±0.3 (*6*)
	2	-61.7±0.5 (*5*)^{e}	-61.7±0.3 (*8*)^{e}	-5.9±0.4 (*5*)	-5.5±0.3 (*8*)
	3	-59.8±0.6 (*3*)	-60.7±0.4 (*4*)	-5.4±0.5 (*3*)	-5.8±0.4 (*4*)
	6	-69.4±0.6 (*6*)^{f}	-66.5±0.5 (*5*)^{df}	-5.2±0.2 (*6*)	-5.4±0.1 (*5*)

'dpf' is days post fertilization. ^{d} indicates values that are significantly different between *sop*$^{-/-}$ mutants and corresponding ages in *sop*$^{+/?}$ siblings. Within *sop*$^{+/?}$ and *sop*$^{-/-}$ groups, ^{e} indicates values that are significantly different from 1 dpf and ^{f} indicates values that are significantly different from 3 dpf. Values are means ± SEM (*n*).

5. Modulation of A-type K_V currents by PKA in white muscle fibers[3]

Ion channels are important phosphorylation targets of protein kinases such as PKA (Hell *et al.*, 1995; Jonas & Kaczmarek, 1996; Johnson *et al.*, 1997; Anderson *et al.*, 2000; Vargas & Lucero, 2002; Hoshi *et al.*, 2003; Vogalis *et al.*, 2003; Vijayaragavan *et al.*, 2004). Channel phosphorylation can lead to many changes in current characteristics, including altered current density and voltage-dependence, similar to those observed in developing muscle fibers. PKA is a heterotetramer composed of various combinations of two catalytic (Cα, Cβ, Cγ) and two regulatory (RIα, RIβ, RIIα, RIIβ) subunits. In neurons, protein complexes consisting of PKA, K_V channels and ancillary subunits such as the K_V channel interacting protein (KChIP3) have been identified (Schrader *et al.*, 2002), and, in many cases, phosphorylation of K_V channels results in a decrease in current amplitude and shifts in the voltage dependence of activation and/or inactivation (Pedarzani & Storm, 1995; Hu & Gereau, 2003; Hu *et al.*, 2003). However, very little is known about the modulation of A-type K_V channels associated with excitable cells other than neurons.

In this study, the ability of PKA to modulate A-type K_V currents in white muscle was investigated at several developmental stages. The A-type K_V currents are fast activating and fast inactivating currents that were first identified in neurons (Hagiwara *et al.*, 1961), but are now known to be

[3] A version of this chapter has been published. Coutts CA, Balt LN, Ali DW 2009. Acta Physiologica. 195(2):259-72.

present in non-neural tissues such as smooth and skeletal muscle (Duval & Leoty, 1978, 1980a, b; Beech & Bolton, 1989). A-type currents are primarily thought to regulate action potential frequency (Connor & Stevens, 1971; Rudy, 1988; Tierney & Harris-Warrick, 1992), but they may also play a role in adjusting action potential shape and size (Zhang & McBain, 1995a, b), in controlling signal propagation (Hoffman *et al.*, 1997) and in underlying membrane potential oscillations (Bourdeau *et al.*, 2007). Factors that modulate A-type currents may therefore also affect cell excitability and action potential frequency, shape and size.

Skeletal muscle fibers are known to express PKA (Chahine *et al.*, 1993; Xu & Salpeter, 1995; Hoover *et al.*, 2001), and it is likely that PKA phosphorylates and modulates muscle ion channels, although little is known about the functional consequences of this modulation in muscle. In neurons, modulation of K_V channels has been shown to alter action potentials and repetitive firing properties. Therefore, since very little is known about the modulation of K_V channels in muscle fibers (Tricarico *et al.*, 1993), and because the white muscle fibers in zebrafish do not fire repetitively, the following hypotheses were tested: 1) skeletal A-type K_V channels are regulated by PKA, and 2) that this regulation affects the firing properties of muscle fibers that are incapable of repetitive firing. This is the first study to directly examine this in skeletal muscle.

Activation of PKA was found to modulate several important characteristics of the A-type K_V current in zebrafish skeletal muscle, which

in turn altered the shape of action potentials. There was no indication of differential modulation by PKA in fish at different ages. These results indicate that modulation of skeletal muscle K_V channel activity by protein kinases may play an important role in muscle excitability, but are not involved in K_V current development.

5.1 Experiments controlling for time and drug solvents

The first goal was to determine if the properties of the A-type currents changed after a 5 minute treatment period and/or in the presence of DMSO. Because the drugs were dissolved in DMSO, currents were recorded after exposing the fibers to DMSO to ensure that this solvent had no effect on any of the properties under investigation. Exposure of preparations to 0.3% DMSO for 5 minutes, resulted in no significant change in the peak current density or kinetics (Figure 5.1A&B; n = 5;), the V_{50} and slope factors of activation (Figure 5.1C&D, Table 5.1) or the V_{50} and slope factors of inactivation (Figure 5.1E&F, Table 5.2). These results indicated that the A-type currents did not change over time and that the DMSO vehicle also had no effect on the properties under investigation. In addition, DMSO time control experiments were recorded for all current clamp experiments; there were no changes in the properties of action potentials in the presence of DMSO after a 5 minute treatment period. Therefore, any significant changes detected after application of the

treatments, were due solely to the effect of the pharmacological agents being applied.

5.2 Modulation of A-type K_V currents by activation of PKA

Initial experiments, performed by L.N. Balt, attempted to increase intracellular levels of cAMP via bath application of Fsk and IBMX independently of one another. Neither the Fsk-only nor the IBMX-only treatments affected K_V currents on their own, however a combination of the two drugs was sufficient to modulate A-type currents (unpublished observations; data not shown). Incubation of white muscle fibers in Fsk (25 μM) and IBMX (500 μM) together resulted in a 58±6% reduction in peak current density, from 214±13 pA pF^{-1} to 92±10 pA pF^{-1} (Figure 5.2A-C; n=7). When muscle fibers were pre-incubated in the specific PKA inhibitor, H-89 (10 μM), the peak current density (recorded at 20 mV) reduced from 199±15 pA pF^{-1} to 154±11 pA pF^{-1}, a reduction of only 24±4%, after Fsk+IBMX application (Figure 5.2D; n=5). Therefore, H-89 blocked approximately 50% of the Fsk+IBMX induced reduction in peak current density. H-89 on its own had no effect on peak current density as indicated by a lack of significant difference between the control and H-89 pre-incubation (Figure 5.2C&D), suggesting that basal levels of PKA phosphorylation are low. In fact, H-89 had no effect on any of the properties examined when compared with controls at the time point t=0 minutes.

Application of Fsk+IBMX changed the shape of the inactivating portion of the K_V current. Prior to treatment, K_V currents decayed with a single exponential time course, $\tau_{inactivation}$, of 37.4±2.6 ms (Figure 5.3, red lines; n=5). However, in the presence of Fsk+IBMX, the currents were poorly fit with a single exponential decay (middle trace) and were much better fit with a double exponential curve (blue line), which consists of a fast (τ_{fast}) and a slow components (τ_{slow}). τ_{fast} and τ_{slow} were 8.4±0.9 ms and 86.6±14.2 ms, respectively (Figure 5.3A&B). τ_{fast} represented 71% of the current amplitude. Pre-incubation in H-89 did not block the change in kinetics (; Figure 5.3A bottom trace and Figure 5.3B&C; n=5), and K_V currents still decayed with fast (τ_{fast} =10.8±1.6 ms) and slow (τ_{slow} =63.3±10.2 ms) components as shown in Figure 5.3A&B. Here, τ_{fast} represented 61% of the current amplitude. Thus, activation of PKA resulted in a reduction in peak current density and possibly an alteration of the decay kinetics. In order to better quantify the effects of PKA activation the width of the K_V current at half amplitude was measured. Application of Fsk+IBMX significantly reduced the half width of the K_V current from 32.8±1.5 ms to 15.0±1.7 ms (Figure 5.3C; n=6). Pre-incubation in H-89 did not block these changes although the mean half width of 21.2 ± 5.2 ms (Figure 5.3D; n=5), was not as small as that found when applying Fsk+IBMX, and the values were more variable as indicated by the large standard error of the mean (Figure 5.3D).

The next goal was to determine if activation of PKA had any significant effect on the voltage dependences of activation and inactivation. Application of Fsk+IBMX had no effect on the V_{50} of activation (Figure 5.4A&B, Table 5.1) but significantly reduced the slope factor from 6.2 to 4.9 (Figure 5.4A&B, Table 5.1). Pre-incubation in H-89 had no significant effect on the V_{50} of activation (Figure 5.4C&D, Table 5.1), but it prevented the Fsk+IBMX-induced change in slope factor (Figure 5.4C&D, Table 5.1). The reduction in slope factor suggests that PKA phosphorylation of K_V channels renders them more readily available for recruitment per unit change in membrane depolarization.

Application of Fsk+IBMX significantly shifted the V_{50} of inactivation from -17.2 mV to -14.1 mV (Figure 5.5A&B, Table 5.2), but had no effect on the slope factor. Pre-incubation of the preparations in H-89 prevented the Fsk+IBMX-induced shift in the inactivation curve (Figure 5.5C&D, Table 5.2) and had no effect on the slope factor. This effect of PKA suggests that it increases the number of channels available to become activated at a given membrane potential.

5.3 Modulation of action potentials by activation of PKA

A number of significant changes were observed in the steady state and kinetic properties of the A-type K_V current in white muscle fibers; the next experiments sought to determine if these changes affected the ability

of the muscle to fire action potentials. The hypothesis was that the PKA-induced decrease in K_V current density may affect one or more of the following characteristics: action potential amplitude, width, voltage threshold and/or amount of current required to reach threshold. Application of Fsk+IBMX resulted in a significant increase in the amplitude of the action potential (Figure 5.6A&B; n=5), but did not change any of the other characteristics that were examined (Figure 5.6C&D; n=5). In the absence of Fsk+IBMX, action potential amplitude was 44.1±10.1 mV, and after addition of Fsk+IBMX the amplitude increased to 60.7±7.6 mV. This increase in amplitude was blocked by H-89 (Figure 5.6B; n=5). Because these fibers are capable of supporting a large passive response to current injection, action potential amplitude was measured from the onset of the active response to the peak of the event, rather than from the resting potential to the peak. Threshold voltage and half width did not change significantly; prior to application of Fsk+IBMX they were -37.5±1.2 mV and 1.0± 0.1 ms and respectively, and following PKA activation were -37.6±2.5 mV and 0.8±0.1 ms (Figure 5.6C&D; n=5). Finally, there was no significant change in the amount of current needed to bring the cell to threshold (data not shown).

It was then determined whether activation of PKA would change the time required for the action potential amplitude to recover after the muscle fiber fired an initial action potential. For this experiment fibers were depolarized with pairs of 1 ms pulses that were separated by intervals

starting at 40 ms and decreasing to 8 ms in 2 ms increments (Figure 5.7A). The time taken for the action potential to recover to full amplitude was examined by plotting the ratio of the second pulse to the first over time (Figure 5.7B). This was done before and after washing on Fsk+IBMX, which had no significant effect on action potential recovery (Figure 5.7B). In the DMSO time controls (n=6) there was a trend towards a faster recovery at the 5 minute time point, but the Fsk+IBMX treated preparations (n=4) showed exactly the same trend, and there was no significant difference between the DMSO recordings and the Fsk+IBMX treated fish at either the t=0 minutes or the t=5 minutes time point (Figure 5.7B).

Zebrafish swim at relatively high rates; therefore, it was important to determine if activation of PKA affected the properties of consecutive action potentials during a bout of high frequency firing. White muscle fibers were stimulated with 20 x 1 ms pulses for 500 ms (40 Hz) as shown in Figure 5.8A. This stimulation paradigm is well within the range of firing frequencies and burst times for bouts of fictive swimming (Buss and Drapeau 2002). Application of Fsk+IBMX significantly increased peak amplitude, as it did in the single pulse experiments of Figure 5.6 (Figure 5.8; n=4), but the width and general shape of the action potential did not change. Indeed, there was no difference in any of the action potential properties within the high frequency burst of firing (Figure 5.8; n=4), and the first (black trace), tenth (red trace) and twentieth (blue trace) action

potential within a burst were virtually identical in size and shape (Figure 5.8B). Figure 5.8C quantifies and compares the properties of the twentieth action potential within the control and Fsk+IBMX treated bursts. The twentieth action potential was chosen because it is most likely to illustrate any additive effects from high frequency firing.

Because the effect of PKA activation on action potentials was not as great as initially anticipated, it was important to determine how much of a role the A-type K_V current played in shaping the action potential. Therefore, the A-type current was completely blocked with 5 mM 4-AP (Figure 5.9A) and action potential properties were examined. Applying 4-AP for 5 minutes completely blocked the A-type current (Figure 5.9A; n=4), and resulted in a significant increase in both the amplitude and width of the action potential (Figure 5.9B-D; n=4). There was no significant difference in the action potential threshold (data not shown). Thus, the A-type K_V current is indeed involved in shaping the muscle action potential.

5.4 Specificity of Fsk+IBMX treatment for PKA activation

In order to confirm that the Fsk+IBMX treatment was activating PKA specifically, various analogs of cAMP were applied intracellularly by including them in the pipette, with the goal of activating PKA directly rather than indirectly (via adenylate cyclase activation and phosphodiesterase inhibition). When the functional cAMP analogs 8-bromo-cAMP (n=5) and

Sp-cAMP (n=4) were applied, peak current density at 20 mV was reduced by approximately 50% (Figure 5.10). In contrast, Rp-cAMP (n=3), a competitive inhibitor of PKA, failed to have an effect. The effects of cAMP analogs on inactivation kinetics were not as clear, however; decay phases of the A-type currents were not consistently fit with either single or double exponential functions (data not shown).

5.5 Activation of PKA during development

After confirming the specificity of the treatment paradigm, the next goal was to investigate whether PKA modulates A-type K_V currents differentially during development. To this end, currents were recorded at two additional ages, 1 and 6 dpf, because they represent the earliest and the latest stages of development studied here. PKA activation was found to have similar effects at all ages examined; namely an approximately 50-60% reduction in A-type K_V current density (Figure 5.11).

Together, the data suggest that activation of PKA leads to a number of significant changes in the steady state and kinetic properties of A-type K_V channels, and that these changes may have small but significant effects on the firing properties of white muscle fibers, but that PKA modulation isn't a likely source of the developmental changes observed in ionic currents.

Figure 5.1 A-type K_V currents did not change after the 5 minute treatment period or in the presence of DMSO. Saline represents the initial recording taken in the absence of DMSO (0.3%), and DMSO refers to the recording taken after bath application of 0.3% DMSO for 5 min. **(A,B)** Bath application of 0.3% DMSO has no significant effect on the peak current density of K_V currents (n=5). The decay of the currents was fit with a single exponential function (red lines) and obtained a time constant of inactivation, which did not change over time. **(C,D)** V_{50} and slope factor of activation (n=6), and **(E,F)** V_{50} and slope factor inactivation (n=5). A liquid junction potential of 6.7 mV was accounted for in all plots.

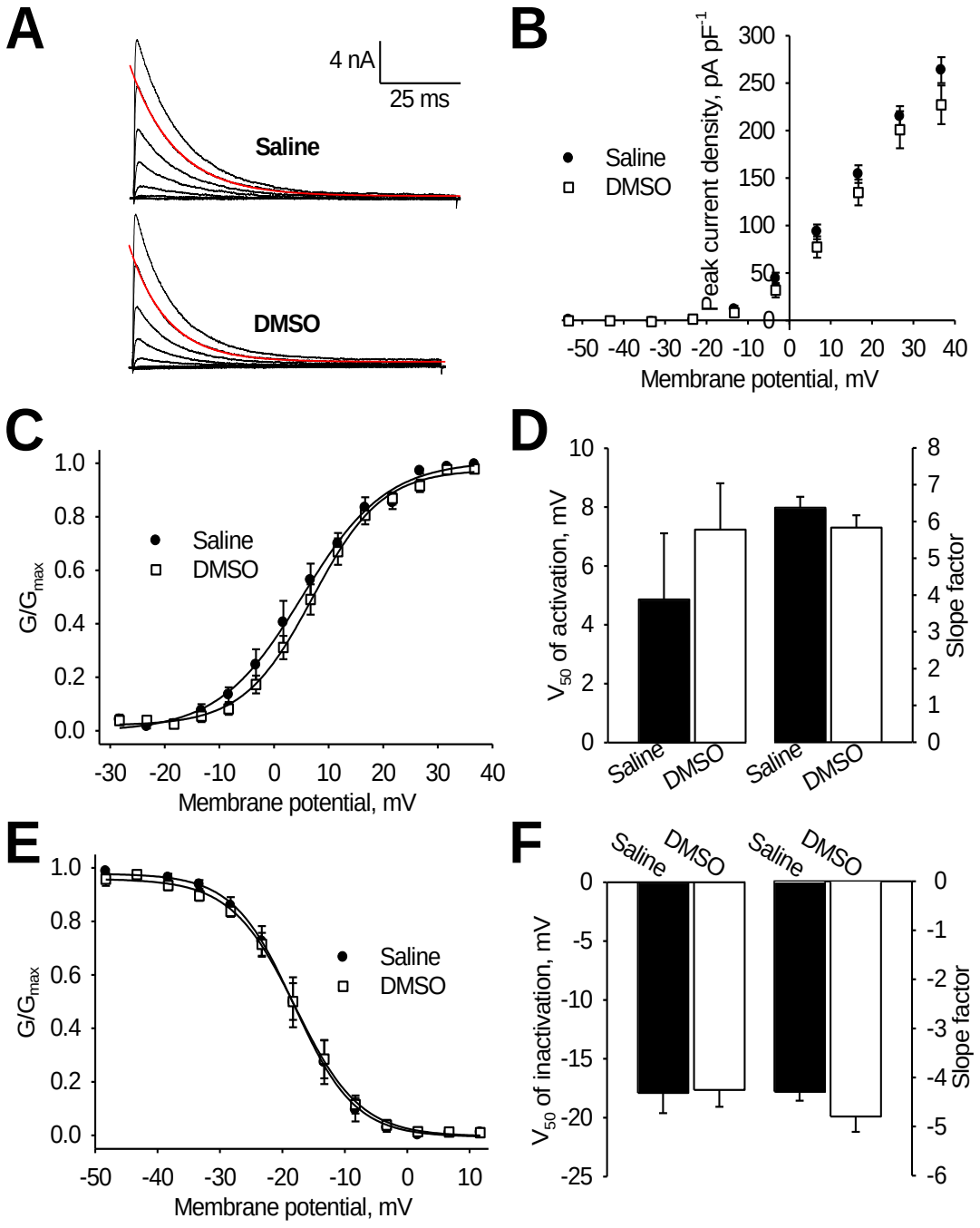
A
4 nA
25 ms
Saline
DMSO
B
Peak current density, pA pF-1
Saline
DMSO
Membrane potential, mV
C
G/Gmax
Saline
DMSO
Membrane potential, mV
D
V50 of activation, mV
Slope factor
Saline
DMSO
Saline
DMSO
E
G/Gmax
Saline
DMSO
Membrane potential, mV
F
V50 of inactivation, mV
Slope factor
Saline
DMSO
Saline
DMSO

Figure 5.2 Application of Fsk+IBMX reduces peak current density of A-type K_V currents. **(A,B)** Stepwise depolarizations from –60 mV to 40 mV in 10 mV increments resulted in outward A-type currents in (controls, n=7) that decreased in peak current density after application of Fsk+IBMX (25 μM + 500 μM) for 5 min. Controls are recordings taken at t=0 min immediately prior to Fsk+IBMX treatment. **(C)** Peak current density of A-type K_V currents recorded at 20 mV in the absence (control) and presence of Fsk+IBMX. **(D)** Pre-incubation of preparations for 5-7 min in H-89 (10 μM) partially blocked the effect of Fsk+IBMX (n=5) on K_V currents recorded at 20 mV. A liquid junction potential of 6.7 mV was accounted for in all plots. * Denotes significance at $p<0.05$, *** at $p<0.001$.

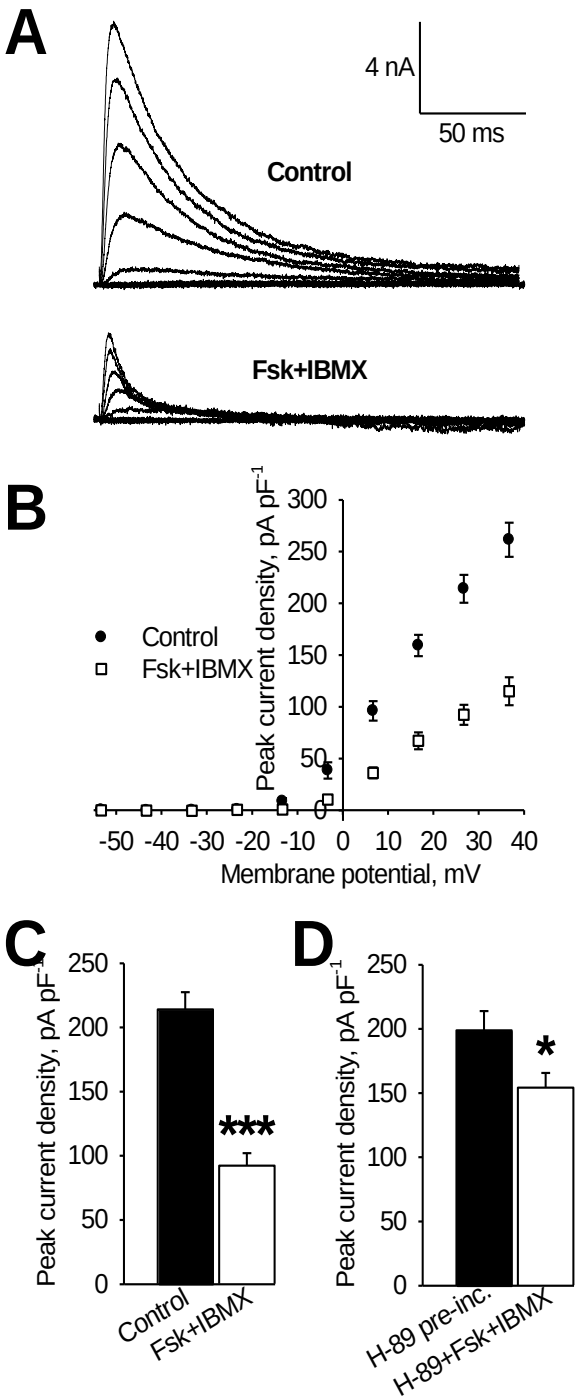
A
4 nA
50 ms
Control
Fsk+IBMX
B
Peak current density, pA pF-1
300
250
200
150
100
50
0
Control
Fsk+IBMX
-50 -40 -30 -20 -10 0 10 20 30 40
Membrane potential, mV
C
Peak current density, pA pF-1
250
200
150
100
50
0
***
Control
Fsk+IBMX
D
Peak current density, pA pF-1
250
200
150
100
50
0
*
H-89 pre-inc.
H-89+Fsk+IBMX

Figure 5.3 Application of Fsk+IBMX changes the decay kinetics of the A-type K_V current. **(A)** A-type currents were recorded during stepwise depolarizations of white muscle fibers and the current decay was fit with single (red lines) or double (blue lines) exponential functions for the current occurring at a depolarization to +20 mV. The decay component of currents recorded in the absence of Fsk+IBMX (25 μM + 500 μM) were equally well fit with single and double exponential decays (top trace). The decay component of currents recorded in the presence of Fsk+IBMX and Fsk+IBMX+H-89 were much better fit with a double exponential decay. **(B,C)** Inactivation time constants (τ, ms) and relative amplitudes for the single exponential fit in the absence of Fsk+IBMX (controls, n=5) and for the double exponential fits in Fsk +IBMX (n=6) and Fsk +IBMX+H-89 (n=5). **(D)** Half-width of the A-type K_V current before (control) and after application of Fsk-IBMX (n=6). Pre-incubation in H-89 does not significantly block the reduction in half width (n=5). * Denotes significance at $p<0.05$, *** at $p<0.001$.

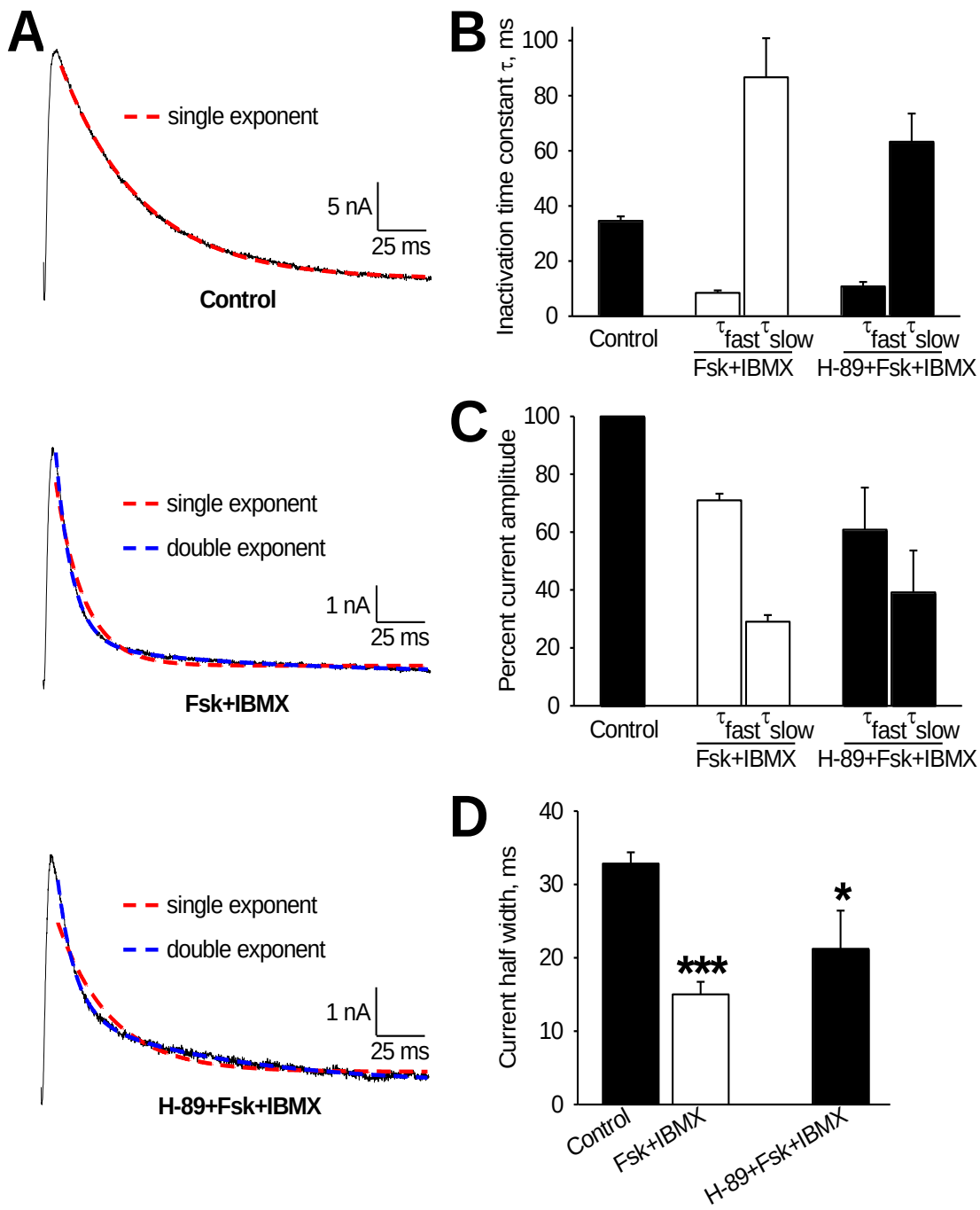
A
single exponent
5 nA
25 ms
Control
single exponent
double exponent
1 nA
25 ms
Fsk+IBMX
single exponent
double exponent
1 nA
25 ms
H-89+Fsk+IBMX
B
Inactivation time constant τ, ms
100
80
60
40
20
0
Control
τfast τslow
Fsk+IBMX
τfast τslow
H-89+Fsk+IBMX
C
Percent current amplitude
100
80
60
40
20
0
Control
τfast τslow
Fsk+IBMX
τfast τslow
H-89+Fsk+IBMX
D
Current half width, ms
40
30
20
10
0
***
*
Control
Fsk+IBMX
H-89+Fsk+IBMX

Figure 5.4 Effects of Fsk+IBMX and H-89 on activation V_{50}s and slope factors of A-type K_V. **(A,B)** Application of Fsk+IBMX (25 μM + 500 μM) for 5 min has no effect on the V_{50} of activation (n=7, p>0.05), but significantly reduces the slope factor (n=7, p<0.05). **(C,D)** Pre-incubation in H-89 (10 μM) for 5-7 min blocks the Fsk+IBMX-induced reduction in slope factor (n=4, p>0.05) and has no effect on the V_{50} of activation (p>0.05). A liquid junction potential of 6.7 mV was accounted for in all plots. ** Denotes significance at p<0.01.

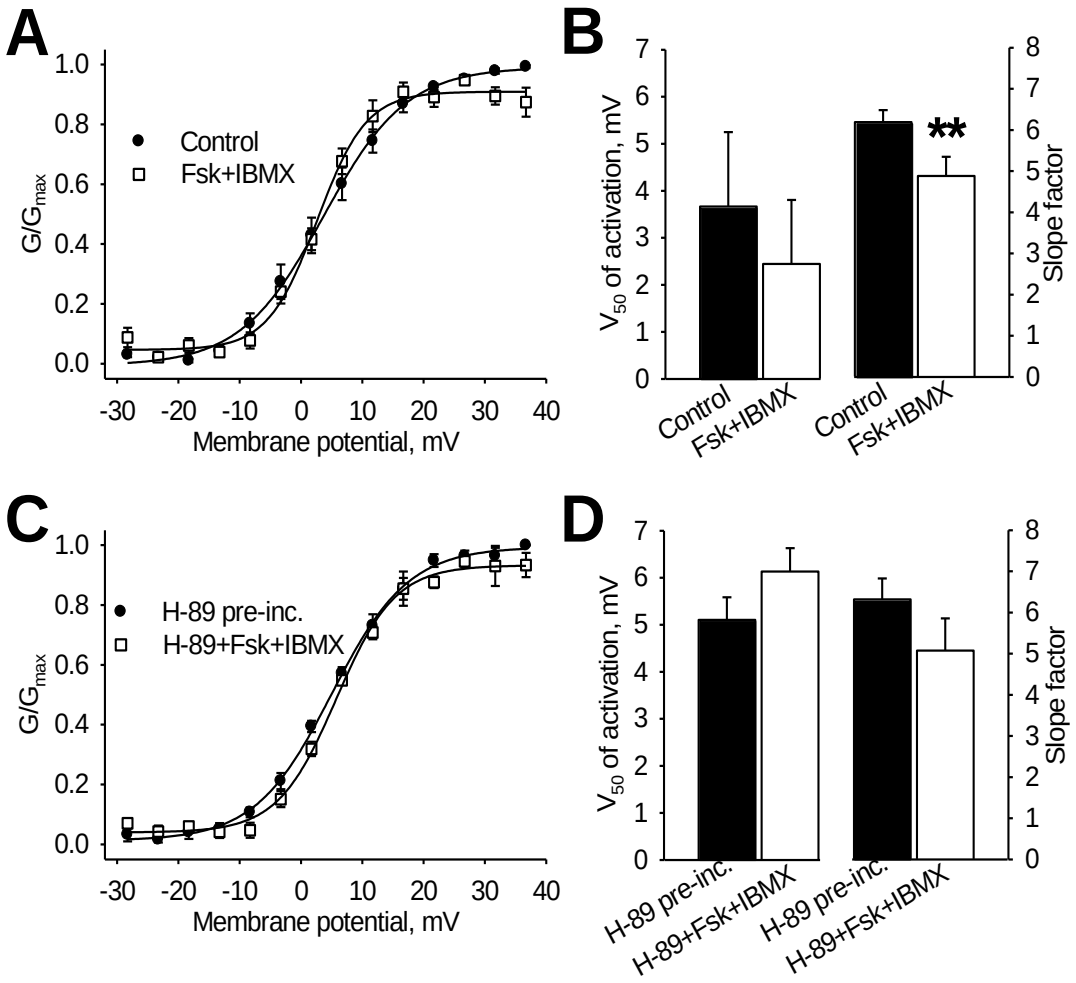
A
B
C
D
Control
Fsk+IBMX
H-89 pre-inc.
H-89+Fsk+IBMX
G/G_max
Membrane potential, mV
V_50 of activation, mV
Slope factor
**

Figure 5.5 Effect of Fsk+IBMX and H-89 on inactivation V_{50}s and slope factors of A-type K_V. **(A,B)** Application of Fsk+IBMX (25 μM + 500 μM) significantly shifts the voltage-dependence of inactivation in the positive direction (n=6, $p<0.05$), but has no effect on the slope factor ($p>0.05$). **(C,D)** Pre-incubation in H-89 (10 μM) for 5-7 min blocks the Fsk+IBMX-induced shift in the V_{50} of inactivation (n=4, $p>0.05$) and has no effect on the slope factor ($p>0.05$). A liquid junction potential of 6.7 mV was accounted for in all plots. * Denotes significance at $p<0.05$.

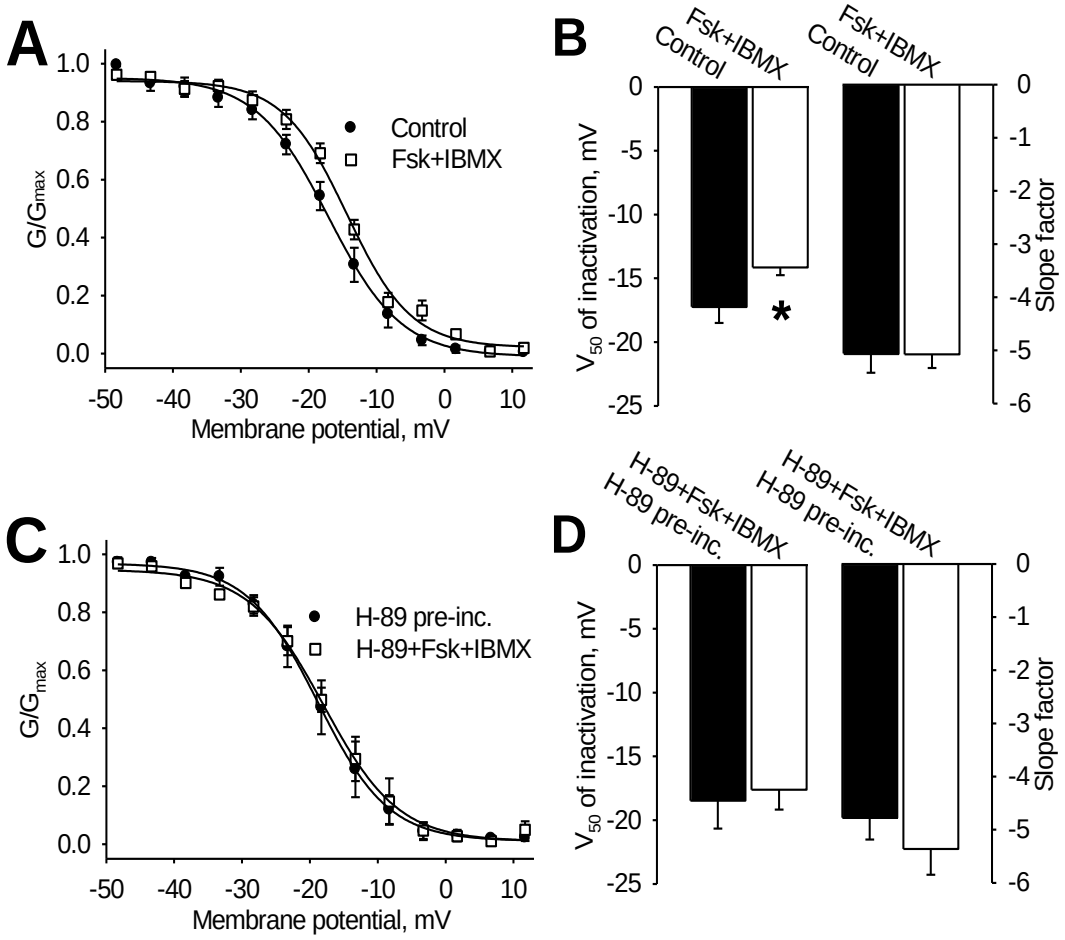
A
1.0
0.8
0.6
0.4
0.2
0.0
G/Gmax
Control
Fsk+IBMX
-50 -40 -30 -20 -10 0 10
Membrane potential, mV
B
Control
Fsk+IBMX
Control
Fsk+IBMX
0
-5
-10
-15
-20
-25
V50 of inactivation, mV
*
0
-1
-2
-3
-4
-5
-6
Slope factor
C
1.0
0.8
0.6
0.4
0.2
0.0
G/Gmax
H-89 pre-inc.
H-89+Fsk+IBMX
-50 -40 -30 -20 -10 0 10
Membrane potential, mV
D
H-89 pre-inc.
H-89+Fsk+IBMX
H-89 pre-inc.
H-89+Fsk+IBMX
0
-5
-10
-15
-20
-25
V50 of inactivation, mV
0
-1
-2
-3
-4
-5
-6
Slope factor

Figure 5.6 Effect of Fsk+IBMX on action potential properties in white muscle. **(A)** Action potentials recorded before (control) and after application of Fsk+IBMX (25 μM + 500 μM) for 5 min. Muscle fibres were held at –70 mV and injected with short current pulses (1 ms in duration) that were 1.2 nA in amplitude. Application of Fsk+IBMX significantly increased action potential amplitude (n=6), which was blocked by pre-incubation in 10 μM H-89 **(B)**; n=5. PKA activation had no significant effect on the half width **(C)** or threshold voltage **(D)**; n=6. * Denotes significance at $p<0.05$.

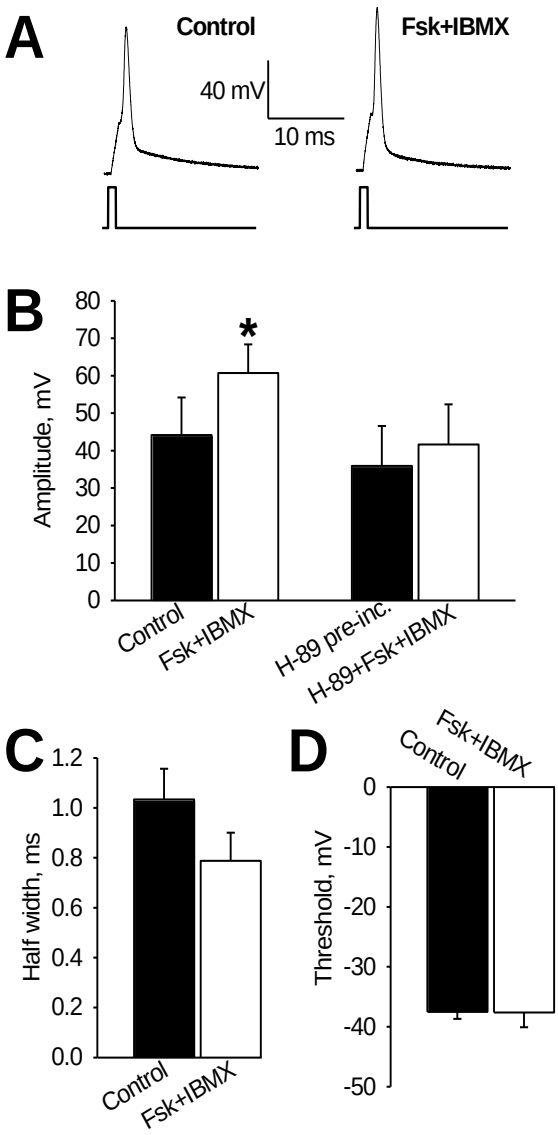
A
Control
Fsk+IBMX
40 mV
10 ms
B
Amplitude, mV
80
70
60
50
40
30
20
10
0
*
Control
Fsk+IBMX
H-89 pre-inc.
H-89+Fsk+IBMX
C
Half width, ms
1.2
1.0
0.8
0.6
0.4
0.2
0.0
Control
Fsk+IBMX
D
Control
Fsk+IBMX
Threshold, mV
0
-10
-20
-30
-40
-50

Figure 5.7 Recovery rate of action potentials was unaffected by Fsk+IBMX treatment. Action potential recovery was measured using a paired two-pulse protocol. **(A)** Representative traces in the absence of Fsk+IBMX (25 μM + 500 μM) at time t=0 min. A 1 ms pulse of current (2 nA in amplitude) was injected in order to depolarize the fibre to threshold. This was followed by a recovery step starting at 40 ms and decreasing to 8 ms, in 2 ms increments. The amplitude of the second current pulse was identical to the first. **(B)** The amplitude of the second action potential relative to the first, was plotted against the duration of the stimulus interval at t = 0 mins and at t = 5 mins for the DMSO time controls, and before (control, t = 0 mins) and after application of Fsk+IBMX for 5 mins. There was no difference in action potential recovery between the DMSO time controls and Fsk+IBMX treatments at either the t = 0 or t = 5 min time points.

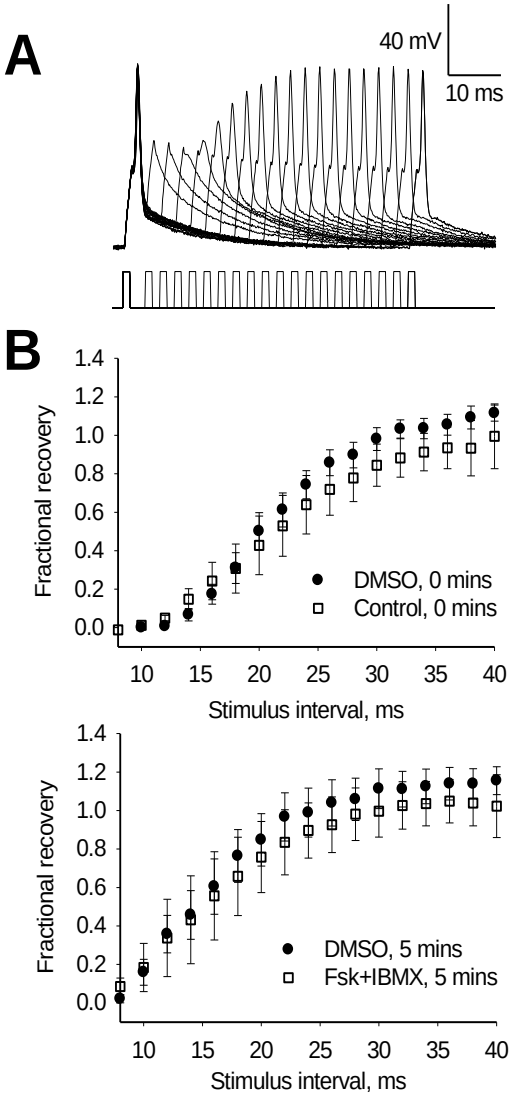
A
40 mV
10 ms
B
Fractional recovery
1.4
1.2
1.0
0.8
0.6
0.4
0.2
0.0
10
15
20
25
30
35
40
Stimulus interval, ms
DMSO, 0 mins
Control, 0 mins
Fractional recovery
Stimulus interval, ms
DMSO, 5 mins
Fsk+IBMX, 5 mins

Figure 5.8 High frequency stimulation of muscle fibers in the presence of Fsk+IBMX. Muscle fibres were depolarized with 20 x 1 ms pulses of current (1.5 nA) over a 500 ms time period (40 Hz). **(A)** Action potentials recorded in the absence (control) and presence of Fsk+IBMX (25 μM + 500 μM). **(B)** The first (black), tenth (red) and twentieth (blue) action potentials in the control (t = 0 min) and Fsk+IBMX (t = 5 min) treated bursts are shown for clarity. Quantification of the amplitude **(C)** and half width **(D)** of the twentieth action potential in the control and Fsk+IBMX treated fibres show that the amplitude is significantly increased, but there is no change in the half width (n=4). ** Denotes significance at $p<0.01$.

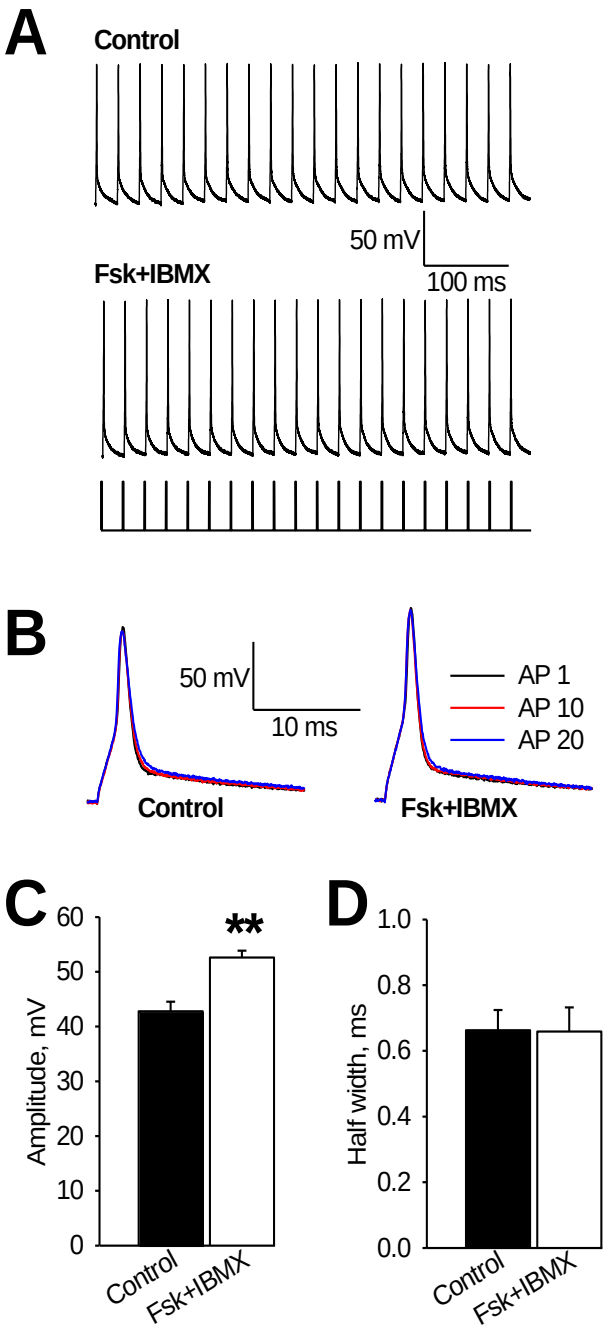
A
Control
50 mV
100 ms
Fsk+IBMX
B
50 mV
10 ms
AP 1
AP 10
AP 20
Control
Fsk+IBMX
C
**
Amplitude, mV
60
50
40
30
20
10
0
Control
Fsk+IBMX
D
Half width, ms
1.0
0.8
0.6
0.4
0.2
0.0
Control
Fsk+IBMX

Figure 5.9 4-Aminopyridine blocks the A-type K_V current and changes the shape of the action potential. A-type K+ currents. **(A)** and muscle action potentials **(B)**, recorded in the absence (black traces) and presence (red traces) of 5 mM 4-AP. Addition of 4-AP completely blocks the K^+ current and significantly increases the amplitude **(C)** and the width **(D)** of the muscle action potential (n=4). * Denotes significance at $p<0.05$, *** at $p<0.001$.

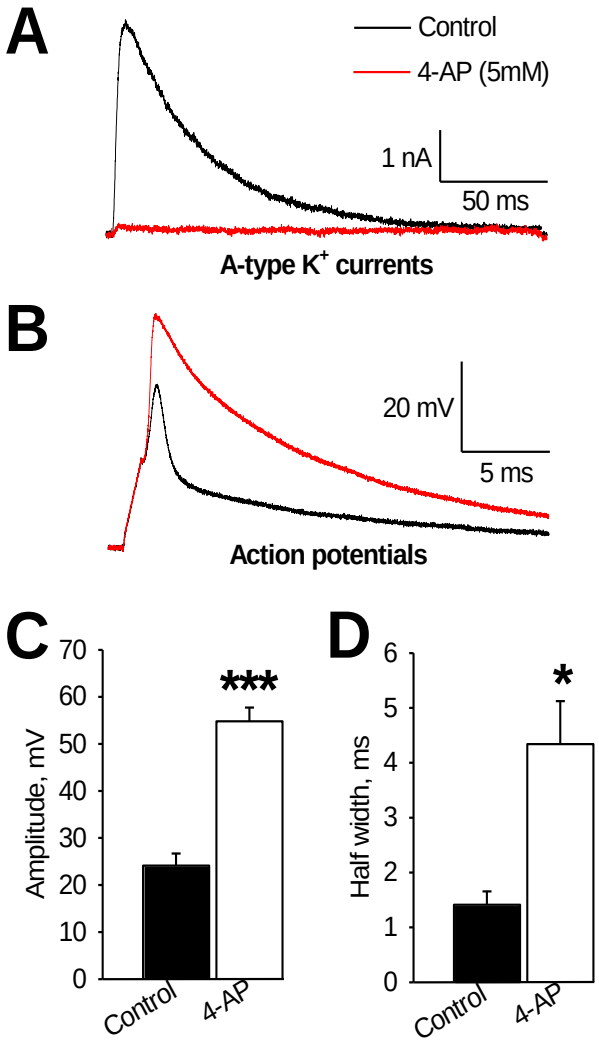
A
Control
4-AP (5mM)
1 nA
50 ms
A-type K+ currents
B
20 mV
5 ms
Action potentials
C
Amplitude, mV
70
60
50
40
30
20
10
0
***
Control
4-AP
D
Half width, ms
6
5
4
3
2
1
0
*
Control
4-AP

Figure 5.10 Effect of intracellular application of cAMP analogues. Peak current density at 20 mV is significantly reduced by intracellular cAMP+IBMX and Sp-cAMP+IBMX treatment, but not Rp-cAMP+IBMX, a competitive inhibitor of PKA. All cAMP analogues were applied intracellularly at a concentration of 500 μM, while IBMX was applied extracellularly (as it was with Fsk) at a concentration of 500 μM. *** Denotes significance from control at $p<0.001$.

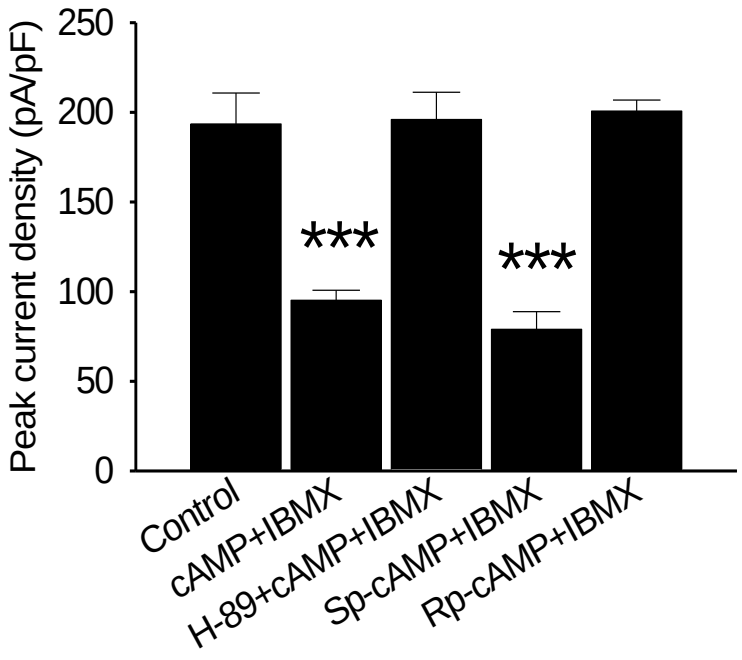
Peak current density (pA/pF)
250
200
150
100
50
0
***
***
Control
cAMP+IBMX
H-89+cAMP+IBMX
Sp-cAMP+IBMX
Rp-cAMP+IBMX

Figure 5.11 Application of Fsk+IBMX modulates A-type K_V currents similarly at all ages examined. **(A)** IV plot at 1 dpf shows Fsk+IBMX treatment reduces peak current density by ~50%, and is quantified at +20 mV in the bar graph. **(B)** IV plot at 6 dpf is very similar. A liquid junction potential of 6.7 mV was accounted for in all plots. *** Denotes significance at $p<0.001$.

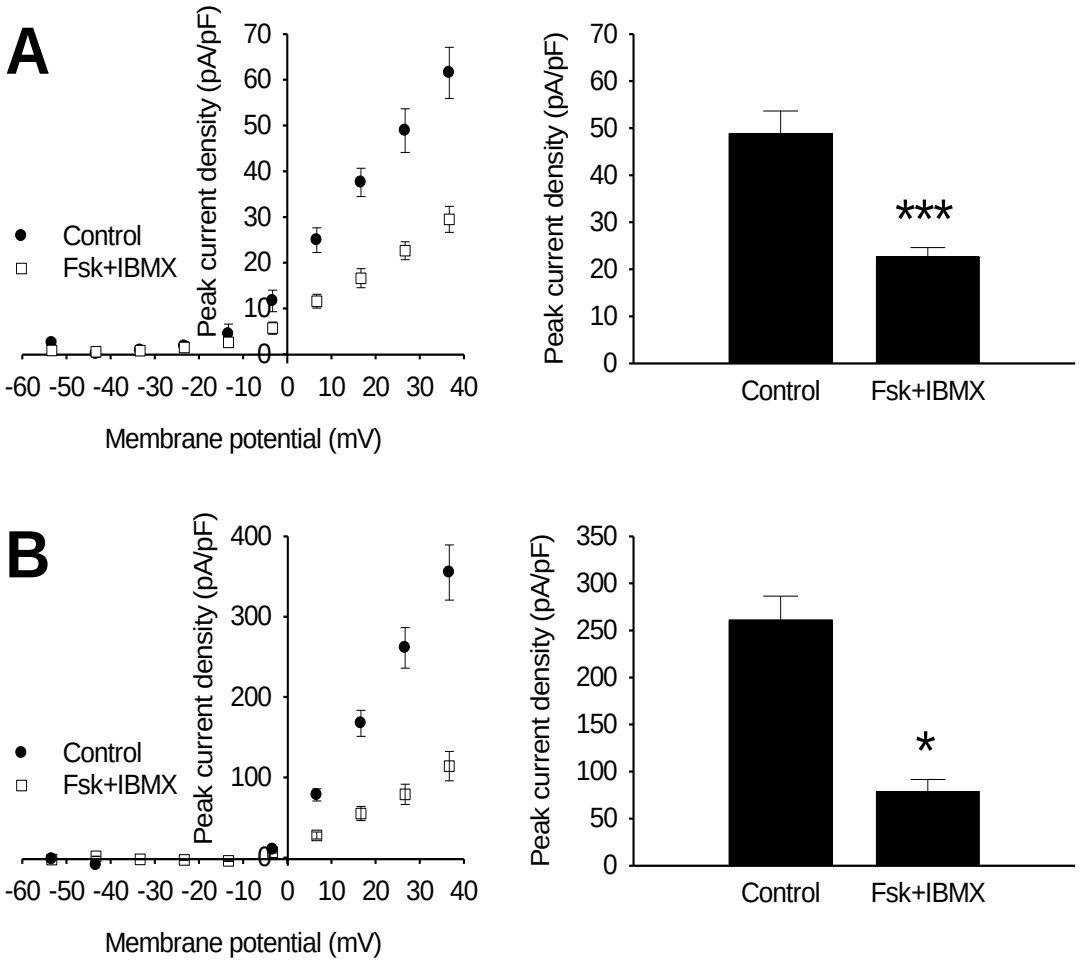
A
Peak current density (pA/pF)
70
60
50
40
30
20
10
0
Control
Fsk+IBMX
-60 -50 -40 -30 -20 -10 0 10 20 30 40
Membrane potential (mV)
***
Control
Fsk+IBMX
B
Peak current density (pA/pF)
400
300
200
100
0
Control
Fsk+IBMX
-60 -50 -40 -30 -20 -10 0 10 20 30 40
Membrane potential (mV)
350
300
250
200
150
100
50
0
*
Control
Fsk+IBMX

Table 5.1 Activation V_{50}s and slope factors of white fibers following PKA activation

Experiment	V_{50} (mV)		Slope factor	
	Initial recording t=0 minutes	Test recording t=5 minutes	Initial recording t=0 minutes	Test recording t=5 minutes
DMSO control	4.9±2.2 (6)	7.2±1.6 (6)	6.4±0.3 (6)	5.8±0.3 (6)
Fsk + IBMX	3.7±1.6 (7)	2.4±1.4 (7)	6.2±0.3 (7)	4.9±0.5 (7)*****
H-89+Fsk+IBMX	5.1±0.5 (4)	6.1±0.5 (4)	6.3±0.5 (4)	5.1±0.8 (4)

In experiments labeled DMSO control and Fsk+IBMX, the initial recording was performed in normal physiological saline and the test recording was performed after 5 minutes application of DMSO (0.3%) or forskolin (25 μM)+IBMX (500 μM) respectively. In experiments labeled H-89+Fsk+IBMX, the initial recording was performed after 5-7 minutes pre-incubation in H-89 (10 μM) followed by 5 minutes application of forskolin+IBMX. ***** denotes significantly different from the initial recording at $p<0.05$.

Table 5.2 Inactivation V_{50}s and slope factors of white fibers following PKA activation

Experiment	V_{50} (mV)		Slope factor	
	Initial recording t=0 minutes	Test recording t=5 minutes	Initial recording t=0 minutes	Test recording t=5 minutes
DMSO control	-17.9±1.7 (5)	-17.6±1.4 (5)	-4.3±0.2 (5)	-4.8±0.3 (5)
Fsk + IBMX	-17.2±1.3 (6)	-14.1±0.6 (6)*****	-5.1±0.4 (6)	-5.1±0.3 (6)
H-89+Fsk+IBMX	-18.5±2.2 (4)	-17.6±1.6 (4)	-4.8±0.4 (4)	-5.4±0.5 (4)

In experiments labeled DMSO control or Fsk+IBMX, the initial recording was performed in normal physiological saline and the test recording was performed after 5 minutes application of DMSO (0.3%) or forskolin (25 μM)+IBMX (500 μM) respectively. In experiments labeled H-89, the initial recording was performed after 5-7 minutes pre-incubation in H-89 (10 μM) followed by 5 minutes application of forskolin+IBMX. ***** denotes significantly different from the initial recording at $p<0.05$.

6. DISCUSSION

Excitable cells have been found to display dynamically regulated changes in the properties of ion channels and their currents during development. These changes are frequently crucial for the proper maturation of cellular excitability, and therefore have the potential to affect more sophisticated functions, including neural circuits, movement, behavior, and disease states. With the abundance of data illustrating the effects of Na_V and K_V current development on cellular excitability, the need arises to understand the mechanisms responsible for bringing these changes about. Recent studies have demonstrated the potential of a variety of mechanisms for cells to utilize in the maturation of excitability; this thesis has focused on the following: synaptic activity as a means of controlling ion channel functions, and modulation of channels by PKA.

6.1 Development of Na_V and K_V currents in zebrafish skeletal muscle

The steady-state and kinetic properties of Na_V and K_V currents were characterized in developing embryonic and larval zebrafish skeletal muscle fibers. In addition, action potentials were recorded in developing twitch muscle. Several interesting developmental changes were documented in the properties of both Na_V and K_V currents, which appear to affect action potentials and may have implications for muscle excitability.

6.1.1 K_V current development

It had previously been shown that the red and white fibers of zebrafish skeletal muscle express different K_V currents in 4-6 dpf larvae (Buckingham & Ali, 2004). The white fibers support an inactivating A-type current that was blocked by micromolar concentrations of 4-AP (Connor & Stevens, 1971; Buckingham & Ali, 2004), whereas the red fibers possess a delayed rectifier-type K_V current. Here, K_V currents in red fibers were found to reach their peak current density very early in development, prior to 1 dpf, and then maintain this density, at least until the end of the first week of maturation. In contrast, the peak current density of the A-type current in white fibers was not achieved until approximately 2 dpf. A developmental increase in peak current density is typical of many systems (Spitzer & Ribera, 1998), and for this reason a gradual increase in the peak current density for the K_V currents in both fibers had been expected for this study; it may be that K_V currents in red fibers of embryos younger than 1 day post fertilization would have exhibited lower peak current densities. A close examination of the development of zebrafish axial muscle has shown that the precursors of red and white fibers are different populations of cells, rather than a single cell precursor which differentiates into the two fiber types (Devoto *et al.*, 1996; Stickney *et al.*, 2000). This is very much like chick embryos, where the red and white fibers have been shown to arise from separate cellular precursors (Stockdale, 1992; Van

Swearingen & Lance-Jones, 1995). Zebrafish red and white fibers are therefore distinct cell types that display very different phenotypes throughout the first week of development. In fact, in zebrafish the red fibers are the first to differentiate (Devoto *et al.*, 1996), suggesting that the development of their ion channels may occur before that of other fibers.

The differences between the ion channel complement and current characteristics of the red and white fibers are striking. The K_V currents in red fibers differ from those in white in almost every property investigated, including the peak current density, which is ~10-fold less than that of the A-type current in white fibers. This is not surprising because during muscle activation these fibers are not depolarized to the same extent as the white fibers (due to a lack of Na_V channels) and therefore the requirement for a strong hyperpolarization is unnecessary. The red fibers have a small inactivating component at potentials greater than 10 mV, which is possibly due to the recruitment of a second type of K_V current such as a high voltage-activated K_V current. The two muscle types, red (tonic) and white (twitch), differ in a number of additional properties. For example, the active zones of the presynaptic terminals of twitch fibers possess a greater number of calcium channels and SNARE complexes per synaptic vesicle; this characteristic is thought to underlie the larger (~10 times) quantal output of twitch fibers compared to tonic fibers (Walrond & Reese, 1985; Connor *et al.*, 1997). Synaptic currents of tonic fibers have lower amplitudes and longer time courses, due to the types of post-synaptic

receptors present; low-conductance nAChRs, which in twitch fibers are only expressed in embryonic and denervated muscle, predominate in tonic fibers (Henderson & Brehm, 1989). One of the overwhelming differences is the lack of Na_V channels and action potentials in red fibers, but this begs the question: what role are K_V channels playing in red fibers if not one of membrane repolarization during the action potential? In addition to their role in the action potential, K_V channels in excitable cells are known to generally lower the effectiveness of excitatory inputs on a cell when they are open (Hille, 2001). This would appear to be a plausible explanation for their presence in red muscle, considering the need for strictly transient muscle activation during fast, undulatory swimming in order to prevent simultaneous bilateral muscle contraction. Future experiments could investigate this possibility by first cloning and then removing or reducing K_V channels in red muscle via genetic manipulation (gene knockout/knockdown technologies) or pharmacological manipulations. Red fibers are also known to be specialized for oxidative metabolism, to express slow isoforms of myosin, and to be innervated by multiple secondary neurons along their entire length (van Raamsdonk *et al.*, 1980; van Raamsdonk *et al.*, 1982; Westerfield *et al.*, 1986; van Asselt *et al.*, 1993). All together, these characteristics strongly suggest that the zebrafish red muscle fibers are, in fact, of the tonic or non-twitch variety.

One of the typical developmental changes exhibited by K_V currents is an overall acceleration of the kinetics (Spitzer & Ribera, 1998). In

zebrafish skeletal muscle, the 10-90% rise time of K_V currents in both red and white fibers was significantly longer in young embryos compared with older animals. In red fibers the rise time fell from ~7 to 2 ms over a 2 day period, whereas in white fibers it fell more gradually to ~2 ms over a 5 day period. An acceleration of the kinetics was also noted for the time course of inactivation (τ_{inact}) of the A-type K_V current. τ_{inact} was found to be large and highly variable in 1 dpf embryos compared with older animals. Interestingly, the developmental expression of the auxiliary subunit, K_V β1.1, is correlated with a decrease in the time constant of inactivation of K_V 1 currents during the development of cultured hippocampal neurons (Falk *et al.*, 2003), suggesting that a similar mechanism may be involved in the acceleration of τ_{inact} in this study. Major developmental events occur between 1 & 2 dpf compared with other ages throughout the first week of development. It was previously found that inhibitory glycinergic, and excitatory glutamatergic synapses in the central nervous system changed properties sometime between 1 and 2 dpf (Ali *et al.*, 2000a; Ali *et al.*, 2000b). In addition, mEPCs at the neuromuscular junction (Nguyen *et al.*, 1999) also changed properties between 1 and 2 dpf. At this stage, zebrafish are still within the chorion (egg case), but will soon hatch around 48 to 52 hpf. Embryos undergo characteristic sequences of motor behaviors throughout development (Saint-Amant & Drapeau, 1998) and the faster kinetics of voltage-gated (this study) and ligand-gated channels may be necessary to prepare the animal for life outside the chorion, where

fast swimming and strong escape responses may mean the difference between life and death. Alternatively, strong coiling and twisting movements needed to tear the egg case during hatching may more likely occur when ion channel kinetics develop into the mature forms.

6.1.2 Na_V current development

There was a significant increase in the peak current density of the inward Na_V currents in the white fibers between 1 and 2 dpf. There was also a significant hyperpolarization in the voltage-dependence of both activation and inactivation during development. These characteristics are similar to mouse skeletal muscle development (Gonoi *et al.*, 1989), where the voltage-dependence of Na_V currents are hyperpolarized by 9-17 mV in the first week after birth. This may be caused by the gradual appearance of the β subunit (Patton *et al.*, 1994). Reconstitution of the α subunit of Na_V channels without the β subunits resulted in a depolarization of the inactivation curve (Wallner *et al.*, 1993; Makita *et al.*, 1994; Patton *et al.*, 1994). Northern blots of rat CNS show that RNA for the β1 subunit is not present until close to day P14, correlating well with physiological changes in the steady state properties of activation and inactivation kinetics that occur at the same time as the onset of β1 expression (Patton *et al.*, 1994).

Na_V channels were found to have recovered from inactivation within 10 ms. In addition, there is no significant change in the speed of recovery during development. The upper limit of tail beat frequency is around 50 Hz

(Budick & O'Malley, 2000), and white muscle fibers are active at frequencies up to around 60Hz during fictive swimming episodes (Buss & Drapeau, 2002). White muscle can follow short trains of stimuli when delivered at frequencies up to 30 Hz (Buss & Drapeau, 2000) and all of these frequencies are well within a theoretical maximum rate of action potential firing of ~100 Hz.

6.1.3 Physiological and behavioral significance

A developmental increase in the density of A-type K_V currents, coupled with a shorter rise time, should result in a faster repolarization of the action potential and possibly a reduction in the amplitude. The timing of these developmental changes is interesting because the peak current density of the Na_V currents also increases dramatically between 1 and 2 dpf. Therefore, the peak current density of both the Na_V and K_V currents in white fibers increase by approximately 3- to 4-fold, approximately simultaneously. The A-type current is associated with white fibers to ensure that the muscle will be rapidly repolarized following an action potential. Because white fibers fire only a single action potential regardless of the duration of the excitatory input, they will need to repolarize to remove Na_V current inactivation in order to fire again. This is critical for fast swimming during the escape response. Zebrafish undergo a series of characteristic behaviors between 17 and 48 hpf: they spontaneously contract between 17 and 27 hpf, they coil in response to

touch starting at 21 hpf and then swim in response to touch after 27 hpf (Saint-Amant & Drapeau, 1998). The speed of evoked coiling increases 3-fold between 19 and 24 hpf, while the speed of contraction also increases approximately 3-fold between 24 and 36 hpf (Saint-Amant & Drapeau, 1998), after which it appears to stabilize. The developmental changes in the peak current density of the Na_V current between 24 and 48 hpf will result in a greater change in voltage per unit time and consequently a faster action potential with faster muscle contractions. Interestingly, the peak current densities of both Na_V and K_V currents increase 3- to 4-fold between 24 and 48 hpf. It is striking that many of the major developmental events in the characteristics of the Na_V and K_V currents appear to occur at precisely the time when zebrafish locomotor behaviors are changed into the adult repertoire.

In conclusion, there are several changes in the steady-state properties of Na_V and K_V currents in developing zebrafish tonic and twitch fibers. The most significant of these changes are the increased peak current density of the Na_V and A-type currents, the acceleration of the K_V current kinetics and the negative shift in the steady-state of inactivation of the Na_V currents. These changes shift the functional working range of the channels to a more appropriate state for the adult animal where muscle resting potentials are more negative (approximately -80 mV) (Westerfield *et al.*, 1990) than in the larva (approximately -60 mV; see APPENDIX 3).

6.2 Synaptic activity and ion current development in zebrafish skeletal muscle

Having established the developmental progression of ion currents, the next goal was to determine whether the normal development of K_V and Na_V currents in zebrafish muscle is dependent upon synaptic activity. There is no evidence to suggest that there is a neurotransmitter other than acetylcholine at the zebrafish neuromuscular junction; therefore, for the purposes of this study, the term “synaptic activity” specifically refers to cholinergic input because the synaptic receptors affected in the *sop* mutation are nAChRs. Advantage was taken of the well-characterized *sop* mutant (Granato *et al.*, 1996; Ono *et al.*, 2001; Li *et al.*, 2003; Ono *et al.*, 2004; Etard *et al.*, 2005; Panzer *et al.*, 2006), which does not possess nAChRs at neuromuscular junctions, and therefore does not receive synaptic input to skeletal muscle fibers. Investigating zebrafish mutants is not without its caveats; although the mutation has been well-characterized and appears to be localized to nAChRs at the neuromuscular junction, it is possible that other proteins may be affected. Attempts were made to mimic and confirm the *sofa potato* phenotype by chronically exposing zebrafish embryos and larvae to nAChR blockers such as D-tubocurarine and α-bungarotoxin; these were not successful, however, due to practical complications and ethical considerations.

6.2.1 K_V currents in developing *sofa potato* mutants

In studying the *sofa potato* mutation it was discovered that the density of K_V currents in red and white muscle is significantly different between the *sop*$^{-/-}$ mutants and their *sop*$^{+/?}$ siblings at 6 dpf, but not at earlier ages. In the *sop*$^{+/?}$ siblings, the current density increases between 3 and 6 dpf, whereas this increase does not occur in the sop mutants. This difference in the peak current density is striking, and may be explained by several possibilities; muscle size in the *sop*$^{-/-}$ mutants may be larger than their siblings at 6 dpf; the trafficking of K_V channels might be affected in an activity-dependent manner, or K_V gene expression might be altered.

The developmental changes that occur with these currents may be due to the appearance of channels with different subunit compositions, the upregulation of auxiliary subunits such as the KChIPs (An *et al.*, 2000; Shibata *et al.*, 2003), or a change in the modulation of the channels via enzymes such as protein kinases (Lin *et al.*, 2006). One of the more recently identified auxiliary subunits, known as KChIP, has been shown to modulate the properties of K_V channels in interesting ways. KChIPs were first identified in rats and were found to associate with the α subunits of K_V channels that are responsible for producing the A-type current (An *et al.*, 2000). In the absence of the KChIPs, A-type currents are several-fold smaller (due to a reduction in K_V channel surface expression), the activation curve is shifted to more positive potentials and the channels inactivate at a faster rate (An *et al.*, 2000). Thus, it is possible that the lack

of synaptic activity affects KChIP function in zebrafish. However, a change in channel kinetics or shifts in the V_{50} of activation in the K_V currents of 6 dpf mutants were not detected, suggesting that an alteration in KChIP activity may not be responsible for the changes in K_V current density in the mutants.

An alternative mechanism for changing current density is an enzyme-dependent trafficking process (Kim *et al.*, 2007; Hammond *et al.*, 2008). Hippocampal neurons that are treated with AMPA undergo an increase in synaptic activity and an internalization of K_V 4.2 channels that is dependent upon PKA (Hammond *et al.*, 2008). These findings suggest that a lack of synaptic activity decreases channel density. One possibility for a reduction in channel expression is regulation at the level of the gene. Thus, the lack of synaptic activity might reduce the transcription or translation of the genes that give rise to the A-type channel. Another possibility is that the channels are produced normally, but are not inserted into the membrane, or are internalized at a greater rate. However, the mechanism for the downregulation of channel expression at 6 dpf remains unknown.

6.2.2 Na_V currents in developing *sofa potato* mutants

Na_V currents in white muscle fibers of *sop*$^{-/-}$ mutants were also affected at 6 dpf. However, the changes were minor compared with those of the K_V currents. Indeed, the only difference was that the voltage-

dependence of inactivation was slightly more positive in *sop*$^{-/-}$ mutants. Na_V channels, like K_V channels, are comprised of several subunits including a primary α subunit and one or more auxiliary subunits (Roberts & Barchi, 1987; Catterall, 1992; Goldin, 2001). The auxiliary subunits serve to shift voltage dependences and modulate channel expression (Catterall, 1992; Goldin, 2001). Thus, it is possible that the function or the developmental onset of one of these auxilliary subunits was altered in the absence of synaptic activity.

6.2.3 Synaptic activity and current development

The role played by synaptic activity in the development of excitability properties of neurons and muscle fibers appears to be very diverse. For instance, in mouse hippocampal neurons, blockade of synaptic activity inhibits the developmental upregulation of some K_V channels (K_V 1.1, 1.2, and 1.4), but not others (K_V 1.3, 1.5, and 1.6) (Grosse *et al.*, 2000). This type of diversity is also evident in this study, where the K_V current density in *sop*$^{-/-}$ mutants is lower in both red and white fibers, but the Na_V current density is not. Similarly, the V_{50} of Na_V current inactivation is different in *sop*$^{-/-}$ mutants, while K_V activation and inactivation are unaffected. Thus, Na_V and K_V currents appear to be differentially regulated by cholinergic input in zebrafish skeletal muscle.

Might these differences be a consequence of secondary changes, such as the loss of gap junctions in the muscle? This is certainly possible,

but only the white muscle fibers appear to lose their coupling by approximately 5 dpf, whereas the red fibers do not. One might therefore expect that if the loss of coupling was involved in the transtion at 6 dpf, then this would affect the A-type K_V currents and the Na_V currents (white muscle) and not the K_V currents in red fibers. However, since the decrease in current density at 6 dpf occurs with K_V currents from both red and white fibers, loss of cell coupling is not likely to be involved in the transition just prior to 6 dpf.

A common intermediary in activity-dependent developmental mechanisms and the control of gene expression is calcium. Calcium signalling can control aspects of cell development at the transcriptional level, including the expression of voltage-gated ion channels (Mennerick & Zorumski, 2000; Spitzer *et al.*, 2002; Moody & Bosma, 2005; Spitzer, 2006). It is possible that ion channel development in zebrafish muscle is influenced by calcium signalling because synaptic activity at the NMJs of zebrafish embryos has been shown to cause calcium release from intracellular stores, resulting in cytosolic calcium transients (Brennan *et al.*, 2005). Removal of synaptic activity abolishes these transients and results in disruptions in myofibril organization (Brennan *et al.*, 2005). Therefore, decreased synaptic activity can compromise structural properties of developing zebrafish muscle, and may also affect electrical properties, as suggested here.

The goal for this aspect of the overall study was to determine if the normal developmental profile of Na_V and K_V currents of zebrafish red and white muscle was activity-dependent. A potential role for cholinergic activity in the regulation of some aspects of K_V and Na_V current development has been demonstrated. However, many developmental changes appear to occur independently of synaptic activity, and thus may be under the control of cell-autonomous genetic programs or other inputs. Synaptic activity leading to muscle excitation is known to be involved in several important aspects of muscle development, including the extrasynaptic repression of nAChR expression and synapse elimination (Sanes & Lichtman, 1999). On the other hand, genes that encode many contractile and synaptic proteins are activated early on in cellular differentiation, prior to innervation. Indeed, these genes are expressed even when muscle fibers are cultured in complete isolation from motorneurons (Sanes & Lichtman, 1999). It is also possible that the development of ion channels is dependent upon neuron-derived signals other than direct electrical stimulation at the NMJ. For example, the clustering of nAChRs at sites of neuron-muscle contact was found to be dependent on agrin, which is synthesized and released by motorneurons to be incorporated into the basal lamina of the NMJ, where it interacts with muscle-specific kinase (MuSK) to cause rapsyn-dependent nAChR clustering (Sanes & Lichtman, 1999). Another example is the synapse-specific transcription of nAChRs by neuregulin via epidermal growth

factor-related (erbB) receptor tyrosine kinase (Si *et al.*, 1996; Tansey *et al.*, 1996; Altiok *et al.*, 1997).

6.3 Modulation of A-type K_V channels by PKA during development

K_V channels play major roles in setting the resting membrane potential, cell excitability and in shaping the action potential (Hille, 2001). Modulation of these channels may therefore be an important aspect of cell functioning. The goals of this study were to test whether activation of PKA was capable of affecting the A-type K_V current found in zebrafish white muscle fibers, whether modulation of these currents affects the muscle firing properties, and, importantly, whether PKA modulation might be involved in the developmental changes observed in A-type currents. In many cells, an A-type current is capable of controlling cell excitability and changes in its properties may affect the production of action potentials (Connor & Stevens, 1971; Rudy, 1988; Tierney & Harris-Warrick, 1992). Activation of PKA resulted in a number of significant changes to the steady state and kinetic properties of the K_V current, which in turn affected the shape of the action potential; this is also the case in neurons. However, contrary to findings in neurons, the effects on K_V described here were insufficient to significantly affect the firing frequency of the muscle cell. The major changes that occur to the K_V current, following application of Fsk+IBMX are, 1) a 50-60% reduction in peak current amplitude, 2) a

change in the kinetics of the decay component, 3) a reduction in the slope factor of activation, and 4) a depolarizing shift in the inactivation curve.

A combination of forskolin and IBMX was utilized to ensure that adenylate cyclase was activated and that cAMP levels increased rapidly and significantly during the short time course of the experiment. This was necessary because whole-cell recordings from these muscle fibers could only be held for a relatively short time period (7-10 minutes maximum). The ability of the specific PKA inhibitor H-89 to block the effects of forskolin and IBMX, together with the use of cAMP analogs, suggests that PKA was indeed activated under these conditions.

6.3.1 Reduction of current density

Activation of PKA consistently and significantly reduced the peak current density and changed the inactivation kinetics of the K_V current. A PKA-induced suppression of A-type currents occurs in dorsal horn neurons (Hu & Gereau, 2003; Hu *et al.*, 2003) and in hippocampal CA1 pyramidal neurons (Hoffman & Johnston, 1998). The reduction in current density may occur via a shift in the voltage-dependence of activation; however the lack of effect of PKA on the V_{50} of activation does not support that hypothesis. Current density could also be diminished via reduced single-channel conductance or a reduction in the number of functional channels associated with the membrane.

One way of removing functional channels is by trafficking them into and out of the plasma membrane, a process that is potentially regulated by phosphorylation mechanisms (Jonas & Kaczmarek, 1996). For instance, in chick ciliary ganglion neurons, the movement of large-conductance Ca^{2+}- and voltage-activated K_V channels (K_{Ca}) into and out of the plasma membrane is negatively regulated by the p38-dependent pathway, which includes MEK6, p38, MAPK-activated protein kinase and HSP27 (Chae & Dryer, 2005). Similarly, activation of the protein kinase Akt leads to the mobilization of functional K_{Ca} to the plasma membrane (Chae *et al.*, 2005). In order to determine whether trafficking of channels is involved in the PKA-induced reduction in current density in zebrafish muscle, future experiments could attempt to block trafficking using clostridial neurotoxins such as tetanus and botulinum. Alternatively, one could assess whether membrane channels were being internalized using immunocytochemistry and/or western blots of membrane and cytosolic fractions of cell lysates. However, one caveat with these results concerns the timing of the PKA-induced change; PKA was activated rapidly, whereby the change in peak current density occurs within 5 minutes of drug application. If trafficking does take place in this preparation, it would need to be very rapid.

Another way to remove channels from the functional pool is to inhibit them by preventing channel activation. For example, PKA phosphorylation of STREX-1 splice variants of K_{Ca} channels results in a

reduction of single-channel activity by ~57%. Interestingly, other splice variants of this channel show unchanged or increased activity following phosphorylation by PKA, indicating that alternative splicing can act as a switch to determine the sensitivity of potassium channels to protein phosphorylation (Tian *et al.*, 2001).

6.3.2 Alteration of inactivation kinetics and voltage-dependence

The ability of Fsk+IBMX to change the inactivation kinetics from a single to a double exponential decay component in a manner that was not blocked by the specific PKA inhibitor, H-89, has also been shown to occur in other systems (Herness *et al.*, 1997; Schrader *et al.*, 2002; Hu & Gereau, 2003; Hu *et al.*, 2003). These results are difficult to interpret and the significance of the kinetic changes, as well as the mechanism underlying these changes, remains unknown. An examination of the current width at half amplitude indicates that the A-type current decays at a faster rate when PKA is activated. The ability of H-89 to block the majority of the PKA-induced decrease in peak current density, the change in slope factor of the activation curve and the shift in the inactivation curve, suggests that much of the effect of Fsk+IBMX is due to the activation of PKA. Further confusing matters were the effects of cAMP analog application, which resulted in either single or double exponential decays in an inconsistent manner. However, it is possible that the Fsk+IBMX treatment was non-specifically activating enzymes other than PKA.

Fsk+IBMX treatment depolarized the steady-state voltage-dependence of inactivation, but only by approximately 4 mV. This minor shift in voltage-dependence, which was inhibited by H-89 pre-incubation, suggests that PKA phosphorylation renders channels more readily available for activation. This would effectively increase K_V current amplitude. The reduction in peak current density and the positive shift in the voltage-dependence of inactivation seem to be at odds since the result of the first is to reduce current while the result of the second is to effectively increase it. However, the reduction in peak current density is dramatic, suggesting that the net effect of PKA activation may be to ensure that action potentials are produced more easily, or that action potential amplitude or width might be increased.

6.3.3 PKA and action potentials

Indeed, when PKA was activated, the action potential amplitude increased, and when the A-type current was completely blocked with 4-AP, both the action potential amplitude and width were significantly increased. In other systems, blocking the A-type K_V current with 4-AP leads to a dramatic increase in the duration of the action potential (Zhang & McBain, 1995a, b), indicating that the K_V current does in fact shape the action potential. It is interesting that completely blocking the A-type current in muscle leads to a significant widening of the action potential, but blocking it by ~60% (following activation of PKA) has no effect on action

potential width. This suggests that rapid repolarization of the action potential requires only a small amount of K^+ efflux, or that the normal movement of K^+ via the A-type current (in the absence of PKA activation) is significantly more than is necessary to repolarize the cell membrane. The functional consequences of an increase in action potential amplitude are difficult to determine. It is possible that PKA modulation of K_V channels, and the subsequent increase in action potential amplitude, increases the safety margin for propagation of the action potential when muscle activity is critical, for example during escape responses, or when fast swimming is necessary. In addition, a greater amplitude action potential may be a more effective means of recruiting muscle mass and increasing swimming speed without affecting swimming frequency.

In neurons, the A-type current also affects the frequency of action potentials (Connor & Stevens, 1971; Rudy, 1988; Tierney & Harris-Warrick, 1992). But the fact that zebrafish muscle fibers only fire once, even in the presence of sustained excitatory input suggests that modulation of the A-type current in this preparation may have little effect on the frequency of firing (Buckingham & Ali, 2004, 2005). This was indeed the case, because muscle fibers never fired more than once after activation of PKA. Furthermore, even when fibers were allowed to repolarize between stimuli to allow for recovery from Na_V channel inactivation, the rate of recovery during the paired pulse stimulation and the shape of the action potential during the high frequency stimulation did

not change. This suggests that the A-type current plays a minor role in firing frequency.

6.3.4 PKA modulation during development

Having characterized PKA modulation at 2 dpf, the next step was to determine whether PKA was able to modulate the A-type currents in an age-dependent manner. Recordings from 1 and 6 dpf fish revealed that activation of PKA had the same effect, primarily a 50-60% reduction in current density, regardless of the stage of development. PKA activation decreases current density, but developmentally there was an increase in current density; therefore, if PKA modulation were involved in this developmental change, it would necessitate a decrease in PKA activity, or perhaps an increase in phosphatase activity. Phosphatases are known to act on a variety of voltage-gated channels, including Na_V channels in the heart, brain and skeletal muscle (Smith & Goldin, 1992; Qu *et al.*, 1994; Bendahhou *et al.*, 1995), and both transient and delayed-rectifier K_V channels (Hescheler *et al.*, 1986; Xiao & McArdle, 1995).

In conclusion, the data support a model for the modulation of K_V channels in zebrafish white skeletal muscle by PKA. This is the first study to show that A-type K_V currents in muscle fibers can be modulated by PKA, which reduces the A-type current and increases the amplitude of the action potential. But, in contrast to neurons, modulation of these currents

does not lead to a change in the firing rates of action potentials when giving either sustained or repetitive, high-frequency stimuli. In addition, it appears that PKA modulation may not underlie the developmental changes observed during development, as there was no differential modulation of A-type currents.

6.4 Excitability and its role in disease states

Because membrane excitability, which is critical for muscle function, is regulated by voltage-gated ion channels, it is no surprise that ion channels are involved in diseases of skeletal muscle. In fact, many insights into ion channel function in general have been inspired by associated diseases, collectively called channelopathies (Lehmann-Horn & Jurkat-Rott, 1999). Channelopathies have common clinical features, recurrent patterns of mutations, and characteristic mechanisms of pathogenesis. In skeletal muscle, disorders are associated with mutations in voltage-gated sodium, potassium, calcium and chloride channels that generally result in one of two conditions - hypoexcitability (causing periodic paralysis) or hyperexcitabilty (causing myotonia or susceptibility to malignant hyperthermia).

Pioneering work on excised muscle tissue of patients with hereditary episodic weakness demonstrated the underlying defect to be a persistent Na_V current, which resulted in chronic depolarization of the membrane, eventually leading to inexcitability and weakness (Lehmann-

Horn *et al.*, 1987). Cloning and analysis of the gene that encodes the Na_V channel of skeletal muscle revealed the first mutations associated with impaired ion channel function and confirmed hyperkalemic periodic paralysis (hyperPP) to be a Na_V channel disorder (Fontaine *et al.*, 1990). Since then, over twenty diseases now termed as channelopathies have been described (Lehmann-Horn & Jurkat-Rott, 1999). The channelopathies first discovered in skeletal muscle now serve as models for understanding episodic disorders of the heart and brain, including cardiac arrhythmia, migraines, and epilepsy.

Examples of disease states caused by problems with the development of excitability are the pediatric seizure disorders. These diseases are known to be quite different from those in the mature brain; the majority of early-onset seizures are neocortical, rather than hippocampal, as in the adult (Mizrahi, 1999). Immature animals, including humans, are also more susceptible to seizures than adults (Sperber *et al.*, 1999). It is therefore likely that the location and increased susceptibility of immature brains to seizures is caused in part by the intrinsic properties of developing neurons, such as those of voltage-gated ion channels underlying excitability. Indeed, the cells of the neural circuits involved undergo a period of spontaneous, synchronized activity during a particular stage of development, which is normally abolished during the maturation process (Moody & Bosma, 2005). Failure to exit this period of spontaneous activity at the normal developmental stage is almost certain

to underlie the increased susceptibility of the immature brain to seizures. In turn, the seizures themselves have been shown to disrupt normal activity-dependent developmental process, including ion channel development (Jacobs *et al.*, 2000; Villeneuve *et al.*, 2000; Chen *et al.*, 2001). It must be stressed that a full understanding of these diseases requires knowledge of the roles that the development of voltage-gated ion channels play in a cellular and systemic context.

6.5 Conclusions and future directions

The properties of voltage-gated ion channels and their currents undergo dramatic changes during development. These developmental processes are often crucial for the proper maturation of cellular excitability, and therefore have the potential to affect more sophisticated functions, including neural circuits, movement, behavior, and disease states. The studies encompassed by this thesis sought to elucidate aspects of voltage-gated ion channel development within this system, with the overall goal of increasing the understanding of processes governing the development of excitability in cells in general.

Zebrafish skeletal muscle is an excellent model for studying the development of ion channels and their contributions to excitability. They possess distinguishable populations of red, tonic and white, twitch muscle fibers, whose biological functions are well understood. Furthermore, properties governing the excitability of these fibers can be studied and

correlated with the simple, well-characterized muscle-driven behavior of the organism as a whole.

A major accomplishment of these studies was the characterization of ion channel and action potential development that underlies the maturation of zebrafish motor activity from spontaneous contractions to beat-and-glide swimming. It is fascinating to think that such subtle alterations in voltage-gated currents may play a huge role in creating such drastically different movements and behaviors. This project would be well-served if the channels responsible for the recorded currents were cloned and identified.

The ability of synaptic activity to regulate developmental processes within excitable cells is well-documented; however it is certainly not required for all aspects of development. The *sofa potato* mutants have revealed that zebrafish skeletal muscle is an example of a system that is reliant on synaptic input for certain aspects of current development, namely K_V current density, but not for others. It would be interesting to determine whether an increase in synaptic activity, such as that reported in *twister* mutants (Lefebvre *et al.*, 2004), would disrupt normal current development in this system.

Phosphorylation of ion channels by kinases such as PKA has been shown to alter channel and current properties in ways similar to those observed in the developing zebrafish skeletal muscle. While the data

presented here certainly demonstrates the potential for PKA to modulate the activity of A-type K_V currents, it does not appear likely that it is involved in their maturation. K_V channels are known to have consensus sequences for several other kinases (PKC, MAPK/ERK, CaMKII) (Adams *et al.*, 2000; Anderson *et al.*, 2000), and it remains to be seen what roles, if any, they may play in muscle fiber physiology and development (see APPENDIX 1).

Overall, these findings provide novel insight into the roles played by voltage-gated currents during the development of excitability in zebrafish skeletal muscle, and expand the rapidly growing body of knowledge about ion channel function in general.

REFERENCES

Adams JP, Anderson AE, Varga AW, Dineley KT, Cook RG, Pfaffinger PJ & Sweatt JD. (2000). The A-type potassium channel Kv4.2 is a substrate for the mitogen-activated protein kinase ERK. *J Neurochem* **75,** 2277-2287.

Adrian RH & Marshall MW. (1977). Sodium currents in mammalian muscle. *J Physiol* **268,** 223-250.

Akerman KE, Enkvist MO & Holopainen I. (1988). Activators of protein kinase C and phenylephrine depolarize the astrocyte membrane by reducing the K+ permeability. *Neurosci Lett* **92,** 265-269.

Ali DW, Buss RR & Drapeau P. (2000a). Properties of miniature glutamatergic EPSCs in neurons of the locomotor regions of the developing zebrafish. *J Neurophysiol* **83,** 181-191.

Ali DW, Drapeau P & Legendre P. (2000b). Development of spontaneous glycinergic currents in the Mauthner neuron of the zebrafish embryo. *J Neurophysiol* **84,** 1726-1736.

Almers W, Roberts WM & Ruff RL. (1984). Voltage clamp of rat and human skeletal muscle: measurements with an improved loose-patch technique. *J Physiol* **347,** 751-768.

Altiok N, Altiok S & Changeux JP. (1997). Heregulin-stimulated acetylcholine receptor gene expression in muscle: requirement for MAP kinase and evidence for a parallel inhibitory pathway independent of electrical activity. *EMBO J* **16,** 717-725.

An WF, Bowlby MR, Betty M, Cao J, Ling HP, Mendoza G, Hinson JW, Mattsson KI, Strassle BW, Trimmer JS & Rhodes KJ. (2000). Modulation of A-type potassium channels by a family of calcium sensors. *Nature* **403,** 553-556.

Anderson AE, Adams JP, Qian Y, Cook RG, Pfaffinger PJ & Sweatt JD. (2000). Kv4.2 phosphorylation by cyclic AMP-dependent protein kinase. *J Biol Chem* **275,** 5337-5346.

Armstrong CM & Hille B. (1998). Voltage-gated ion channels and electrical excitability. *Neuron* **20,** 371-380.

Arnaout R, Ferrer T, Huisken J, Spitzer K, Stainier DY, Tristani-Firouzi M & Chi NC. (2007). Zebrafish model for human long QT syndrome. *Proc Natl Acad Sci U S A* **104,** 11316-11321.

Awad SS, Lightowlers RN, Young C, Chrzanowska-Lightowlers ZM, Lomo T & Slater CR. (2001). Sodium channel mRNAs at the neuromuscular junction: distinct patterns of accumulation and effects of muscle activity. *J Neurosci* **21,** 8456-8463.

Bahrey HL & Moody WJ. (2003). Voltage-gated currents, dye and electrical coupling in the embryonic mouse neocortex. *Cereb Cortex* **13,** 239-251.

Bahring R, Dannenberg J, Peters HC, Leicher T, Pongs O & Isbrandt D. (2001). Conserved Kv4 N-terminal domain critical for effects of Kv channel-interacting protein 2.2 on channel expression and gating. *J Biol Chem* **276,** 23888-23894.

Baines RA, Uhler JP, Thompson A, Sweeney ST & Bate M. (2001). Altered electrical properties in Drosophila neurons developing without synaptic transmission. *J Neurosci* **21,** 1523-1531.

Barish ME. (1986). Differentiation of voltage-gated potassium current and modulation of excitability in cultured amphibian spinal neurones. *J Physiol* **375,** 229-250.

Bassett DI & Currie PD. (2003). The zebrafish as a model for muscular dystrophy and congenital myopathy. *Hum Mol Genet* **12 Spec No 2,** R265-270.

Batty RS. (1984). Development of swimming movements and musculature of larval herring (Clupea harengus). *J Exp Biol* **110,** 217-229.

Beech DJ & Bolton TB. (1989). A voltage-dependent outward current with fast kinetics in single smooth muscle cells isolated from rabbit portal vein. *J Physiol* **412,** 397-414.

Bendahhou S, Cummins TR, Potts JF, Tong J & Agnew WS. (1995). Serine-1321-independent regulation of the mu 1 adult skeletal muscle Na+ channel by protein kinase C. *Proc Natl Acad Sci U S A* **92,** 12003-12007.

Blagden CS, Currie PD, Ingham PW & Hughes SM. (1997). Notochord induction of zebrafish slow muscle mediated by Sonic hedgehog. *Genes Dev* **11,** 2163-2175.

Bourdeau ML, Morin F, Laurent CE, Azzi M & Lacaille JC. (2007). Kv4.3-mediated A-type K+ currents underlie rhythmic activity in hippocampal interneurons. *J Neurosci* **27,** 1942-1953.

Brennan C, Mangoli M, Dyer CE & Ashworth R. (2005). Acetylcholine and calcium signalling regulates muscle fibre formation in the zebrafish embryo. *J Cell Sci* **118,** 5181-5190.

Bringmann A, Biedermann B & Reichenbach A. (1999). Expression of potassium channels during postnatal differentiation of rabbit Muller glial cells. *Eur J Neurosci* **11,** 2883-2896.

Buckingham SD & Ali DW. (2004). Sodium and potassium currents of larval zebrafish muscle fibres. *J Exp Biol* **207,** 841-852.

Buckingham SD & Ali DW. (2005). Computer simulations of high-pass filtering in zebrafish larval muscle fibres. *J Exp Biol* **208,** 3055-3063.

Budick SA & O'Malley DM. (2000). Locomotor repertoire of the larval zebrafish: swimming, turning and prey capture. *J Exp Biol* **203,** 2565-2579.

Buss RR & Drapeau P. (2000). Physiological properties of zebrafish embryonic red and white muscle fibers during early development. *J Neurophysiol* **84,** 1545-1557.

Buss RR & Drapeau P. (2002). Activation of embryonic red and white muscle fibers during fictive swimming in the developing zebrafish. *J Neurophysiol* **87,** 1244-1251.

Butler A, Wei AG, Baker K & Salkoff L. (1989). A family of putative potassium channel genes in Drosophila. *Science* **243,** 943-947.

Camacho J, Delay MJ, Vazquez M, Arguello C & Sanchez JA. (1996). Transient outward K+ channels in vesicles derived from frog skeletal muscle plasma membranes. *Biophys J* **71,** 171-181.

Campbell DT & Hille B. (1976). Kinetic and pharmacological properties of the sodium channel of frog skeletal muscle. *J Gen Physiol* **67,** 309-323.

Carlin KP, Liu J & Jordan LM. (2008). Postnatal changes in the inactivation properties of voltage-gated sodium channels contribute to the mature firing pattern of spinal motoneurons. *J Neurophysiol* **99,** 2864-2876.

Casadei JM, Gordon RD & Barchi RL. (1986). Immunoaffinity isolation of Na+ channels from rat skeletal muscle. Analysis of subunits. *J Biol Chem* **261,** 4318-4323.

Catterall WA. (1988). Structure and function of voltage-sensitive ion channels. *Science* **242,** 50-61.

Catterall WA. (1992). Cellular and molecular biology of voltage-gated sodium channels. *Physiol Rev* **72,** S15-48.

Catterall WA, Goldin AL & Waxman SG. (2005). International Union of Pharmacology. XLVII. Nomenclature and structure-function relationships of voltage-gated sodium channels. *Pharmacol Rev* **57,** 397-409.

Chae KS & Dryer SE. (2005). The p38 mitogen-activated protein kinase pathway negatively regulates Ca2+-activated K+ channel trafficking in developing parasympathetic neurons. *J Neurochem* **94,** 367-379.

Chae KS, Martin-Caraballo M, Anderson M & Dryer SE. (2005). Akt activation is necessary for growth factor-induced trafficking of functional K(Ca) channels in developing parasympathetic neurons. *J Neurophysiol* **93,** 1174-1182.

Chahine KG, Baracchini E & Goldman D. (1993). Coupling muscle electrical activity to gene expression via a cAMP-dependent second messenger system. *J Biol Chem* **268,** 2893-2898.

Chen K, Aradi I, Thon N, Eghbal-Ahmadi M, Baram TZ & Soltesz I. (2001). Persistently modified h-channels after complex febrile seizures convert the seizure-induced enhancement of inhibition to hyperexcitability. *Nat Med* **7,** 331-337.

Chen TC, Law B, Kondratyuk T & Rossie S. (1995). Identification of soluble protein phosphatases that dephosphorylate voltage-sensitive sodium channels in rat brain. *J Biol Chem* **270,** 7750-7756.

Chouinard SW, Wilson GF, Schlimgen AK & Ganetzky B. (1995). A potassium channel beta subunit related to the aldo-keto reductase superfamily is encoded by the Drosophila hyperkinetic locus. *Proc Natl Acad Sci U S A* **92,** 6763-6767.

Connaughton VP & Maguire G. (1998). Differential expression of voltage-gated K+ and Ca2+ currents in bipolar cells in the zebrafish retinal slice. *Eur J Neurosci* **10,** 1350-1362.

Connor EA, Dunaevsky A, Griffiths DJ, Hardwick JC & Parsons RL. (1997). Transmitter release differs at snake twitch and tonic endplates during potassium-induced nerve terminal depolarization. *J Neurophysiol* **77,** 749-760.

Connor JA & Stevens CF. (1971). Inward and delayed outward membrane currents in isolated neural somata under voltage clamp. *J Physiol* **213,** 1-19.

Covarrubias M, Wei A, Salkoff L & Vyas TB. (1994). Elimination of rapid potassium channel inactivation by phosphorylation of the inactivation gate. *Neuron* **13,** 1403-1412.

Currie DA & Moody WJ. (1999). Time course of ion channel development in Xenopus muscle induced in vitro by activin. *Dev Biol* **209,** 40-51.

Dargent B, Paillart C, Carlier E, Alcaraz G, Martin-Eauclaire MF & Couraud F. (1994). Sodium channel internalization in developing neurons. *Neuron* **13,** 683-690.

Dascal N & Lotan I. (1991). Activation of protein kinase C alters voltage dependence of a Na+ channel. *Neuron* **6,** 165-175.

Davis AK, Greaves AA, Dallman JE & Moody WJ. (1995). Comparison of ionic currents expressed in immature and mature muscle cells of an ascidian larva. *J Neurosci* **15,** 4875-4884.

Denac H, Mevissen M & Scholtysik G. (2000). Structure, function and pharmacology of voltage-gated sodium channels. *Naunyn Schmiedebergs Arch Pharmacol* **362,** 453-479.

Depaoli-Roach AA, Park IK, Cerovsky V, Csortos C, Durbin SD, Kuntz MJ, Sitikov A, Tang PM, Verin A & Zolnierowicz S. (1994). Serine/threonine protein phosphatases in the control of cell function. *Adv Enzyme Regul* **34,** 199-224.

DeRiemer SA, Strong JA, Albert KA, Greengard P & Kaczmarek LK. (1985). Enhancement of calcium current in Aplysia neurones by phorbol ester and protein kinase C. *Nature* **313,** 313-316.

Devoto SH, Melancon E, Eisen JS & Westerfield M. (1996). Identification of separate slow and fast muscle precursor cells in vivo, prior to somite formation. *Development* **122,** 3371-3380.

Duval A & Leoty C. (1978). Ionic currents in mammalian fast skeletal muscle. *J Physiol* **278,** 403-423.

Duval A & Leoty C. (1980a). Comparison between the delayed outward current in slow and fast twitch skeletal muscle in the rat. *J Physiol* **307,** 43-57.

Duval A & Leoty C. (1980b). Ionic currents in slow twitch skeletal muscle in the rat. *J Physiol* **307,** 23-41.

Eisen JS, Myers PZ & Westerfield M. (1986). Pathway selection by growth cones of identified motoneurones in live zebra fish embryos. *Nature* **320,** 269-271.

Eliasof S, Barnes S & Werblin F. (1987). The interaction of ionic currents mediating single spike activity in retinal amacrine cells of the tiger salamander. *J Neurosci* **7,** 3512-3524.

Engeszer RE, Patterson LB, Rao AA & Parichy DM. (2007). Zebrafish in the wild: a review of natural history and new notes from the field. *Zebrafish* **4,** 21-40.

Etard C, Behra M, Ertzer R, Fischer N, Jesuthasan S, Blader P, Geisler R & Strahle U. (2005). Mutation in the delta-subunit of the nAChR suppresses the muscle defects caused by lack of Dystrophin. *Dev Dyn* **234,** 1016-1025.

Falk T, Kilani RK, Strazdas LA, Borders RS, Steidl JV, Yool AJ & Sherman SJ. (2003). Developmental regulation of the A-type potassium-channel current in hippocampal neurons: role of the Kvbeta 1.1 subunit. *Neuroscience* **120,** 387-404.

Fein AJ, Wright MA, Slat EA, Ribera AB & Isom LL. (2008). scn1bb, a zebrafish ortholog of SCN1B expressed in excitable and nonexcitable cells, affects motor neuron axon morphology and touch sensitivity. *J Neurosci* **28,** 12510-12522.

Fetcho JR. (1987). A review of the organization and evolution of motoneurons innervating the axial musculature of vertebrates. *Brain Res* **434,** 243-280.

Fetcho JR. (1992). The spinal motor system in early vertebrates and some of its evolutionary changes. *Brain Behav Evol* **40,** 82-97.

Fontaine B, Khurana TS, Hoffman EP, Bruns GA, Haines JL, Trofatter JA, Hanson MP, Rich J, McFarlane H, Yasek DM & et al. (1990).

Hyperkalemic periodic paralysis and the adult muscle sodium channel alpha-subunit gene. *Science* **250,** 1000-1002.

Frohnwieser B, Chen LQ, Schreibmayer W & Kallen RG. (1997). Modulation of the human cardiac sodium channel alpha-subunit by cAMP-dependent protein kinase and the responsible sequence domain. *J Physiol* **498 (Pt 2),** 309-318.

Gao BX & Ziskind-Conhaim L. (1998). Development of ionic currents underlying changes in action potential waveforms in rat spinal motoneurons. *J Neurophysiol* **80,** 3047-3061.

Gershon E, Weigl L, Lotan I, Schreibmayer W & Dascal N. (1992). Protein kinase A reduces voltage-dependent Na+ current in Xenopus oocytes. *J Neurosci* **12,** 3743-3752.

Goldin AL. (2001). Resurgence of sodium channel research. *Annu Rev Physiol* **63,** 871-894.

Goldin AL. (2002). Evolution of voltage-gated Na(+) channels. *J Exp Biol* **205,** 575-584.

Gonoi T, Hagihara Y, Kobayashi J, Nakamura H & Ohizumi Y. (1989). Geographutoxin-sensitive and insensitive sodium currents in mouse skeletal muscle developing in situ. *J Physiol* **414,** 159-177.

Granato M & Nusslein-Volhard C. (1996). Fishing for genes controlling development. *Curr Opin Genet Dev* **6,** 461-468.

Granato M, van Eeden FJ, Schach U, Trowe T, Brand M, Furutani-Seiki M, Haffter P, Hammerschmidt M, Heisenberg CP, Jiang YJ, Kane DA, Kelsh RN, Mullins MC, Odenthal J & Nusslein-Volhard C. (1996). Genes controlling and mediating locomotion behavior of the zebrafish embryo and larva. *Development* **123,** 399-413.

Grande M, Suarez E, Vicente R, Canto C, Coma M, Tamkun MM, Zorzano A, Guma A & Felipe A. (2003). Voltage-dependent K+ channel beta subunits in muscle: differential regulation during postnatal development and myogenesis. *J Cell Physiol* **195,** 187-193.

Grega DS, Werz MA & Macdonald RL. (1987). Forskolin and phorbol esters reduce the same potassium conductance of mouse neurons in culture. *Science* **235,** 345-348.

Grosse G, Draguhn A, Hohne L, Tapp R, Veh RW & Ahnert-Hilger G. (2000). Expression of Kv1 potassium channels in mouse

hippocampal primary cultures: development and activity-dependent regulation. *J Neurosci* **20,** 1869-1882.

Guo W, Kamiya K & Toyama J. (1996). Modulated expression of transient outward current in cultured neonatal rat ventricular myocytes: comparison with development in situ. *Cardiovasc Res* **32,** 524-533.

Guo W, Kamiya K & Toyama J. (1997). Roles of the voltage-gated K+ channel subunits, Kv 1.5 and Kv 1.4, in the developmental changes of K+ currents in cultured neonatal rat ventricular cells. *Pflugers Arch* **434,** 206-208.

Gurantz D, Lautermilch NJ, Watt SD & Spitzer NC. (2000). Sustained upregulation in embryonic spinal neurons of a Kv3.1 potassium channel gene encoding a delayed rectifier current. *J Neurobiol* **42,** 347-356.

Gurantz D, Ribera AB & Spitzer NC. (1996). Temporal regulation of Shaker- and Shab-like potassium channel gene expression in single embryonic spinal neurons during K+ current development. *J Neurosci* **16,** 3287-3295.

Gutman GA, Chandy KG, Adelman JP, Aiyar J, Bayliss DA, Clapham DE, Covarriubias M, Desir GV, Furuichi K, Ganetzky B, Garcia ML, Grissmer S, Jan LY, Karschin A, Kim D, Kuperschmidt S, Kurachi Y, Lazdunski M, Lesage F, Lester HA, McKinnon D, Nichols CG, O'Kelly I, Robbins J, Robertson GA, Rudy B, Sanguinetti M, Seino S, Stuehmer W, Tamkun MM, Vandenberg CA, Wei A, Wulff H & Wymore RS. (2003). International Union of Pharmacology. XLI. Compendium of voltage-gated ion channels: potassium channels. *Pharmacol Rev* **55,** 583-586.

Gutman GA, Chandy KG, Grissmer S, Lazdunski M, McKinnon D, Pardo LA, Robertson GA, Rudy B, Sanguinetti MC, Stuhmer W & Wang X. (2005). International Union of Pharmacology. LIII. Nomenclature and molecular relationships of voltage-gated potassium channels. *Pharmacol Rev* **57,** 473-508.

Hagiwara S, Kusano K & Saito N. (1961). Membrane changes of Onchidium nerve cell in potassium-rich media. *J Physiol* **155,** 470-489.

Hammond RS, Lin L, Sidorov MS, Wikenheiser AM & Hoffman DA. (2008). Protein kinase a mediates activity-dependent Kv4.2 channel trafficking. *J Neurosci* **28,** 7513-7519.

Hassel D, Scholz EP, Trano N, Friedrich O, Just S, Meder B, Weiss DL, Zitron E, Marquart S, Vogel B, Karle CA, Seemann G, Fishman MC, Katus HA & Rottbauer W. (2008). Deficient zebrafish ether-a-go-go-related gene channel gating causes short-QT syndrome in zebrafish reggae mutants. *Circulation* **117,** 866-875.

Hattori S, Murakami F & Song WJ. (2003). Quantitative relationship between Kv4.2 mRNA and A-type K+ current in rat striatal cholinergic interneurons during development. *J Neurophysiol* **90,** 175-183.

Heinemann SH, Rettig J, Graack HR & Pongs O. (1996). Functional characterization of Kv channel beta-subunits from rat brain. *J Physiol* **493 (Pt 3),** 625-633.

Hell JW, Yokoyama CT, Breeze LJ, Chavkin C & Catterall WA. (1995). Phosphorylation of presynaptic and postsynaptic calcium channels by cAMP-dependent protein kinase in hippocampal neurons. *EMBO J* **14,** 3036-3044.

Henderson LP & Brehm P. (1989). The single-channel basis for the slow kinetics of synaptic currents in vertebrate slow muscle fibers. *Neuron* **2,** 1399-1405.

Herness MS, Sun XD & Chen Y. (1997). cAMP and forskolin inhibit potassium currents in rat taste receptor cells by different mechanisms. *Am J Physiol* **272,** C2005-2018.

Hescheler J, Kameyama M & Trautwein W. (1986). On the mechanism of muscarinic inhibition of the cardiac Ca current. *Pflugers Arch* **407,** 182-189.

Hille B. (2001). *Ion channels of excitable membranes*. Sinauer, Sunderland, Mass.

Hodgkin AL & Huxley AF. (1952a). The components of membrane conductance in the giant axon of Loligo. *J Physiol* **116,** 473-496.

Hodgkin AL & Huxley AF. (1952b). Currents carried by sodium and potassium ions through the membrane of the giant axon of Loligo. *J Physiol* **116,** 449-472.

Hodgkin AL & Huxley AF. (1952c). A quantitative description of membrane current and its application to conduction and excitation in nerve. *J Physiol* **117,** 500-544.

Hodgkin AL, Huxley AF & Katz B. (1952). Measurement of current-voltage relations in the membrane of the giant axon of Loligo. *J Physiol* **116,** 424-448.

Hoffman DA & Johnston D. (1998). Downregulation of transient K+ channels in dendrites of hippocampal CA1 pyramidal neurons by activation of PKA and PKC. *J Neurosci* **18,** 3521-3528.

Hoffman DA, Magee JC, Colbert CM & Johnston D. (1997). K+ channel regulation of signal propagation in dendrites of hippocampal pyramidal neurons. *Nature* **387,** 869-875.

Hoger JH, Walter AE, Vance D, Yu L, Lester HA & Davidson N. (1991). Modulation of a cloned mouse brain potassium channel. *Neuron* **6,** 227-236.

Holley SA & Nusslein-Volhard C. (2000). Somitogenesis in zebrafish. *Curr Top Dev Biol* **47,** 247-277.

Hoover F, Mathiesen I, Skalhegg BS, Lomo T & Tasken K. (2001). Differential expression and regulation of the PKA signalling pathway in fast and slow skeletal muscle. *Anat Embryol (Berl)* **203,** 193-201.

Hoshi N, Zhang JS, Omaki M, Takeuchi T, Yokoyama S, Wanaverbecq N, Langeberg LK, Yoneda Y, Scott JD, Brown DA & Higashida H. (2003). AKAP150 signaling complex promotes suppression of the M-current by muscarinic agonists. *Nat Neurosci* **6,** 564-571.

Hu CL, Zeng XM, Zhou MH, Shi YT, Cao H & Mei YA. (2008). Kv 1.1 is associated with neuronal apoptosis and modulated by protein kinase C in the rat cerebellar granule cell. *J Neurochem* **106,** 1125-1137.

Hu HJ & Gereau RWt. (2003). ERK integrates PKA and PKC signaling in superficial dorsal horn neurons. II. Modulation of neuronal excitability. *J Neurophysiol* **90,** 1680-1688.

Hu HJ, Glauner KS & Gereau RWt. (2003). ERK integrates PKA and PKC signaling in superficial dorsal horn neurons. I. Modulation of A-type K+ currents. *J Neurophysiol* **90,** 1671-1679.

Huang XC, Sumners C & Richards EM. (1996). Angiotensin II stimulates protein phosphatase 2A activity in cultured neuronal cells via type 2 receptors in a pertussis toxin sensitive fashion. *Adv Exp Med Biol* **396,** 209-215.

Ingham PW & Kim HR. (2005). Hedgehog signalling and the specification of muscle cell identity in the zebrafish embryo. *Exp Cell Res* **306,** 336-342.

Isom LL, Scheuer T, Brownstein AB, Ragsdale DS, Murphy BJ & Catterall WA. (1995). Functional co-expression of the beta 1 and type IIA alpha subunits of sodium channels in a mammalian cell line. *J Biol Chem* **270,** 3306-3312.

Jacobs KM, Graber KD, Kharazia VN, Parada I & Prince DA. (2000). Postlesional epilepsy: the ultimate brain plasticity. *Epilepsia* **41 Suppl 6,** S153-161.

Jeck CD & Boyden PA. (1992). Age-related appearance of outward currents may contribute to developmental differences in ventricular repolarization. *Circ Res* **71,** 1390-1403.

Johnson BD, Brousal JP, Peterson BZ, Gallombardo PA, Hockerman GH, Lai Y, Scheuer T & Catterall WA. (1997). Modulation of the cloned skeletal muscle L-type Ca2+ channel by anchored cAMP-dependent protein kinase. *J Neurosci* **17,** 1243-1255.

Jonas EA & Kaczmarek LK. (1996). Regulation of potassium channels by protein kinases. *Curr Opin Neurobiol* **6,** 318-323.

Kaczmarek LK & Strumwasser F. (1984). A voltage-clamp analysis of currents underlying cyclic AMP-induced membrane modulation in isolated peptidergic neurons of Aplysia. *J Neurophysiol* **52,** 340-349.

Kallen RG, Sheng ZH, Yang J, Chen LQ, Rogart RB & Barchi RL. (1990). Primary structure and expression of a sodium channel characteristic of denervated and immature rat skeletal muscle. *Neuron* **4,** 233-242.

Kamb A, Iverson LE & Tanouye MA. (1987). Molecular characterization of Shaker, a Drosophila gene that encodes a potassium channel. *Cell* **50,** 405-413.

Kang J, Posner P & Sumners C. (1994). Angiotensin II type 2 receptor stimulation of neuronal K+ currents involves an inhibitory GTP binding protein. *Am J Physiol* **267,** C1389-1397.

Katz LC & Shatz CJ. (1996). Synaptic activity and the construction of cortical circuits. *Science* **274,** 1133-1138.

Kilborn MJ & Fedida D. (1990). A study of the developmental changes in outward currents of rat ventricular myocytes. *J Physiol* **430,** 37-60.

Kim J, Jung SC, Clemens AM, Petralia RS & Hoffman DA. (2007). Regulation of dendritic excitability by activity-dependent trafficking of the A-type K+ channel subunit Kv4.2 in hippocampal neurons. *Neuron* **54,** 933-947.

Kim SJ, Choi WS, Han JS, Warnock G, Fedida D & McIntosh CH. (2005). A novel mechanism for the suppression of a voltage-gated potassium channel by glucose-dependent insulinotropic polypeptide: protein kinase A-dependent endocytosis. *J Biol Chem* **280,** 28692-28700.

Kondratyuk T & Rossie S. (1997). Depolarization of rat brain synaptosomes increases phosphorylation of voltage-sensitive sodium channels. *J Biol Chem* **272,** 16978-16983.

Langheinrich U, Vacun G & Wagner T. (2003). Zebrafish embryos express an orthologue of HERG and are sensitive toward a range of QT-prolonging drugs inducing severe arrhythmia. *Toxicol Appl Pharmacol* **193,** 370-382.

Lara A, Dargent B, Julien F, Alcaraz G, Tricaud N, Couraud F & Jover E. (1996). Channel activators reduce the expression of sodium channel alpha-subunit mRNA in developing neurons. *Brain Res Mol Brain Res* **37,** 116-124.

Lefebvre JL, Ono F, Puglielli C, Seidner G, Franzini-Armstrong C, Brehm P & Granato M. (2004). Increased neuromuscular activity causes axonal defects and muscular degeneration. *Development* **131,** 2605-2618.

Lehmann-Horn F & Jurkat-Rott K. (1999). Voltage-gated ion channels and hereditary disease. *Physiol Rev* **79,** 1317-1372.

Lehmann-Horn F, Kuther G, Ricker K, Grafe P, Ballanyi K & Rudel R. (1987). Adynamia episodica hereditaria with myotonia: a non-inactivating sodium current and the effect of extracellular pH. *Muscle Nerve* **10,** 363-374.

Leicher T, Bahring R, Isbrandt D & Pongs O. (1998). Coexpression of the KCNA3B gene product with Kv1.5 leads to a novel A-type potassium channel. *J Biol Chem* **273,** 35095-35101.

Lerche H, Mitrovic N, Dubowitz V & Lehmann-Horn F. (1996). Paramyotonia congenita: the R1448P Na+ channel mutation in adult human skeletal muscle. *Ann Neurol* **39,** 599-608.

Li M, West JW, Lai Y, Scheuer T & Catterall WA. (1992). Functional modulation of brain sodium channels by cAMP-dependent phosphorylation. *Neuron* **8,** 1151-1159.

Li M, West JW, Numann R, Murphy BJ, Scheuer T & Catterall WA. (1993). Convergent regulation of sodium channels by protein kinase C and cAMP-dependent protein kinase. *Science* **261,** 1439-1442.

Li W, Ono F & Brehm P. (2003). Optical measurements of presynaptic release in mutant zebrafish lacking postsynaptic receptors. *J Neurosci* **23,** 10467-10474.

Li Y, Um SY & McDonald TV. (2006). Voltage-gated potassium channels: regulation by accessory subunits. *Neuroscientist* **12,** 199-210.

Liao L, Zeng XM, Gao PJ, Zhu DL & Mei YA. (2005). PKC pathway associated with the expression of an A-type K+ channel induced by TGF-beta1 in rat vascular myofibroblasts. *Biochem Biophys Res Commun* **336,** 854-859.

Lin MT, Hessinger DA, Pearce WJ & Longo LD. (2006). Modulation of BK channel calcium affinity by differential phosphorylation in developing ovine basilar artery myocytes. *Am J Physiol Heart Circ Physiol* **291,** H732-740.

Liu DW & Westerfield M. (1988). Function of identified motoneurones and co-ordination of primary and secondary motor systems during zebra fish swimming. *J Physiol* **403,** 73-89.

Liu YR, Ye WL, Zeng XM, Ren WH, Zhang YQ & Mei YA. (2008). K+ channels and the cAMP-PKA pathway modulate TGF-beta1-induced migration of rat vascular myofibroblasts. *J Cell Physiol* **216,** 835-843.

Lockery SR & Spitzer NC. (1992). Reconstruction of action potential development from whole-cell currents of differentiating spinal neurons. *J Neurosci* **12,** 2268-2287.

Luna VM & Brehm P. (2006). An electrically coupled network of skeletal muscle in zebrafish distributes synaptic current. *J Gen Physiol* **128,** 89-102.

Luna VM, Wang M, Ono F, Gleason MR, Dallman JE, Mandel G & Brehm P. (2004). Persistent electrical coupling and locomotory dysfunction in the zebrafish mutant shocked. *J Neurophysiol* **92,** 2003-2009.

MacVicar BA, Crichton SA, Burnard DM & Tse FW. (1987). Membrane conductance oscillations in astrocytes induced by phorbol ester. *Nature* **329,** 242-243.

Majumder K, De Biasi M, Wang Z & Wible BA. (1995). Molecular cloning and functional expression of a novel potassium channel beta-subunit from human atrium. *FEBS Lett* **361,** 13-16.

Makielski JC. (1996). The heart sodium channel phenotype for inactivation and lidocaine block. *Jpn Heart J* **37,** 733-739.

Makita N, Bennett PB, Jr. & George AL, Jr. (1994). Voltage-gated Na+ channel beta 1 subunit mRNA expressed in adult human skeletal muscle, heart, and brain is encoded by a single gene. *J Biol Chem* **269,** 7571-7578.

McCormack K, McCormack T, Tanouye M, Rudy B & Stuhmer W. (1995). Alternative splicing of the human Shaker K+ channel beta 1 gene and functional expression of the beta 2 gene product. *FEBS Lett* **370,** 32-36.

Meis S & Deitmer JW. (1997). Developmental changes of potassium currents of embryonic leech ganglion cells in primary culture. *J Neurosci Res* **50,** 967-978.

Melancon E, Liu DW, Westerfield M & Eisen JS. (1997). Pathfinding by identified zebrafish motoneurons in the absence of muscle pioneers. *J Neurosci* **17,** 7796-7804.

Mennerick S & Zorumski CF. (2000). Neural activity and survival in the developing nervous system. *Mol Neurobiol* **22,** 41-54.

Messner DJ, Feller DJ, Scheuer T & Catterall WA. (1986). Functional properties of rat brain sodium channels lacking the beta 1 or beta 2 subunit. *J Biol Chem* **261,** 14882-14890.

Miller C. (2000). Ion channels: doing hard chemistry with hard ions. *Curr Opin Chem Biol* **4,** 148-151.

Mittelstadt SW, Hemenway CL, Craig MP & Hove JR. (2008). Evaluation of zebrafish embryos as a model for assessing inhibition of hERG. *J Pharmacol Toxicol Methods* **57,** 100-105.

Mizrahi EM. (1999). Acute and chronic effects of seizures in the developing brain: lessons from clinical experience. *Epilepsia* **40 Suppl 1,** S42-50; discussion S64-46.

Moody WJ & Bosma MM. (2005). Ion channel development, spontaneous activity, and activity-dependent development in nerve and muscle cells. *Physiol Rev* **85,** 883-941.

Morin-Kensicki EM & Eisen JS. (1997). Sclerotome development and peripheral nervous system segmentation in embryonic zebrafish. *Development* **124,** 159-167.

Murphy BJ, Rossie S, De Jongh KS & Catterall WA. (1993). Identification of the sites of selective phosphorylation and dephosphorylation of the rat brain Na+ channel alpha subunit by cAMP-dependent protein kinase and phosphoprotein phosphatases. *J Biol Chem* **268,** 27355-27362.

Murray KT, Fahrig SA, Deal KK, Po SS, Hu NN, Snyders DJ, Tamkun MM & Bennett PB. (1994). Modulation of an inactivating human cardiac K+ channel by protein kinase C. *Circ Res* **75,** 999-1005.

Myers PZ, Eisen JS & Westerfield M. (1986). Development and axonal outgrowth of identified motoneurons in the zebrafish. *J Neurosci* **6,** 2278-2289.

Nakamura TY & Coetzee WA. (2008). Functional and pharmacological characterization of a Shal-related K+ channel subunit in Zebrafish. *BMC Physiol* **8,** 2.

Nakamura TY, Coetzee WA, Vega-Saenz De Miera E, Artman M & Rudy B. (1997). Modulation of Kv4 channels, key components of rat ventricular transient outward K+ current, by PKC. *Am J Physiol* **273,** H1775-1786.

Nakayama H & Oda Y. (2004). Common sensory inputs and differential excitability of segmentally homologous reticulospinal neurons in the hindbrain. *J Neurosci* **24,** 3199-3209.

Nasevicius A & Ekker SC. (2000). Effective targeted gene 'knockdown' in zebrafish. *Nat Genet* **26,** 216-220.

Nguyen PV, Aniksztejn L, Catarsi S & Drapeau P. (1999). Maturation of neuromuscular transmission during early development in zebrafish. *J Neurophysiol* **81,** 2852-2861.

Noda M, Shimizu S, Tanabe T, Takai T, Kayano T, Ikeda T, Takahashi H, Nakayama H, Kanaoka Y, Minamino N & et al. (1984). Primary structure of Electrophorus electricus sodium channel deduced from cDNA sequence. *Nature* **312,** 121-127.

Novak AE, Jost MC, Lu Y, Taylor AD, Zakon HH & Ribera AB. (2006a). Gene duplications and evolution of vertebrate voltage-gated sodium channels. *J Mol Evol* **63,** 208-221.

Novak AE, Taylor AD, Pineda RH, Lasda EL, Wright MA & Ribera AB. (2006b). Embryonic and larval expression of zebrafish voltage-gated sodium channel alpha-subunit genes. *Dev Dyn* **235,** 1962-1973.

Numann R, Catterall WA & Scheuer T. (1991). Functional modulation of brain sodium channels by protein kinase C phosphorylation. *Science* **254,** 115-118.

Nuss HB & Marban E. (1994). Electrophysiological properties of neonatal mouse cardiac myocytes in primary culture. *J Physiol* **479 (Pt 2),** 265-279.

Nuss HB, Tomaselli GF & Marban E. (1995). Cardiac sodium channels (hH1) are intrinsically more sensitive to block by lidocaine than are skeletal muscle (mu 1) channels. *J Gen Physiol* **106,** 1193-1209.

O'Dowd DK, Ribera AB & Spitzer NC. (1988). Development of voltage-dependent calcium, sodium, and potassium currents in Xenopus spinal neurons. *J Neurosci* **8,** 792-805.

O'Leary ME. (1998). Characterization of the isoform-specific differences in the gating of neuronal and muscle sodium channels. *Can J Physiol Pharmacol* **76,** 1041-1050.

Ochi H & Westerfield M. (2007). Signaling networks that regulate muscle development: lessons from zebrafish. *Dev Growth Differ* **49,** 1-11.

Ono F, Higashijima S, Shcherbatko A, Fetcho JR & Brehm P. (2001). Paralytic zebrafish lacking acetylcholine receptors fail to localize rapsyn clusters to the synapse. *J Neurosci* **21,** 5439-5448.

Ono F, Mandel G & Brehm P. (2004). Acetylcholine receptors direct rapsyn clusters to the neuromuscular synapse in zebrafish. *J Neurosci* **24,** 5475-5481.

Paillart C, Boudier JL, Boudier JA, Rochat H, Couraud F & Dargent B. (1996). Activity-induced internalization and rapid degradation of sodium channels in cultured fetal neurons. *J Cell Biol* **134,** 499-509.

Panzer JA, Song Y & Balice-Gordon RJ. (2006). In vivo imaging of preferential motor axon outgrowth to and synaptogenesis at prepatterned acetylcholine receptor clusters in embryonic zebrafish skeletal muscle. *J Neurosci* **26,** 934-947.

Papazian DM, Schwarz TL, Tempel BL, Jan YN & Jan LY. (1987). Cloning of genomic and complementary DNA from Shaker, a putative potassium channel gene from Drosophila. *Science* **237,** 749-753.

Parcej DN, Scott VE & Dolly JO. (1992). Oligomeric properties of alpha-dendrotoxin-sensitive potassium ion channels purified from bovine brain. *Biochemistry* **31,** 11084-11088.

Patten SA, Sihra RK, Dhami KS, Coutts CA & Ali DW. (2007). Differential expression of PKC isoforms in developing zebrafish. *Int J Dev Neurosci* **25,** 155-164.

Patton DE, Isom LL, Catterall WA & Goldin AL. (1994). The adult rat brain beta 1 subunit modifies activation and inactivation gating of multiple sodium channel alpha subunits. *J Biol Chem* **269,** 17649-17655.

Pedarzani P & Storm JF. (1995). Protein kinase A-independent modulation of ion channels in the brain by cyclic AMP. *Proc Natl Acad Sci U S A* **92,** 11716-11720.

Personius K, Chang Q, Bittman K, Panzer J & Balice-Gordon R. (2001). Gap junctional communication among motor and other neurons shapes patterns of neural activity and synaptic connectivity during development. *Cell Commun Adhes* **8,** 329-333.

Pineda RH, Heiser RA & Ribera AB. (2005). Developmental, molecular, and genetic dissection of INa in vivo in embryonic zebrafish sensory neurons. *J Neurophysiol* **93,** 3582-3593.

Pineda RH, Svoboda KR, Wright MA, Taylor AD, Novak AE, Gamse JT, Eisen JS & Ribera AB. (2006). Knockdown of Nav1.6a Na+ channels affects zebrafish motoneuron development. *Development* **133,** 3827-3836.

Pongs O, Kecskemethy N, Muller R, Krah-Jentgens I, Baumann A, Kiltz HH, Canal I, Llamazares S & Ferrus A. (1988). Shaker encodes a

family of putative potassium channel proteins in the nervous system of Drosophila. *EMBO J* **7,** 1087-1096.

Qu Y, Rogers J, Tanada T, Scheuer T & Catterall WA. (1994). Modulation of cardiac Na+ channels expressed in a mammalian cell line and in ventricular myocytes by protein kinase C. *Proc Natl Acad Sci U S A* **91,** 3289-3293.

Randall DJ, Burggren WW, French K & Eckert R. (2002). *Eckert animal physiology : mechanisms and adaptations*. W.H. Freeman and Co., New York.

Rettig J, Heinemann SH, Wunder F, Lorra C, Parcej DN, Dolly JO & Pongs O. (1994). Inactivation properties of voltage-gated K+ channels altered by presence of beta-subunit. *Nature* **369,** 289-294.

Ribera AB. (1999). Potassium currents in developing neurons. *Ann N Y Acad Sci* **868,** 399-405.

Ribera AB & Nusslein-Volhard C. (1998). Zebrafish touch-insensitive mutants reveal an essential role for the developmental regulation of sodium current. *J Neurosci* **18,** 9181-9191.

Roberts RH & Barchi RL. (1987). The voltage-sensitive sodium channel from rabbit skeletal muscle. Chemical characterization of subunits. *J Biol Chem* **262,** 2298-2303.

Roeper J, Lorra C & Pongs O. (1997). Frequency-dependent inactivation of mammalian A-type K+ channel KV1.4 regulated by Ca2+/calmodulin-dependent protein kinase. *J Neurosci* **17,** 3379-3391.

Rottbauer W, Baker K, Wo ZG, Mohideen MA, Cantiello HF & Fishman MC. (2001). Growth and function of the embryonic heart depend upon the cardiac-specific L-type calcium channel alpha1 subunit. *Dev Cell* **1,** 265-275.

Rudy B. (1988). Diversity and ubiquity of K channels. *Neuroscience* **25,** 729-749.

Ruff RL. (1996a). Single-channel basis of slow inactivation of Na+ channels in rat skeletal muscle. *Am J Physiol* **271,** C971-981.

Ruff RL. (1996b). Sodium channel slow inactivation and the distribution of sodium channels on skeletal muscle fibres enable the performance

properties of different skeletal muscle fibre types. *Acta Physiol Scand* **156,** 159-168.

Sada H, Ban T, Fujita T, Ebina Y & Sperelakis N. (1995). Developmental change in fast Na channel properties in embryonic chick ventricular heart cells. *Can J Physiol Pharmacol* **73,** 1475-1484.

Saint-Amant L & Drapeau P. (1998). Time course of the development of motor behaviors in the zebrafish embryo. *J Neurobiol* **37,** 622-632.

Saint-Amant L & Drapeau P. (2000). Motoneuron activity patterns related to the earliest behavior of the zebrafish embryo. *J Neurosci* **20,** 3964-3972.

Sanchez-Chapula J, Elizalde A, Navarro-Polanco R & Barajas H. (1994). Differences in outward currents between neonatal and adult rabbit ventricular cells. *Am J Physiol* **266,** H1184-1194.

Sanes JR & Lichtman JW. (1999). Development of the vertebrate neuromuscular junction. *Annu Rev Neurosci* **22,** 389-442.

Schiffmann SN, Desdouits F, Menu R, Greengard P, Vincent JD, Vanderhaeghen JJ & Girault JA. (1998). Modulation of the voltage-gated sodium current in rat striatal neurons by DARPP-32, an inhibitor of protein phosphatase. *Eur J Neurosci* **10,** 1312-1320.

Schilling TF & Webb J. (2007). Considering the zebrafish in a comparative context. *J Exp Zoolog B Mol Dev Evol* **308,** 515-522.

Scholz EP, Niemer N, Hassel D, Zitron E, Burgers HF, Bloehs R, Seyler C, Scherer D, Thomas D, Kathofer S, Katus HA, Rottbauer WA & Karle CA. (2009). Biophysical properties of zebrafish ether-a-go-go related gene potassium channels. *Biochem Biophys Res Commun* **381,** 159-164.

Schrader LA, Anderson AE, Mayne A, Pfaffinger PJ & Sweatt JD. (2002). PKA modulation of Kv4.2-encoded A-type potassium channels requires formation of a supramolecular complex. *J Neurosci* **22,** 10123-10133.

Schreibmayer W, Frohnwieser B, Dascal N, Platzer D, Spreitzer B, Zechner R, Kallen RG & Lester HA. (1994). Beta-adrenergic modulation of currents produced by rat cardiac Na+ channels expressed in Xenopus laevis oocytes. *Receptors Channels* **2,** 339-350.

Scott VE, Rettig J, Parcej DN, Keen JN, Findlay JB, Pongs O & Dolly JO. (1994). Primary structure of a beta subunit of alpha-dendrotoxin-sensitive K+ channels from bovine brain. *Proc Natl Acad Sci U S A* **91,** 1637-1641.

Shatz CJ. (1994). Viktor Hamburger Award review. Role for spontaneous neural activity in the patterning of connections between retina and LGN during visual system development. *Int J Dev Neurosci* **12,** 531-546.

Shi G, Nakahira K, Hammond S, Rhodes KJ, Schechter LE & Trimmer JS. (1996). Beta subunits promote K+ channel surface expression through effects early in biosynthesis. *Neuron* **16,** 843-852.

Shibata R, Misonou H, Campomanes CR, Anderson AE, Schrader LA, Doliveira LC, Carroll KI, Sweatt JD, Rhodes KJ & Trimmer JS. (2003). A fundamental role for KChIPs in determining the molecular properties and trafficking of Kv4.2 potassium channels. *J Biol Chem* **278,** 36445-36454.

Shuster MJ, Camardo JS, Siegelbaum SA & Kandel ER. (1985). Cyclic AMP-dependent protein kinase closes the serotonin-sensitive K+ channels of Aplysia sensory neurones in cell-free membrane patches. *Nature* **313,** 392-395.

Si J, Luo Z & Mei L. (1996). Induction of acetylcholine receptor gene expression by ARIA requires activation of mitogen-activated protein kinase. *J Biol Chem* **271,** 19752-19759.

Sigel E & Baur R. (1988). Activation of protein kinase C differentially modulates neuronal Na+, Ca2+, and gamma-aminobutyrate type A channels. *Proc Natl Acad Sci U S A* **85,** 6192-6196.

Simoncini L & Moody WJ. (1991). Dependence of Ca2+ and K+ current development on RNA and protein synthesis in muscle-lineage cells of the ascidian Boltenia villosa. *J Neurosci* **11,** 1413-1420.

Smith RD & Goldin AL. (1992). Protein kinase A phosphorylation enhances sodium channel currents in Xenopus oocytes. *Am J Physiol* **263,** C660-666.

Smith RD & Goldin AL. (1996). Phosphorylation of brain sodium channels in the I--II linker modulates channel function in Xenopus oocytes. *J Neurosci* **16,** 1965-1974.

Soliven B, Szuchet S, Arnason BG & Nelson DJ. (1988). Forskolin and phorbol esters decrease the same K+ conductance in cultured oligodendrocytes. *J Membr Biol* **105,** 177-186.

Sontheimer H, Ransom BR & Waxman SG. (1992). Different Na+ currents in P0- and P7-derived hippocampal astrocytes in vitro: evidence for a switch in Na+ channel expression in vivo. *Brain Res* **597,** 24-29.

Sperber EF, Veliskova J, Germano IM, Friedman LK & Moshe SL. (1999). Age-dependent vulnerability to seizures. *Adv Neurol* **79,** 161-169.

Spitzer NC. (1991). A developmental handshake: neuronal control of ionic currents and their control of neuronal differentiation. *J Neurobiol* **22,** 659-673.

Spitzer NC. (2006). Electrical activity in early neuronal development. *Nature* **444,** 707-712.

Spitzer NC, Kingston PA, Manning TJ & Conklin MW. (2002). Outside and in: development of neuronal excitability. *Curr Opin Neurobiol* **12,** 315-323.

Spitzer NC & Ribera AB. (1998). Development of electrical excitability in embryonic neurons: mechanisms and roles. *J Neurobiol* **37,** 190-197.

Spitzer NC, Vincent A & Lautermilch NJ. (2000). Differentiation of electrical excitability in motoneurons. *Brain Res Bull* **53,** 547-552.

Stanfield PR. (1972). Electrical properties of white and red muscle fibres of the elasmobranch fish Scyliorhinus canicula. *J Physiol* **222,** 161-186.

Stickney HL, Barresi MJ & Devoto SH. (2000). Somite development in zebrafish. *Dev Dyn* **219,** 287-303.

Stockdale FE. (1992). Myogenic cell lineages. *Dev Biol* **154,** 284-298.

Stoiber W & Sanger AM. (1996). An electron microscopic investigation into the possible source of new muscle fibres in teleost fish. *Anat Embryol (Berl)* **194,** 569-579.

Strong JA. (1984). Modulation of potassium current kinetics in bag cell neurons of Aplysia by an activator of adenylate cyclase. *J Neurosci* **4,** 2772-2783.

Stuhmer W, Conti F, Suzuki H, Wang XD, Noda M, Yahagi N, Kubo H & Numa S. (1989). Structural parts involved in activation and inactivation of the sodium channel. *Nature* **339,** 597-603.

Summerton J & Weller D. (1997). Morpholino antisense oligomers: design, preparation, and properties. *Antisense Nucleic Acid Drug Dev* **7,** 187-195.

Sutkowski EM & Catterall WA. (1990). Beta 1 subunits of sodium channels. Studies with subunit-specific antibodies. *J Biol Chem* **265,** 12393-12399.

Tansey MG, Chu GC & Merlie JP. (1996). ARIA/HRG regulates AChR epsilon subunit gene expression at the neuromuscular synapse via activation of phosphatidylinositol 3-kinase and Ras/MAPK pathway. *J Cell Biol* **134,** 465-476.

Tempel BL, Papazian DM, Schwarz TL, Jan YN & Jan LY. (1987). Sequence of a probable potassium channel component encoded at Shaker locus of Drosophila. *Science* **237,** 770-775.

Tian L, Duncan RR, Hammond MS, Coghill LS, Wen H, Rusinova R, Clark AG, Levitan IB & Shipston MJ. (2001). Alternative splicing switches potassium channel sensitivity to protein phosphorylation. *J Biol Chem* **276,** 7717-7720.

Ticho BS, Stainier DY, Fishman MC & Breitbart RE. (1996). Three zebrafish MEF2 genes delineate somitic and cardiac muscle development in wild-type and mutant embryos. *Mech Dev* **59,** 205-218.

Tierney AJ & Harris-Warrick RM. (1992). Physiological role of the transient potassium current in the pyloric circuit of the lobster stomatogastric ganglion. *J Neurophysiol* **67,** 599-609.

Todd KJ, Slatter CA & Ali DW. (2004). Activation of ionotropic glutamate receptors on peripheral axons of primary motoneurons mediates transmitter release at the zebrafish NMJ. *J Neurophysiol* **91,** 828-840.

Tricarico D, Wagner R, Bryant SH & Camerino DC. (1993). Regulation of resting ionic conductances in frog skeletal muscle. *Pflugers Arch* **423,** 189-192.

Trimmer JS, Cooperman SS, Tomiko SA, Zhou JY, Crean SM, Boyle MB, Kallen RG, Sheng ZH, Barchi RL, Sigworth FJ & et al. (1989).

Primary structure and functional expression of a mammalian skeletal muscle sodium channel. *Neuron* **3,** 33-49.

Trimmer JS & Rhodes KJ. (2004). Localization of voltage-gated ion channels in mammalian brain. *Annu Rev Physiol* **66,** 477-519.

Tsai CW, Tseng JJ, Lin SC, Chang CY, Wu JL, Horng JF & Tsay HJ. (2001). Primary structure and developmental expression of zebrafish sodium channel Na(v)1.6 during neurogenesis. *DNA Cell Biol* **20,** 249-255.

van Asselt E, de Graaf F & van Raamsdonk W. (1993). Ultrastructural characteristics of zebrafish spinal motoneurons innervating glycolytic white, and oxidative red and intermediate muscle fibers. *Acta Histochem* **95,** 31-44.

van Raamsdonk W, Smit-Onel M, Scholten G, Hemrika W & Robbe B. (1987). Metabolic specialization of spinal neurons and the myotomal muscle in post-hatching stages of the zebrafish, Brachydanio rerio. A histochemical study. *Z Mikrosk Anat Forsch* **101,** 318-330.

van Raamsdonk W, Tekronnie G, Pool CW & van de Laarse W. (1980). An immune histochemical and enzymic characterization of the muscle fibres in myotomal muscle of the teleost Brachydanio rerio, Hamilton-Buchanan. *Acta Histochem* **67,** 200-216.

van Raamsdonk W, van't Veer L, Veeken K, Heyting C & Pool CW. (1982). Differentiation of muscle fiber types in the teleost Brachydanio rerio, the zebrafish. Posthatching development. *Anat Embryol (Berl)* **164,** 51-62.

Van Swearingen J & Lance-Jones C. (1995). Slow and fast muscle fibers are preferentially derived from myoblasts migrating into the chick limb bud at different developmental times. *Dev Biol* **170,** 321-337.

Vargas G & Lucero MT. (2002). Modulation by PKA of the hyperpolarization-activated current (Ih) in cultured rat olfactory receptor neurons. *J Membr Biol* **188,** 115-125.

Vassilev P, Scheuer T & Catterall WA. (1989). Inhibition of inactivation of single sodium channels by a site-directed antibody. *Proc Natl Acad Sci U S A* **86,** 8147-8151.

Veggetti A, Mascarello F, Scapolo PA, Rowlerson A & Carnevali C. (1993). Muscle growth and myosin isoform transitions during

development of a small teleost fish, Poecilia reticulata (Peters) (Atheriniformes, Poeciliidae): a histochemical, immunohistochemical, ultrastructural and morphometric study. *Anat Embryol (Berl)* **187,** 353-361.

Vessey JP, Stratis AK, Daniels BA, Da Silva N, Jonz MG, Lalonde MR, Baldridge WH & Barnes S. (2005). Proton-mediated feedback inhibition of presynaptic calcium channels at the cone photoreceptor synapse. *J Neurosci* **25,** 4108-4117.

Vijayaragavan K, Boutjdir M & Chahine M. (2004). Modulation of Nav1.7 and Nav1.8 peripheral nerve sodium channels by protein kinase A and protein kinase C. *J Neurophysiol* **91,** 1556-1569.

Villeneuve N, Ben-Ari Y, Holmes GL & Gaiarsa JL. (2000). Neonatal seizures induced persistent changes in intrinsic properties of CA1 rat hippocampal cells. *Ann Neurol* **47,** 729-738.

Vincent A, Lautermilch NJ & Spitzer NC. (2000). Antisense suppression of potassium channel expression demonstrates its role in maturation of the action potential. *J Neurosci* **20,** 6087-6094.

Vogalis F, Harvey JR & Furness JB. (2003). PKA-mediated inhibition of a novel K+ channel underlies the slow after-hyperpolarization in enteric AH neurons. *J Physiol* **548,** 801-814.

Wahler GM, Dollinger SJ, Smith JM & Flemal KL. (1994). Time course of postnatal changes in rat heart action potential and in transient outward current is different. *Am J Physiol* **267,** H1157-1166.

Wallner M, Weigl L, Meera P & Lotan I. (1993). Modulation of the skeletal muscle sodium channel alpha-subunit by the beta 1-subunit. *FEBS Lett* **336,** 535-539.

Walrond JP & Reese TS. (1985). Structure of axon terminals and active zones at synapses on lizard twitch and tonic muscle fibers. *J Neurosci* **5,** 1118-1131.

Weinberg ES, Allende ML, Kelly CS, Abdelhamid A, Murakami T, Andermann P, Doerre OG, Grunwald DJ & Riggleman B. (1996). Developmental regulation of zebrafish MyoD in wild-type, no tail and spadetail embryos. *Development* **122,** 271-280.

West JW, Numann R, Murphy BJ, Scheuer T & Catterall WA. (1991). A phosphorylation site in the Na+ channel required for modulation by protein kinase C. *Science* **254,** 866-868.

West JW, Patton DE, Scheuer T, Wang Y, Goldin AL & Catterall WA. (1992). A cluster of hydrophobic amino acid residues required for fast Na(+)-channel inactivation. *Proc Natl Acad Sci U S A* **89,** 10910-10914.

Westerfield M. (1995). *The Zebrafish Book: A Guide for the laboratory use of zebrafish (Brachydanio rerio)*. University of Oregon Press, Eugene.

Westerfield M, Liu DW, Kimmel CB & Walker C. (1990). Pathfinding and synapse formation in a zebrafish mutant lacking functional acetylcholine receptors. *Neuron* **4,** 867-874.

Westerfield M, McMurray JV & Eisen JS. (1986). Identified motoneurons and their innervation of axial muscles in the zebrafish. *J Neurosci* **6,** 2267-2277.

Wible BA, Yang Q, Kuryshev YA, Accili EA & Brown AM. (1998). Cloning and expression of a novel K+ channel regulatory protein, KChAP. *J Biol Chem* **273,** 11745-11751.

Wickenden AD, Kaprielian R, Parker TG, Jones OT & Backx PH. (1997). Effects of development and thyroid hormone on K+ currents and K+ channel gene expression in rat ventricle. *J Physiol* **504 (Pt 2),** 271-286.

Wood JN & Baker M. (2001). Voltage-gated sodium channels. *Curr Opin Pharmacol* **1,** 17-21.

Xiao YF & McArdle JJ. (1995). Activation of protein kinase A partially reverses the effects of 2,3-butanedione monoxime on the transient outward K+ current of rat ventricular myocytes. *Life Sci* **57,** 335-343.

Xu H, Dixon JE, Barry DM, Trimmer JS, Merlie JP, McKinnon D & Nerbonne JM. (1996). Developmental analysis reveals mismatches in the expression of K+ channel alpha subunits and voltage-gated K+ channel currents in rat ventricular myocytes. *J Gen Physiol* **108,** 405-419.

Xu R & Salpeter MM. (1995). Protein kinase A regulates the degradation rate of Rs acetylcholine receptors. *J Cell Physiol* **165,** 30-39.

Yao WD & Wu CF. (2001). Distinct roles of CaMKII and PKA in regulation of firing patterns and K(+) currents in Drosophila neurons. *J Neurophysiol* **85,** 1384-1394.

Yonkers MA & Ribera AB. (2008). Sensory neuron sodium current requires nongenomic actions of thyroid hormone during development. *J Neurophysiol* **100,** 2719-2725.

Yu CJ & Li L. (2005). Dopamine modulates voltage-activated potassium currents in zebrafish retinal on bipolar cells. *J Neurosci Res* **82,** 368-376.

Yuan LL, Adams JP, Swank M, Sweatt JD & Johnston D. (2002). Protein kinase modulation of dendritic K+ channels in hippocampus involves a mitogen-activated protein kinase pathway. *J Neurosci* **22,** 4860-4868.

Zhang L & McBain CJ. (1995a). Potassium conductances underlying repolarization and after-hyperpolarization in rat CA1 hippocampal interneurones. *J Physiol* **488 (Pt 3),** 661-672.

Zhang L & McBain CJ. (1995b). Voltage-gated potassium currents in stratum oriens-alveus inhibitory neurones of the rat CA1 hippocampus. *J Physiol* **488 (Pt 3),** 647-660.

APPENDICES

1. Modulation of voltage-gated currents by PKC[4]

Introduction

Ion channels are important phosphorylation targets of protein kinases such as PKC (Numann *et al.*, 1991; West *et al.*, 1991). Channel phosphorylation can lead to many changes in current characteristics, including altered current density and voltage-dependence, similar to those observed in developing muscle fibers. Na_V and K_V channels have consensus sequences for various protein kinases. For example, Na_V channels possess multiple potential phosphorylation targets for both PKA and PKC, which are located on the intracellular loops linking α subunit domains I-II and III-IV (Sigel & Baur, 1988; Dascal & Lotan, 1991; Chen *et al.*, 1995). K_V channels possess consensus sequences for phosphorylation by multiple kinases (PKA, PKC, MAPK/ERK, CaMKII) on the intracellular C-terminal portions of each α subunit, and a potential site for PKA modulation was also identified on the N-terminal (Adams *et al.*, 2000; Anderson *et al.*, 2000).

Among the different K_V currents known to be modulated by PKC, the A-type currents are one of the most well-documented (Grega *et al.*, 1987; Werz & Macdonald, 1987; Colby & Blaustein, 1988). The A-type K_V currents have already been described above (RESULTS 3). Briefly, they

[4]A version of this chapter has been published. Patten SA, Sihra RK, Dhami KS, Coutts CA, Ali DW 2009. International Journal of Developmental Neuroscience. 25(3):155-64.

are fast activating and fast inactivating currents that were first identified in neurons, but are now known to be present in non-neural tissues such as smooth and skeletal muscle. They can perform various functions, such as adjusting action potential shape and size (Zhang & McBain, 1995a, b), controlling signal propagation (Hoffman *et al.*, 1997) and underlying membrane potential oscillations (Bourdeau *et al.*, 2007). Factors that modulate A-type currents may therefore also affect cell excitability and action potential frequency, shape and size.

PKC is a family of kinases composed of approximately 11 different isozymes that have been categorized into three groups depending on their ligand sensitivities and structural properties (Newton, 2001; Nakashima, 2002; Ohno & Nishizuka, 2002). The first group, known as the classical or conventional PKCs (α, βI, βII, γ), require phosphatidylserine (PS), diacylglycerol (DAG) and Ca^{2+} for optimal activation. The second group, known as the novel PKCs (δ, ε, θI, θII, η), require PS and DAG, but not Ca^{2+} for activation. Lastly, the atypical PKCs (ζ, τ/λ) require PS but neither DAG nor Ca^{2+} for activation (Newton, 2001; Ohno & Nishizuka, 2002). The expression of different PKC isoforms varies greatly between tissues, but certain isoforms are generally thought to be more widely expressed in the CNS (for instance PKCα, βII, γ, δ, θ and ζ) (Battaini, 2001) or in skeletal muscle (PKCβII and θ) (Osada *et al.*, 1992; Battaini, 2001). PKC has been shown to modulate many types of channels.

Because PKC is known to be expressed in skeletal muscle, and it is a well-known modulator of A-type K_V channels, a study was initiated to determine: 1) whether PKC is expressed in zebrafish skeletal muscle, and 2) whether PKC modulates the A-type K_V and/or Na_V currents in white skeletal muscle fibers.

Methods

PKCs βII and θ were identified using rabbit polyclonal antibodies obtained from Santa Cruz Biotechnology (Santa Cruz, CA). Both PKC antibodies were generated against the C terminal portion of the enzyme and were used at a dilution of 1:500. The secondary antiserum was a goat anti-rabbit IgG coupled to Cy3 (1:2000).

For electrophysiological recordings, 2 dpf zebrafish were maintained and dissected as described above (see METHODS 1). K^+-isolating salines were prepared as in Tables 1 and 2, with the following exceptions. 1,2-dioctanoyl-*sn*-glycerol (DOG) and GFX were purchased from Calbiochem (San Diego, CA). DOG and GFX (GF109203X; Bisindoylmaleimide I) were prepared in dimethyl sulfoxide (DMSO), aliquoted, and stored at -20°C. Samples were thawed just prior to use and were diluted in K_V -isolating extracellular bathing saline to final concentration of 50 μM for DOG, and 2 μM for GFX. Cells were pre-incubated in GFX for 5-7 minutes prior to obtaining the initial recording

('GFX'), followed by bath application of both GFX and DOG for 5 minutes, at which point a second recording was obtained ('GFX+DOG'). The vehicle (DMSO) and time control experiments were shared with the study on PKA modulation of A-type K_V currents, as detailed in METHODS 3.3 and RESULTS 3.1 above, and therefore have been excluded here. Voltage-protocols were the same as those detailed in METHODS and Figure M2.

Results

Anti-PKC βII intensely labeled the intersegmental boundaries and lightly stained skeletal muscle fibers (Figure A1.1 A; n=63). This staining pattern was consistent up to 2 weeks of age and was punctate in nature (Figure A1.1 A, inset). The lack of staining in the immune serum preabsorption controls (Figure A1.1 B; n=7) suggested that the labeling of muscle tissue by anti-PKC βII was specific.

Anti-PKC θ staining was very similar to that of anti-PKC βII. PKC θ strongly labeled intersegmental boundaries and labeled muscle fibers (Figure A1.2 A and B; n=49); however, staining at the segmental boundaries was smooth and continuous, rather than punctate, like that found with anti-PKC βII. There was very light, diffuse staining of the spinal cord (between arrowheads, Figure A1.2 C), and individual cells were difficult to identify. Immune serum preabsorption controls exhibited no

positive staining in immunohistochemistry experiments (Figure A1.2 D; n=8).

Having established the expression of PKC in skeletal muscle, subsequent experiments were aimed at activating PKC to determine whether K_V currents in white muscle were modulated. Activation of PKC via DOG application for 5 minutes had no effect on the peak current density of A-type K_V currents, as shown by the current-voltage relationship and the peak current density at 20 mV before and after drug treatment (Figure A1.3 A and B). PKC activation did, however, depolarize the voltage-dependence of steady state activation (Figure A1.4; from 2.774±1.524 mV to 7.446±0.591 mV; n=8) and inactivation (Figure A1.5; from -21.678±1.371 mV to -17.178±1.029 mV) by ~5 mV each. Interestingly, the specific PKC inhibitor, GFX, was able to block the effect on activation only, whereas the shift in inactivation V50 was present even after pre-incubation in GFX. The activation slope factor was increased slightly by DOG treatment (Figure A1.4C; from 5.853±0.148 to 6.853±0.347, n=8), and this effect was blocked by GFX pre-incubation, but the inactivation slope factor was unaffected (Figure A1.5 C).

In preparation for studies that were aimed at investigating the possible modulation of Na_V currents by kinases like PKA and PKC, the first step taken was to ensure that the currents were stable over the time frame required to perform such experiments. When recordings were made of Na_V currents every minute for 10 minutes, in the absence of any kinase

activators, it was discovered that the peak current density of Na_V currents fluctuated drastically and inconsistently over time (Figure A1.6). Na_V currents were highly variable over time; they would sometimes increase or decrease drastically, often by as much as 50%, during the recordings. These currents were deemed too variable to obtain reliable control data, therefore experiments to test for channel modulation by PKA and PKC were aborted.

Discussion

K^+ channels play major roles in setting the resting membrane potential, cell excitability and in shaping the action potential (Hille, 2001). Modulation of these channels may therefore be an important aspect of cell functioning. The first goal of this study was to determine whether PKC is expressed in zebrafish skeletal muscle; both the βII and the θ isoforms of PKC were labeled by fluorescently-tagged antibodies in skeletal muscle, although there were some differences in the staining patterns between them. PKC βII staining differed from that of θ in that it didn't label cells in the spinal cord and the segmental boundaries were labeled in a punctuate fashion.

Zebrafish white fibers had previously been shown to express at least two main kinds of voltage sensitive ionic currents: a Na_V current and an inactivating A-type K_V current (Buckingham & Ali, 2004). In many cells,

an A-type current is capable of controlling cell excitability and changes in its properties may affect the production of action potentials (Connor & Stevens, 1971; Rudy, 1988; Tierney & Harris-Warrick, 1992). The major changes that occur to the A-type K_V current in white fibers following application of DOG were a depolarization of the voltage-dependence of activation, and a slight, but significant, increase in the activation slope factor. Application of DOG also resulted in a depolarization of inactivation voltage-dependence, however it appears to have been the result of a non-specific action of DOG, because this effect was not inhibited by GFX.

The A-type K_V currents of zebrafish white fibers were not reduced following activation of PKC, which is somewhat at odds with the fact that the voltage-dependence underwent a depolarization following DOG treatment. The depolarized activation V_{50} is caused by a fewer number of channels being activated at a given membrane potential, which should result in a decreased current density in the current voltage relationship, if all other variables remain equal. The equal but opposite effect of the depolarization of inactivation voltage-dependence cannot account for this discrepancy either, as it is not a factor at the interstimulus holding potential of -90 mV used in the voltage protocol. This paradox has no known explanation at this point, and together with the non-specific effects of DOG on the voltage-dependence of inactivation, the reliability of this entire set of experiments becomes questionable.

There was a high degree of variability between recordings of Na_V currents in white fibers. This variability would likely have rendered any modulatory effects of PKC, had they existed, indistinguishable; this line of questioning was therefore subsequently abandoned.

In conclusion, there may have been some modulation of the voltage-dependent properties of A-type channels by PKC, however the validity of the results was put into doubt by inconsistencies within the data. Na_V channels may very well be modulated by kinases such as PKC and PKA, however they don't appear to be stable enough over time to be able to obtain useful data.

Figure A1.1 Anti-PKC βII immunoreactivity in zebrafish. **(A)** Positive immunostaining in a 6 dpf larva (and inset) shows strong punctate labeling of segmental boundaries. This staining pattern was identical at all ages until 2 weeks post fertilization (data not shown). Note that individual muscle fibers are also labeled. **(B)** Control experiment in a 2 dpf larva using anti-PKC βII preabsorbed with blocking peptide to confirm the specificity of the staining. Scale bars: (A and inset, B) = 50 μm.

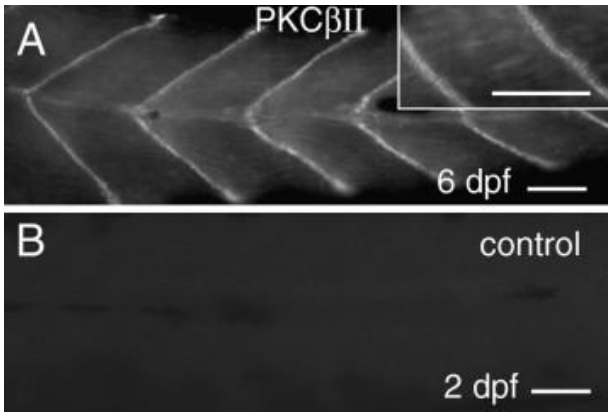
A
PKCβII
6 dpf
B
control
2 dpf

Figure A1.2 Anti-PKC θ immunoreactivity in zebrafish. Trunk region of a 2 dpf **(A)** and 6 dpf larva **(B)** showing intense labeling of regions at the segmental boundaries. **(C)** Very light staining of the spinal cord can be ascertained in 6 dpf fish (arrowheads) suggesting the presence of PKC θ in the CNS at this age. **(D)** Control experiment using anti-PKC θ preabsorbed with blocking peptide to confirm the specificity of the staining. Scale bars: (A–D) = 50 μm.

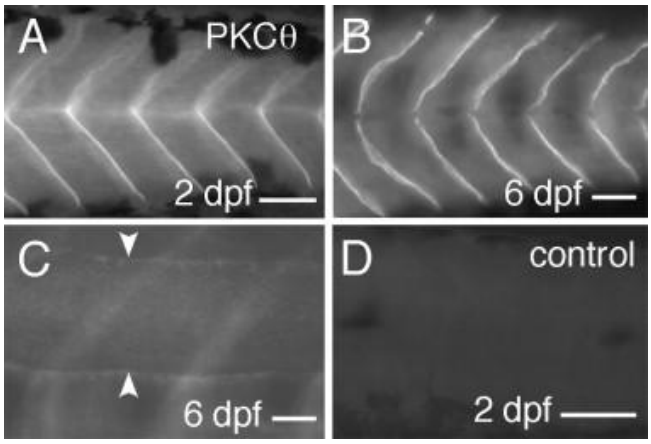
A
PKCθ
2 dpf
B
6 dpf
C
6 dpf
D
control
2 dpf

Figure A1.3 Activation of PKC via DOG has no effect on peak current density of A-type K_V currents. Currents were evoked by stepwise depolarizations from a holding potential of -90 mV to a range of potentials from -60 to 30 mV in 10 mV increments. **(A)** Current density – voltage plot indicates there is no effect after 5 mins DOG (50 μM) treatment. **(B)** Quantification of peak current density at 20 mV. A liquid junction potential of 6.7 mV was accounted for in all plots. '**b'** denotes significance from GFX on its own.

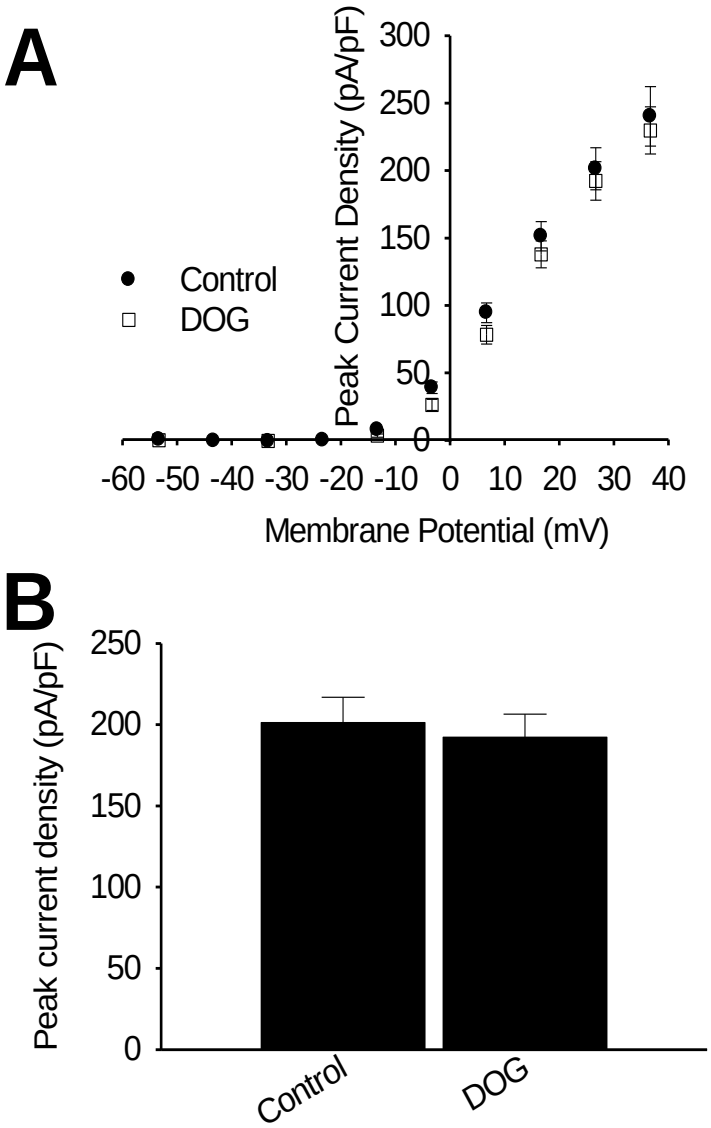
A
Peak Current Density (pA/pF)
300
250
200
150
100
50
0
Control
DOG
-60 -50 -40 -30 -20 -10 0 10 20 30 40
Membrane Potential (mV)
B
Peak current density (pA/pF)
250
200
150
100
50
0
Control
DOG

Figure A1.4 Activation of PKC via DOG alters the voltage-dependence of activation of A-type KV currents. **(A)** The activation curve is depolarized after DOG (50 μM) application for 5 mins. **(B)** The activation V_{50} is more depolarized following DOG application; this effect is blocked by the PKC inhibitor GFX (2 μM). **(C)** The activation slope factor is also increased following DOG treatment, and is also blocked by GFX pre-incubation. A liquid junction potential of 6.7 mV was accounted for in all plots. '**a'** denotes significance from control group.

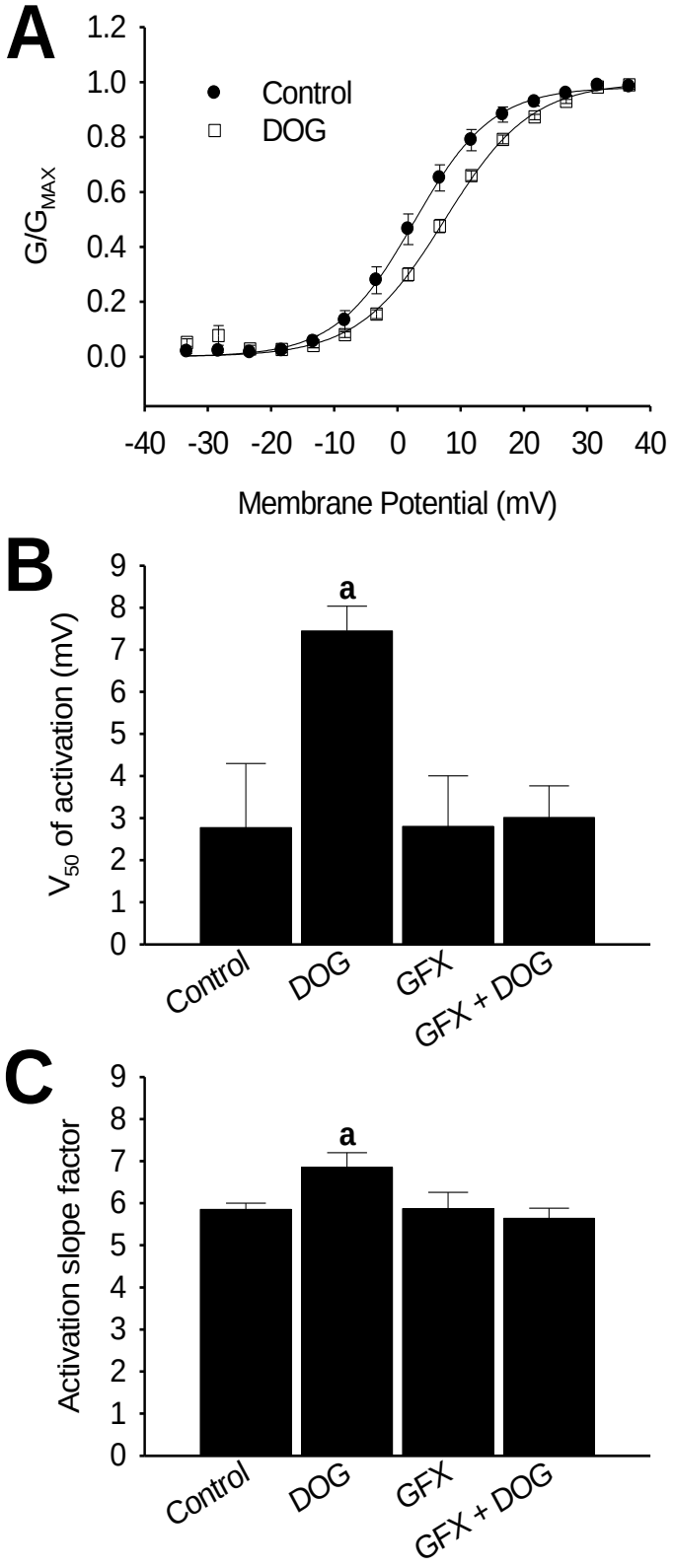
A
1.2
1.0
0.8
0.6
0.4
0.2
0.0
G/G_MAX
Control
DOG
-40 -30 -20 -10 0 10 20 30 40
Membrane Potential (mV)
B
9
8
7
6
5
4
3
2
1
0
V50 of activation (mV)
a
Control
DOG
GFX
GFX + DOG
C
9
8
7
6
5
4
3
2
1
0
Activation slope factor
a
Control
DOG
GFX
GFX + DOG

Figure A1.5 Activation of PKC via DOG alters the voltage-dependence of inactivation of A-type KV currents. **(A)** The inactivation curve is depolarized after DOG application for 5 minutes. **(B)** The inactivation V_{50} is more depolarized following DOG (50 μM) application, but this effect is not blocked by the PKC inhibitor GFX (2 μM); on the contrary, DOG appears to have the same effect even in the presence of GFX. **(C)** The inactivation slope factor is not affected by DOG. GFX also has no effect on the slope factor. A liquid junction potential of 6.7 mV was accounted for in all plots. '**a'** denotes significance from control group; '**b**' denotes significance from GFX on its own.

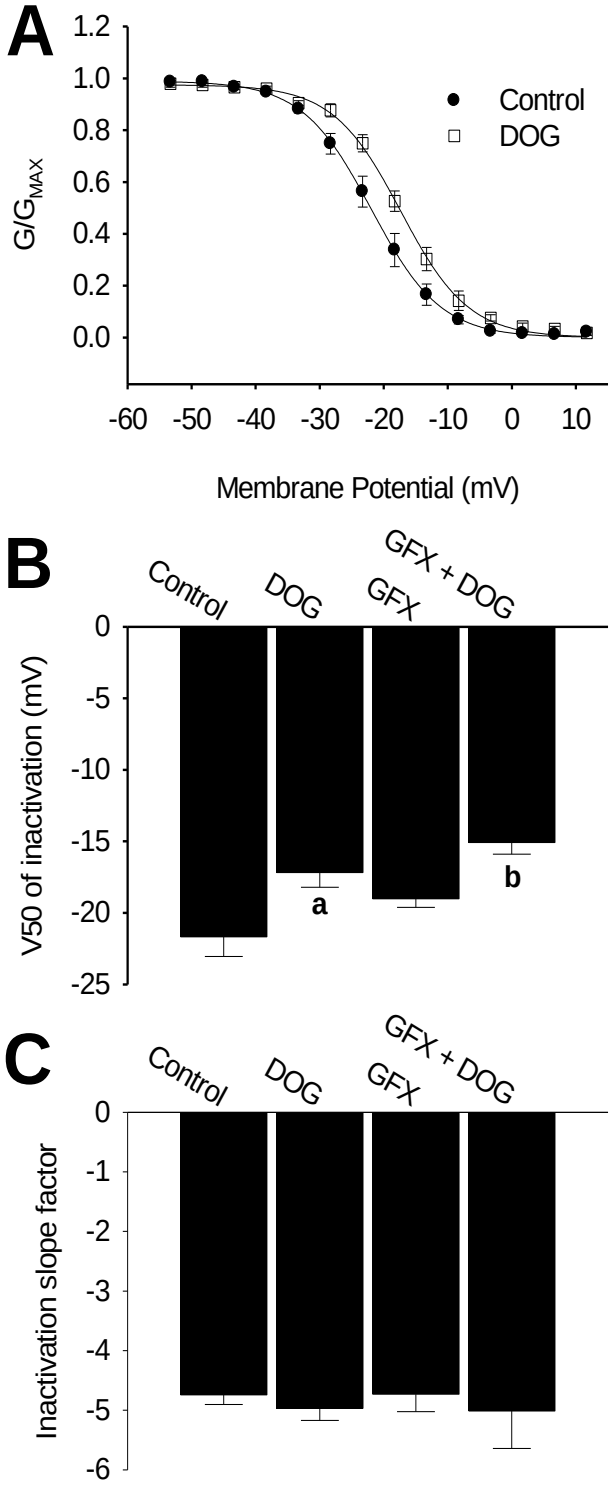
A
1.2
1.0
0.8
0.6
0.4
0.2
0.0
G/G_MAX
Control
DOG
-60
-50
-40
-30
-20
-10
0
10
Membrane Potential (mV)
B
Control
DOG
GFX
GFX + DOG
0
-5
-10
-15
-20
-25
V50 of inactivation (mV)
a
b
C
Control
DOG
GFX
GFX + DOG
0
-1
-2
-3
-4
-5
-6
Inactivation slope factor

Figure A1.6 Peak current density of NaV currents fluctuates drastically and inconsistently over time under normal conditions. Na_V currents were recorded every minute for 10 minutes in order to determine whether they were stable enough to obtain reliable recordings over time under different experimental treatments. Na_V currents were highly variable over time; they would sometimes increase or decrease drastically during the recordings. These currents were deemed too variable to obtain reliable control data, therefore experiments to test for channel modulation by PKA and PKC were aborted.

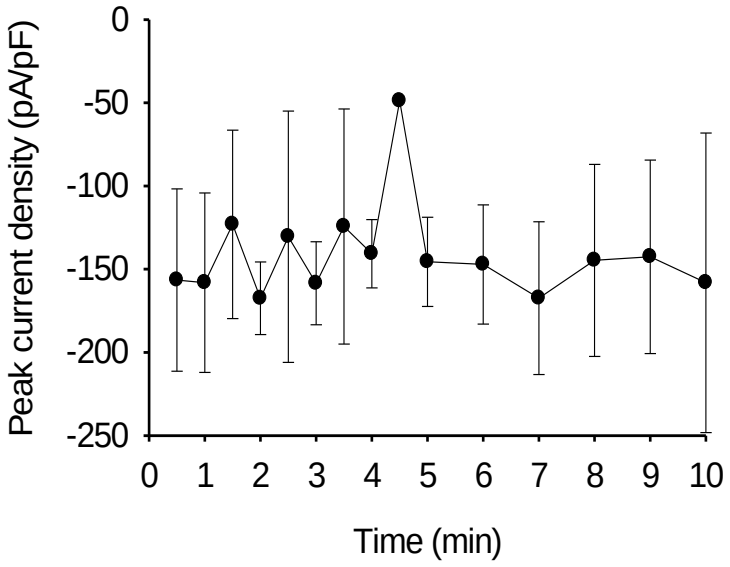
Peak current density (pA/pF)
0
-50
-100
-150
-200
-250
0 1 2 3 4 5 6 7 8 9 10
Time (min)

2. Na_V currents recorded in the cell-attached patch clamp configuration

Introduction

Very large cells and those with large axons or extensive dendritic arbours, can pose problems for the whole-cell patch-clamp configuration. Voltage errors can arise, whereby the voltage that the cell membrane experiences at a given point along the membrane deviates significantly from the command voltage set at the amplifier. Just as the the patch electrode itself possesses some (small) resistance to current flow which causes the voltage at the tip of the electrode to deviate from the command voltage, so too does the cytoplasm in a cellular process (e.g. dendrite or axon) possess resistance to current flow. Thus, the voltage in distal parts of cellular processes or simply very large or oblong cells (e.g. muscle fibers) deviates from the voltage at the tip of the electrode. In general, the membrane potential will deviate from the command potential to a degree that varies with the distance from the patch electrode. This deviation in voltage causes several tell-tale artifacts to appear in recordings.

One such artifact is the superposition of poorly clamped currents over properly clamped currents. This is because areas of membrane near enough to the electrode will still be properly voltage-clamped, however more distant regions of membrane will experience a large deviation from the command voltage, and the voltage change takes a longer time to

spread to these regions. Thus poorly clamped currents can appear as delayed currents superimposed upon properly clamped currents (Sontheimer *et al.*, 1992). The overall kinetics of currents that are not clamped properly will be slower as well, due to so-called low pass filter effects that result from having to travel a greater distance to reach the electrode. In addition, Na_V channels in poorly clamped distant regions can be depolarized above threshold, and therefore produce regenerative inward currents that can overwhelm the ability of the patch-clamp amplifier to control or clamp the membrane potential (Eliasof *et al.*, 1987).

For these reasons, attempts were made to confirm that zebrafish red and white muscle fibers, which are cylindrical in shape, and fairly large, were adequately space-clamped. This was done by ensuring that the peak of the Na_V currents all occurred within 500 μs of the onset of depolarization, that tail currents were super-imposable when normalized, and that there were never any uncontrolled regenerative inward currents.

However, the best way to ensure that space-clamping is not an issue is to have complete control over the entire membrane that you are recording from, which is what the cell-attached patch-clamp configuration allows. Only currents produced by channels in the membrane directly beneath the patch pipette are recorded, and the voltage across that small patch of membrane can be completely controlled by the amplifier.

Thus, the cell-attached recordings detailed below were aimed at confirming that these fibers can be adequately space-clamped, even at the oldest age (and therefore the largest fiber size) examined.

Methods

Zebrafish, aged 6 dpf, were maintained and dissected as described above (see METHODS 1). For these experiments, both the extracellular bath solution and the pipette-filling solution were the same – Na^+-isolating extracellular saline (Table 1) with the addition of curare (15μM) to block neuromuscular transmission and 4-aminopyridine (4-AP; 5 mM) to block K_V channels. Currents were evoked by stepwise depolarizations from a holding potential of -90 mV to a range of potentials from -80 to 60 mV in 10 mV increments.

Results

Properties of Na_V currents obtained in cell-attached patch clamp configuration from 6 dpf white muscle fibers closely resemble those of their whole-cell counterparts (n=12). The currents appeared to be very similar in shape and kinetics to those obtained from whole-cell recordings, but amplitude is lower due to a reduced number of contributing channels (Figure A2A). A current-voltage plot of cell-attached Na_V currents indicates

that the maximum amount of inward current occurs at ~0 mV, which is consistent with whole-cell currents (Figure A2B). Most importantly, the time-course of inactivation of cell-attached Na_V currents at various membrane potentials is virtually identical to that seen in 6 dpf whole-cell recordings, indicating that whole-cell recordings were adequately space-clamped (Figure A2C).

Discussion

These results serve as confirmation that all whole-cell recordings made from zebrafish skeletal muscle fibers up to at least 6 dpf are adequately space-clamped. Thus, the properties of whole-cell currents are indeed accurate representations of true currents in terms of voltage-dependent and kinetic properties.

Figure A2. Properties of NaV currents obtained in cell-attached patch lamp configuration from 6 dpf white muscle fibers closely resemble those of their whole-cell counterparts. **(A)** A representative recording of Na_V currents in a small patch of membrane. The currents appear to be very similar in shape and kinetics to those obtained from whole-cell recordings, but amplitude is lower due to a reduced number of contributing channels. **(B)** Current-voltage plot of cell-attached Na_V currents indicates that the maximum amount of inward current occurs at ~0 mV, which is consistent with whole-cell currents. **(C)** The time-course of inactivation of cell-attached Na_V currents at various membrane potentials is virtually identical to that seen in 6 dpf whole-cell recordings, indicating that whole-cell recordings were adequately space-clamped.

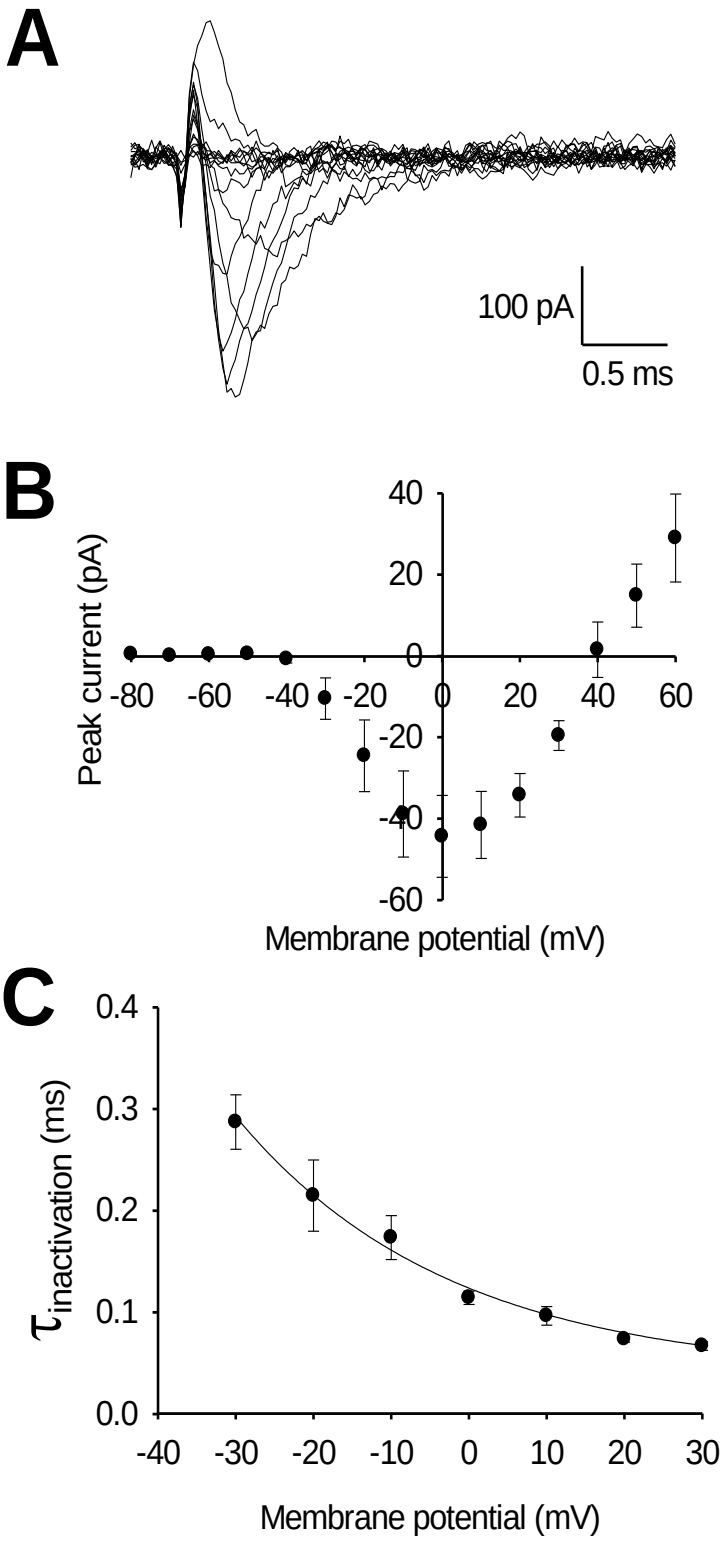
A
100 pA
0.5 ms
B
Peak current (pA)
40
20
0
-20
-40
-60
-80
-60
-40
-20
0
20
40
60
Membrane potential (mV)
C
$\tau_{inactivation}$ (ms)
0.4
0.3
0.2
0.1
0.0
-40
-30
-20
-10
0
10
20
30
Membrane potential (mV)

3. Resting membrane potentials in red and white muscle fibers of larval zebrafish.

Introduction

Resting membrane potentials have previously been reported in zebrafish red and white muscle fibers; rest potential in red fibers changed from -73 mV to -56 mV during the first 5 dpf, whereas in white fibers it went from -78 mV to -71 mV. These potentials were measured using the whole-cell patch clamp technique, however, which raises concerns about their accuracy (Buss & Drapeau, 2000). Although membrane potentials can be measured using the whole-cell patch clamp technique, they are not necessarily accurate of the true rest membrane potentials of cells due to the fact that you are displacing both the extracellular and intracellular milieu. A better approach is to use sharp electrode recording techniques, where the tips of the electrodes are small enough that displacement of intracellular milieu is negligible.

Methods

Transmembrane potentials were recorded using standard procedures (Westerfield et al, 1986). Briefly, wild type zebrafish larvae

between 2 dpf and 4 dpf were continuously bathed in fresh aerated physiological saline containing (in mM) 116 NaCl, 2 KCl, 0.9 CaCl2, 15 glucose, 5 HEPES, buffered to pH 7.8. Single muscle fibers were penetrated for intracellular recording with high resistance (20-40 MΩ) glass micropipettes containing a 3M KCl solution in water.

Results

Intracellular recordings were obtained from red and white muscle fibers of zebrafish larvae (2-4 dpf). There was no significant change in resting membrane potentials between 2 and 4 dpf in either red or white muscle fibers, therefore recordings were pooled into red and white groups. Figure A3A shows a representative recording of the transmembrane potential from a red fiber at rest. The potential is initially zero before contact is made with the muscle fiber. As the electrode penetrates the cell membrane, the potential difference between the recording electrode and the reference electrode in the bath drops sharply into negative values and settles at a rest potential of approximately -60 mV. This potential remains relatively steady until the pipette is pulled out of the cell, at which point the potential quickly reverts back to zero. Rest potential in red fibers appears to be more depolarized, at -36±2 mV (n=15), whereas white fibers rest at -59±5 mV (n=9).

Discussion

The rest potentials measured in white fibers are similar to those previously reported in 36 hpf wild type fish (-59±12 mV) as well as *nic-1*(b107) mutants (-56±10 mV), which, similar to *sop* mutants, lack AchRs (Westerfield *et al.*, 1990). The same group has also recorded from juvenile and adult wild type zebrafish muscle fibers and reported rest potentials of -82±7 mV, leading to the conclusion that rest potential hyperpolarizes in white muscle during development. The rest potential of zebrafish red muscle appeared to be ~25 mV more depolarized than white muscle. According to the steady state inactivation properties of K_V currents in white muscle (Figure R4B), regardless of age, virtually 100% of K_V channels would be in a non-inactivated state at a resting membrane potential of around -60 mV, and would therefore be available to be activated upon depolarization. The availability of Na_V channels, on the other hand, would change drastically during development; from ~ 75% at 1 dpf to ~30% at 6 dpf (Figure R7B). This would result in fibers becoming gradually less excitable as they mature, and may be tied to their changing behaviors during this time period; fibers are more easily excited during periods of spontaneous contractions than when undergoing beat-and-glide swimming behaviors.

Relative to their twitch (white) fiber counterparts, depolarized resting potentials have previously been observed in tonic (red) fibers; however, this was deemed to be due to the higher input resistance of tonic

fibers (Table 3), which makes them more sensitive to leak currents produced by impalement by the sharp electrode (Stefani & Steinbach, 1969).

Resting membrane potentials could have major implications for the steady state properties of Na_V and K_V currents, and therefore muscle activity itself. Future work in this area should aim to complete the characterization of resting membrane potentials in wild-type fish by recording from 1 dpf animals in order to see if there is a developmental shift occurring between 1 and 2 dpf, which appears to be a period of much developmental change for ionic currents.

Figure A3. Resting membrane potentials in red and white muscle fibers of larval zebrafish. **(A)** Representative recording of resting membrane potential (approximately -60 mV) in a white muscle fiber. Resting potential was measured as the potential to which the current fell immediately after the cell membrane was penetrated by the sharp electrode. **(B)** The average resting membrane potentials in red fibers was more depolarized (-36±2 mV, n=15) than in white fibers (-59±5 mV, n=9).

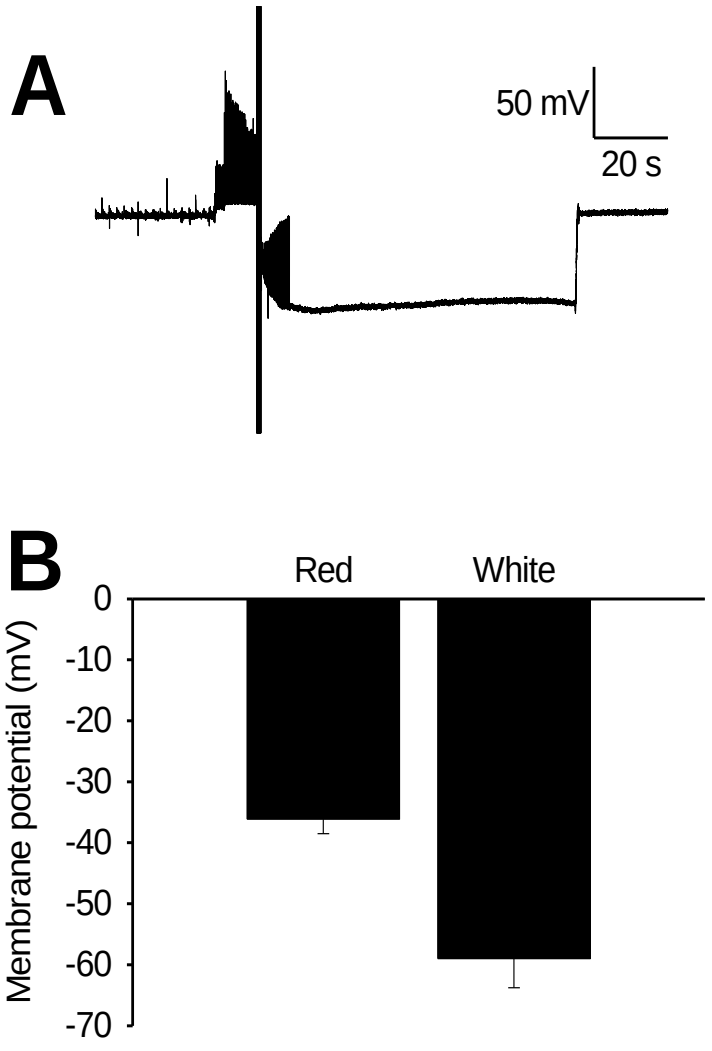
A
50 mV
20 s
B
Red
White
0
-10
-20
-30
-40
-50
-60
-70
Membrane potential (mV)

REFERENCES

Adams JP, Anderson AE, Varga AW, Dineley KT, Cook RG, Pfaffinger PJ & Sweatt JD. (2000). The A-type potassium channel Kv4.2 is a substrate for the mitogen-activated protein kinase ERK. *J Neurochem* **75,** 2277-2287.

Anderson AE, Adams JP, Qian Y, Cook RG, Pfaffinger PJ & Sweatt JD. (2000). Kv4.2 phosphorylation by cyclic AMP-dependent protein kinase. *J Biol Chem* **275,** 5337-5346.

Battaini F. (2001). Protein kinase C isoforms as therapeutic targets in nervous system disease states. *Pharmacol Res* **44,** 353-361.

Bourdeau ML, Morin F, Laurent CE, Azzi M & Lacaille JC. (2007). Kv4.3-mediated A-type K+ currents underlie rhythmic activity in hippocampal interneurons. *J Neurosci* **27,** 1942-1953.

Buckingham SD & Ali DW. (2004). Sodium and potassium currents of larval zebrafish muscle fibres. *J Exp Biol* **207,** 841-852.

Buss RR & Drapeau P. (2000). Physiological properties of zebrafish embryonic red and white muscle fibers during early development. *J Neurophysiol* **84,** 1545-1557.

Chen TC, Law B, Kondratyuk T & Rossie S. (1995). Identification of soluble protein phosphatases that dephosphorylate voltage-sensitive sodium channels in rat brain. *J Biol Chem* **270,** 7750-7756.

Colby KA & Blaustein MP. (1988). Inhibition of voltage-gated K channels in synaptosomes by sn-1,2-dioctanoylglycerol, an activator of protein kinase C. *J Neurosci* **8,** 4685-4692.

Connor JA & Stevens CF. (1971). Inward and delayed outward membrane currents in isolated neural somata under voltage clamp. *J Physiol* **213,** 1-19.

Dascal N & Lotan I. (1991). Activation of protein kinase C alters voltage dependence of a Na+ channel. *Neuron* **6,** 165-175.

Eliasof S, Barnes S & Werblin F. (1987). The interaction of ionic currents mediating single spike activity in retinal amacrine cells of the tiger salamander. *J Neurosci* **7,** 3512-3524.

Grega DS, Werz MA & Macdonald RL. (1987). Forskolin and phorbol esters reduce the same potassium conductance of mouse neurons in culture. *Science* **235,** 345-348.

Hille B. (2001). *Ion channels of excitable membranes*. Sinauer, Sunderland, Mass.

Hoffman DA, Magee JC, Colbert CM & Johnston D. (1997). K+ channel regulation of signal propagation in dendrites of hippocampal pyramidal neurons. *Nature* **387,** 869-875.

Nakashima S. (2002). Protein kinase C alpha (PKC alpha): regulation and biological function. *J Biochem* **132,** 669-675.

Newton AC. (2001). Protein kinase C: structural and spatial regulation by phosphorylation, cofactors, and macromolecular interactions. *Chem Rev* **101,** 2353-2364.

Numann R, Catterall WA & Scheuer T. (1991). Functional modulation of brain sodium channels by protein kinase C phosphorylation. *Science* **254,** 115-118.

Ohno S & Nishizuka Y. (2002). Protein kinase C isotypes and their specific functions: prologue. *J Biochem* **132,** 509-511.

Osada S, Mizuno K, Saido TC, Suzuki K, Kuroki T & Ohno S. (1992). A new member of the protein kinase C family, nPKC theta, predominantly expressed in skeletal muscle. *Mol Cell Biol* **12,** 3930-3938.

Rudy B. (1988). Diversity and ubiquity of K channels. *Neuroscience* **25,** 729-749.

Sigel E & Baur R. (1988). Activation of protein kinase C differentially modulates neuronal Na+, Ca2+, and gamma-aminobutyrate type A channels. *Proc Natl Acad Sci U S A* **85,** 6192-6196.

Sontheimer H, Black JA, Ransom BR & Waxman SG. (1992). Ion channels in spinal cord astrocytes in vitro. I. Transient expression of high levels of Na+ and K+ channels. *J Neurophysiol* **68,** 985-1000.

Stefani E & Steinbach AB. (1969). Resting potential and electrical properties of frog slow muscle fibres. Effect of different external solutions. *J Physiol* **203,** 383-401.

Tierney AJ & Harris-Warrick RM. (1992). Physiological role of the transient potassium current in the pyloric circuit of the lobster stomatogastric ganglion. *J Neurophysiol* **67,** 599-609.

Werz MA & Macdonald RL. (1987). Phorbol esters: voltage-dependent effects on calcium-dependent action potentials of mouse central and peripheral neurons in cell culture. *J Neurosci* **7,** 1639-1647.

West JW, Numann R, Murphy BJ, Scheuer T & Catterall WA. (1991). A phosphorylation site in the Na+ channel required for modulation by protein kinase C. *Science* **254,** 866-868.

Westerfield M, Liu DW, Kimmel CB & Walker C. (1990). Pathfinding and synapse formation in a zebrafish mutant lacking functional acetylcholine receptors. *Neuron* **4,** 867-874.

Zhang L & McBain CJ. (1995a). Potassium conductances underlying repolarization and after-hyperpolarization in rat CA1 hippocampal interneurones. *J Physiol* **488 (Pt 3),** 661-672.

Zhang L & McBain CJ. (1995b). Voltage-gated potassium currents in stratum oriens-alveus inhibitory neurones of the rat CA1 hippocampus. *J Physiol* **488 (Pt 3),** 647-660.